

Finite-round quantum error correction on symmetric quantum sensors

Yingkai Ouyang^{1,*} and Gavin K. Brennen²

¹*Department of Physics & Astronomy, University of Sheffield, Sheffield, S3 7RH, United Kingdom*

²*Center for Engineered Quantum Systems, Dept. of Physics & Astronomy, Macquarie University, 2109 NSW, Australia*

The Heisenberg limit provides a quadratic improvement over the standard quantum limit, and is the maximum quantum advantage that linear quantum sensors could provide over classical methods. It remains elusive, however, because of the inevitable presence of noise decohering quantum sensors. Namely, if infinite rounds of quantum error correction corrects any part of a quantum sensor's signal, a no-go result purports that the standard quantum limit scaling can not be exceeded. We side-step this no-go result by using an optimal finite number of rounds of quantum error correction, such that even if part of the signal is corrected away, our quantum field sensing protocol can approach the Heisenberg limit in the face of a linear rate of deletion errors. Here, we focus on quantum error correction codes within the symmetric subspace. Symmetric states of collective angular momentum are good candidates for multi-qubit probe states in quantum sensors because they are easy to prepare and can be controlled without requiring individual addressability. We show how the representation theory of the symmetric group can inform practical decoding algorithms for permutation-invariant codes. These decoding algorithms involve measurements of total angular momentum, quantum Schur transforms or logical state teleportations, and geometric pulse gates. Our completion of the theory of permutation-invariant codes allows near-term implementation of quantum error correction using simple quantum control techniques.

I. INTRODUCTION

Quantum sensors exploit entangled quantum probe states to estimate physical parameters with unprecedented precision. However, the difficulty of reliably preparing and preserving entangled probe states in the face of noise invariably degrades the performance of practical quantum sensors. Is it possible to recover the quantum advantage of noisy quantum sensors using using a quantum error correction scheme that admits near term implementations?

Erasure errors and energy losses are common noise processes that degrade the performance of quantum sensors. Energy losses, or amplitude damping errors, arise when an excited quantum state couples with a lower temperature bath [1]. Erasure errors can occur for a variety of reasons including actual particle losses due to the escape of qubits from a region of confinement, or, more frequently, due to errors which map the information carrying states to an orthogonal subspace, aka detectable leakage. Erasure errors due to absorption dominate in many architectures using photonic qubits and notably it has been shown that in trapped Rydberg atoms nearly all qubit errors can be converted into erasure errors [2]. A particularly severe situation occurs when the location of the erasure is not kept track of. Such errors are called deletion errors [3–5]. Deletion errors can be extremely punitive on Quantum Error Correction (QEC) codes that are not well-chosen: even a single deletion error can introduce errors on all of the remaining qubits. In view of this, it is especially important to use special QEC codes that can correct deletion errors.

When no active QEC is available, but where there is a negligible amount of noise, such as a constant number of errors, the quantum advantage in quantum sensing can still be retained [6–8]. Practically speaking however, a scenario with a constant number of errors while the number of particles becomes large is not very realistic. Indeed, there is strong evidence that a linear number of errors completely destroys the quantum advantage of quantum sensors [9].

The promise of using active QEC to recover the maximum quantum advantage in quantum sensors, that is Heisenberg scaling for their precision, is well-studied [10–19]. In these papers, QEC is applied an infinite number of times. However, the proposed schemes do not consider QEC codes that can correct deletion errors, do not admit near-term implementations, and do not use a finite number of QEC rounds.

The ultimate limits of QEC-enhanced metrology using infinite rounds of QEC has been discussed [15, 20]. Namely, a strong no-go result was shown: for quantum sensors to recover the Heisenberg scaling for their precision in the face of a linear rate of errors using infinite rounds of QEC, the QEC code (1) must not correct away any part of the signal and (2) the signal cannot lie within the span of the errors. Failing this, the standard quantum limit cannot be surpassed [15, 20]. However this does not rule out the possibility of having quantum sensors' precision approach the Heisenberg scaling when (1) and (2) are violated, but we use a finite number of rounds of QEC. This gives rise to the following question:

Can we optimize the quantum advantage of quantum sensors in the face of a linear rate of errors by varying the number of QEC rounds per unit time?

* y.ouyang@sheffield.ac.uk

In this paper, we answer this question. We depart from the oft-considered infinite rate of QEC; in an explicit QEC-enhanced sensing scheme, we optimize the number of QEC rounds, and prove that the precision can approach the Heisenberg scaling. Moreover, we show how our scheme admits near-term implementations using simple quantum control techniques.

Our scheme builds upon the theory of quantum sensing using symmetric states that support QEC. Such states reside in permutation-invariant codes, which not only comprise of states that are invariant under any permutation of the underlying qubits, but also support quantum error correction. Permutation-invariant codes [5, 21–26], have several features that make them attractive candidates for use in quantum sensors. First their controllability by global fields could allow for their scalable physical implementations [27] in near-term devices such as NV centres in diamond, trapped ions, or trapped neutral atoms where addressability without cross-talk is difficult. Second, such permutation-invariant codes can correct deletions [5], which conventional QEC codes cannot correct. Third, there are families of permutation-invariant codes parametrized by only a few integers, namely gnu codes [23] and their variants [5, 25], and this makes optimising the best such codes to use in quantum sensors a tractable computation problem.

Permutation-invariant codes, particularly gnu codes [23] and shifted gnu codes [5, 25] which we review in Section III B, are attractive candidates to consider for QEC. However, a full theory of QEC for permutation-invariant codes remains lacking. In particular, while the optimal recovery map that performs the QEC for permutation-invariant codes exists, and its Kraus operators can be written down, it was not known how one could concretely implement these recovery operations using a sequence of simple operations.

The first main contribution here is our completion of the theory of QEC for permutation-invariant codes.

Applying tools from the representation theory of the symmetric group, we devise a sequence of simple operations that performs QEC for *any* permutation-invariant quantum code. These operations require only measurements of total angular momenta, quantum Schur transforms, and geometric phase gates. When we specialize to deletion errors, the recovery operation is even simpler; we just need to measure in the modulo Dicke basis, and apply geometric phase gates.

The second main contribution of our work is a protocol for QEC-enhanced sensing using symmetric probe states in the face of a linear rate of deletion errors. We prove that with a non-trivial amount of prior information about the signal, we can have a quantum advantage in estimating its value when the signal accumulates for a constant amount of time. This advantage can approach the maximum possible for noiseless sensing, in the limit of a large number of qubits.

The third main contribution of our work are our protocols for implementing the algorithms in our paper using

near-term quantum control techniques.

II. OVERVIEW OF OUR MAIN RESULTS

We establish the following main results.

★ **Field sensing with symmetric states:-** We discuss field sensing along with permutation-invariant codes. This discussion lays the foundation for subsequent analysis of field sensing with a finite number of rounds of QEC. In Theorem 1 of Section III, we derive the optimal quantum measurement that maximizes the precision for a fixed symmetric probe state.

We give a simple expression of any logical plus shifted gnu state’s quantum Fisher information (QFI) in Lemma 2 of Section III C.

We give a simple expression for the Fisher information (FI) by projecting into the shifted gnu code’s logical plus-minus basis after accumulating a phase signal in Theorem 3.

We discuss the impact of noise on field sensing using symmetric states in Section III D. We calculate in Lemma 4 and Lemma 6 what deletions and amplitude damping errors do to arbitrary pure symmetric states. In Lemma 5 and Lemma 7, we give the QFI of shifted gnu plus states after deletions and amplitude damping errors happen.

★ **From representation theory to QEC:-** In Section IV, we develop a complete theory for the QEC of permutation-invariant codes. We explain in Section IV A how to perform QEC for any permutation-invariant code in a two-stage procedure. Stage 1 projects the corrupted state onto the irreducible representations of the symmetric group by measuring the total angular momentum of subsets of qubits. The error-syndrome extracted at this point corresponds to a standard Young tableaux. Stage 2 does further projections within the irreducible representations and finally performs a unitary to bring the state back to the codespace.

We explain how to correct deletion errors in Section IV C. The QEC procedure for correcting deletions is far simpler than that of correcting general errors. Namely, it suffices to just count the number of deletions that occurred, perform projections within the symmetric subspace. This will correct the errors, and map us to a permutation-invariant code with fewer qubits. If we like to recover the original number of qubits, we can perform teleportation.

★ **A proposal for QEC-enhanced field sensing, with a finite number of rounds of QEC:-** In Section V, we propose a quantum sensing scheme using a finite number of QEC rounds with precision that approaches the Heisenberg scaling.

First, we show that each round of QEC on an accumulated signal on a specific permutation-invariant codestate

amounts to an effective evolution of the probe state within the codespace.

Second, to extract the signal after multiple rounds of QEC, we propose measurement of the evolved probe state within the logical basis of the codespace. We are able to calculate the Fisher information of the unknown signal that can be extracted in this procedure. We call this scheme as Protocol 1.

We show that with a suitable number of repetitions of Protocol 1 and with a suitable choice of coding parameters for the shifted gnu codes we use, we can estimate field strengths with a quantum advantage that can approach the Heisenberg limit. We achieve this by deriving a linear program whose objective function equals the logarithm of the signal's Fisher information, and the linear constraints of the linear program impose the requirement of having the distortion in the signal brought about by QEC to be negligible.

*** Quantum control techniques to implement of QEC and field sensing for permutation-invariant codes:-**

We discuss in detail in Section VI how we may physically implement the subroutines that our QEC and quantum sensing protocols require using quantum control techniques. The quantum control techniques require only the introduction of a small number of catalytic coherent states, a linear coupling between the spin-system and the coherent states, and geometric pulse gates. First, we explain in Section VIA how to measure the total angular momentum. In Section VIB, we explain how to measure the modulo weights of Dicke states. In Section VIC, we discuss geometric phase gates and unitary synthesis on Dicke states. In Section VID, we explain how to perform gates related to code-teleportation for shifted gnu codes. In Section VIE we explain how to perform optimal measurements for field-estimation when the initial probe state is a pure symmetric state.

III. SYMMETRIC PROBE STATES FOR FIELD SENSING

A. Field sensing

Before we discuss the use of quantum codes for field-sensing in quantum sensors, let us review at an abstract level how we can use quantum sensors for field sensing. Imagine that we have N qubits that are sensitive to a classical field, and that we want to use them to estimate a classical field's magnitude E . Sensing in a quantum sensor proceeds in three stages, which are (1) state preparation, (2) signal accumulation, and (3) measurement. In the state-preparation stage, one carefully initializes a chosen probe state ρ , and awaits the arrival of the signal (the classical field). In the signal accumulation stage, the classical field of magnitude E interacts with the qubits

via the interaction Hamiltonian $\mu E \hat{J}^z$.¹ Here, μ is the coupling strength, $\hat{J}^z = \frac{1}{2} \sum_j Z_j$ is the collective spin operator, and Z_j applies a phase-flip on only the j -th qubit. The signal in this case, maps ρ to $\rho_\theta = U_\theta \rho U_\theta^\dagger$ where

$$U_\theta = \exp(-i\theta \hat{J}^z) \quad (1)$$

and θ is directly proportional to E and the duration of the signal accumulation. In the measurement stage, one measures ρ_θ in a well-chosen basis. After these three stages are repeated, one can embark on the parameter estimation stage. Using the measurement statistics, one constructs a locally unbiased estimator $\hat{\theta}$ for the true value of θ with the smallest possible variance. With this estimator, one estimates the field strength.

The field sensing problem is a canonical problem in quantum metrology. Using the language of quantum metrology, given a probe state ρ_θ that depends on a parameter θ , we want to find the minimum variance estimator $\hat{\theta}$ of θ that is furthermore locally unbiased. The celebrated quantum Cramér-Rao bound gives an attainable lower bound on $\text{Var}(\hat{\theta})$ [28]:

$$\text{Var}(\hat{\theta}) \geq Q(\rho_\theta, \frac{d\rho_\theta}{d\theta})^{-1} \quad (2)$$

where $Q(\rho_\theta, \frac{d\rho_\theta}{d\theta}) = \text{tr}(\rho_\theta L^2)$ denotes the quantum Fisher information (QFI) and L , the symmetric logarithmic derivative (SLD), is any Hermitian solution of the Lyapunov equation

$$\frac{d\rho_\theta}{d\theta} = \frac{1}{2}(L\rho_\theta + \rho_\theta L). \quad (3)$$

In this work we focus on using symmetric states as probe states for field sensing. Symmetric states are invariant under any permutation of the underlying particles. The symmetric space of N qubits is spanned by the Dicke states defined as

$$|D_w^N\rangle = \frac{1}{\sqrt{\binom{N}{w}}} \sum_{\substack{x_1, \dots, x_N \in \{0,1\} \\ x_1 + \dots + x_N = w}} |x_1, \dots, x_N\rangle, \quad (4)$$

where $w = 0, \dots, N$ is denoted the weight of $|D_w^N\rangle$, such that $N/2 - w$ is the eigenvalue of \hat{J}^z acting on the state.

For any pure symmetric state $|\psi\rangle = \sum_w a_w |D_w^N\rangle$, the variance of \hat{J}^z with respect to the Dicke basis is v_ψ where

$$v_\psi = \sum_w |a_w|^2 w^2 - \left(\sum_w |a_w| w \right)^2. \quad (5)$$

When ρ_θ is pure symmetric state used for noiseless field-sensing and $\frac{d\rho}{d\theta} = -i[\hat{J}^z, \rho]$, we derive a corresponding rank two SLD and find its spectral decomposition in Theorem 1.

¹ Hereafter we set $\hbar \equiv 1$.

Theorem 1 (SLD for pure symmetric states). *Let $\rho_\theta = |\psi\rangle\langle\psi|$ be a pure symmetric state where $|\psi\rangle = \sum_w a_w |D_w^N\rangle$. For $j = 1, 2$, let $m_j = \sum_{w=1}^N |a_w|^2 w^j$, and let $v_\psi = m_2 - m_1^2$. Then an SLD solution to (3) has the spectral decomposition*

$$L = \sqrt{v_\psi} (|\psi\rangle + i|b\rangle)(\langle\psi| - i\langle b|) - \sqrt{v_\psi} (|\psi\rangle - i|b\rangle)(\langle\psi| + i\langle b|) \quad (6)$$

where

$$|b\rangle = \left(\sum_w a_w w |D_w^N\rangle - m_1 |\psi\rangle \right) / \sqrt{v_\psi}, \quad (7)$$

and $\{|\psi\rangle, |b\rangle\}$ is an orthonormal basis.

We detail the proof of Theorem 1 in Appendix A. Based on Theorem 1, since the QFI is $\langle\psi|L^2|\psi\rangle$, we can ascertain that for symmetric states, the QFI is indeed $4v_\psi$ as expected. Hence, for any pure symmetric state $|\psi\rangle$, and when $\rho_\theta = U_\theta|\psi\rangle\langle\psi|U_\theta^\dagger$, we can write

$$\text{Var}(\hat{\theta}) \geq Q(\rho_\theta, \frac{d\rho_\theta}{d\theta})^{-1} = 1/(4v_\psi). \quad (8)$$

B. Permutation-invariant codes

Permutation-invariant codes are subspaces of the symmetric subspace that support a non-trivial amount of QEC. There is a rich theory of permutation-invariant codes [21–25, 29], with a variety of applications such as for storing quantum data in quantum ferromagnets [30], for unprotected quantum sensing [7], and for decoherence-free subspace communication in quantum buses [26].

We focus on so called gnu codes [23], which use $N = g \times n \times u$ qubits and have a distance of $d = \min\{g, n\}$ errors. We can visualize the logical codewords of gnu codes in terms of a binomial distribution on $(n+1)$ Dicke states, where the weights of the Dicke states are spaced g apart. In particular, gnu codes encode a single logical qubit, and have logical codes

$$|0_{g,n,u}\rangle = 2^{-(n-1)/2} \sum_{\substack{k \text{ even} \\ 0 \leq k \leq n}} \sqrt{\binom{n}{k}} |D_{gk}^{gnu}\rangle, \quad (9)$$

$$|1_{g,n,u}\rangle = 2^{-(n-1)/2} \sum_{\substack{k \text{ odd} \\ 0 \leq k \leq n}} \sqrt{\binom{n}{k}} |D_{gk}^{gnu}\rangle. \quad (10)$$

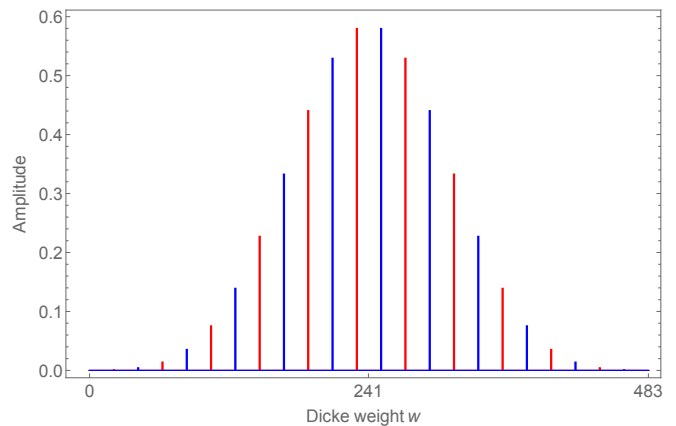


FIG. 1: Illustration of a gnu state $|+_{g,n,u,s}\rangle$ where $g = 21$, $n = 2\lfloor g/2\rfloor + 1$, $u = 1 + 1/n$, and $s = g$ so that the number of qubits is $N = gn + 2g = 483$. Here the horizontal axis depicts the weights w of the Dicke states, and the vertical axis depicts the values of amplitude $\langle D_w^{gnu+s} | +_{g,n,u,s}\rangle$. The colors red and blue correspond to the Dicke states of $|0_{g,n,u,s}\rangle$ and $|1_{g,n,u,s}\rangle$ respectively, and which are related by a global bit flip.

Here the positive integers g and n correspond to the bit-flip and phase-flip distance of the gnu code, and the real number $u \geq 1$ is a scaling parameter that does not affect the error correction property of the permutation-invariant code. Gnu codes can be generalized to s -shifted gnu codes [5, 25] that use $N = gnu + s$ qubits, with logical codewords

$$|0_{g,n,u,s}\rangle = 2^{-(n-1)/2} \sum_{\substack{k \text{ even} \\ 0 \leq k \leq n}} \sqrt{\binom{n}{k}} |D_{gk+s}^{gnu+s}\rangle \quad (11)$$

$$|1_{g,n,u,s}\rangle = 2^{-(n-1)/2} \sum_{\substack{k \text{ odd} \\ 0 \leq k \leq n}} \sqrt{\binom{n}{k}} |D_{gk+s}^{gnu+s}\rangle. \quad (12)$$

Again the distance of s -shifted gnu codes is $\min\{g, n\}$.

In this paper, we focus our attention of s -shifted gnu codes for which both g and n are sublinear in N and where $(gk + s) - N/2 = o(N)$ for all $k = 0, \dots, n$. We can visualize these shifted gnu codes to be concentrated around the half-Dicke state $|D_{N/2}^N\rangle$, as shown in Fig. 1. In particular, we use the logical plus state as the probe state, given by

$$|+_{g,n,u,s}\rangle = (|0_{g,n,u,s}\rangle + |1_{g,n,u,s}\rangle) / \sqrt{2}. \quad (13)$$

C. Permutation-invariant quantum sensors

Here, Lemma 2 calculates how much QFI we can get if we use $|+_{g,n,u,s}\rangle$ as a probe state to estimate θ in the noiseless setting.

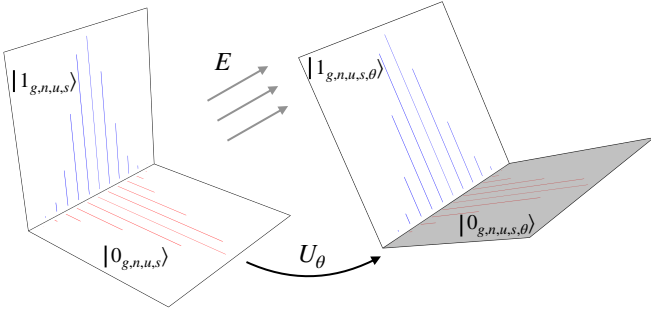


FIG. 2: Quantum sensing with the shifted gnu code to infer the strength of the field E which acts uniformly on the spins. The logical basis is rotated to a new logical frame, which satisfies the same error correction criteria, by a unitary $U_\theta = e^{-i\theta\hat{J}^z}$ where $\theta = \mu E\tau$ is the angle to be estimated and τ the interrogation time.

Lemma 2. *The QFI of $|+_{g,n,u,s}\rangle$ with respect to the signal U_θ is g^2n .*

Proof. The QFI is four times of the variance of the state $|+_{g,n,u,s}\rangle$. Note that

$$\sum_{k=0}^n \binom{n}{k} k = 2^{n-1}n, \quad \sum_{k=0}^n \binom{n}{k} k^2 = 2^{n-2}n(n+1). \quad (14)$$

Hence the variance of $|+_{g,n,u,s}\rangle$ is

$$\frac{1}{2^n} \sum_{k=0}^n \binom{n}{k} (g^2k^2 + 2gks + s^2) - \left(\frac{1}{2^n} \sum_{k=0}^n \binom{n}{k} (gk + s) \right)^2. \quad (15)$$

Using binomial identities, this variance is $\frac{g^2n(n+1)}{4} + \frac{2gsn}{2} + s^2 - \left(\frac{gn}{2} + s\right)^2$, and simplifies to $\frac{g^2n}{4}$. The result follows. \square

Theorem 3 shows that the FI can be proportional to g^2 by measuring an evolved gnu probe state in the code basis, spanned by the logical plus and minus operators.

Theorem 3. *Consider a shifted gnu state $\sum_w a_w |D_w^N\rangle$ with parameters g, n, u, s , where $a_{gk+s} = \sqrt{\binom{n}{k}} 2^{-n/2}$ for $k = 0, 1, \dots, n$ and $a_w = 0$ for all w that cannot be written as $gk + s$. After U_θ applies on the probe state, the FI of estimating θ by measuring in the gnu code's logical plus-minus basis is*

$$4g^2n^2 \left(\sin^2(g\theta) \cos^{2n-2}(g\theta) + \cos^2(g\theta) \sin^{2n-2}(g\theta) \right). \quad (16)$$

We provide the details of the proof in the Appendix.

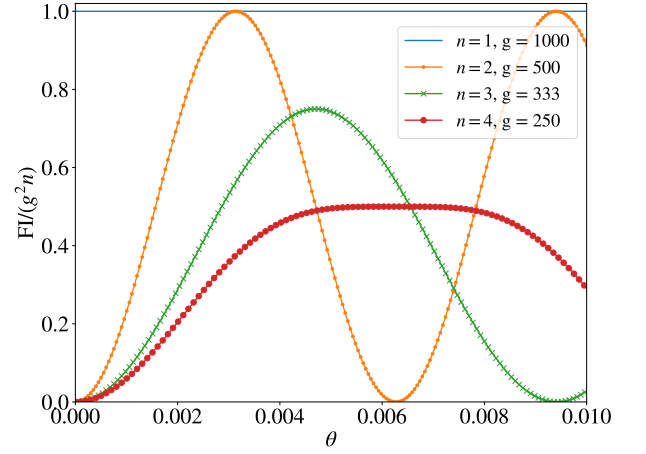


FIG. 3: The FI and QFI of shifted gnu codes ($u = 1$) on 1000 qubits in the absence of noise. The QFI for shifted gnu codes is g^2n . The FI is obtained by measuring the evolved shifted gnu states in the code's logical plus-minus basis. The plot shows how the ratio of the FI to the QFI depends on the true value of θ . For reference, the 1000-qubit GHZ state corresponds to $g = 1000, n = 1$.

Using Theorem 3, we can compute the performance of the FI obtained by measuring evolved shifted gnu states on the logical plus-minus basis, and compare this FI to the QFI in Fig. 3. Fig. 3 shows that the FI can be within a constant factor of the QFI, and also the tradeoff between increasing the distance of the code $d = \min\{g, n\}$ and the ratio of the FI to the QFI. Note that Theorem 3 also shows that the FI is exponentially suppressed with increasing n , and for this reason, we focus our attention on shifted gnu codes with constant n .

When shifted gnu codes accumulate the signal given by the unitary U_θ , they transform into what we call θ -rotated and s -shifted gnu codes. Such codes have logical codewords

$$|0_{g,n,u,s,\theta}\rangle = U_\theta |0_{g,n,u,s}\rangle, \quad (17)$$

$$|1_{g,n,u,s,\theta}\rangle = U_\theta |1_{g,n,u,s}\rangle. \quad (18)$$

Using the same proof technique as in [23], we can see that these θ -rotated codes also have a distance of $\min(g, n)$. This is because for any multi-qubit Pauli operator P that acts on at most $\min(g, n) - 1$ qubits, we can see that the Knill-Laflamme error criterion [31] for shifted gnu codes is equivalent to that for θ -rotated codes:

$$\langle 0_{g,n,u,s,\theta} | P | 0_{g,n,u,s,\theta} \rangle = \langle 0_{g,n,u,s} | P | 0_{g,n,u,s} \rangle \quad (19)$$

$$\langle 1_{g,n,u,s,\theta} | P | 1_{g,n,u,s,\theta} \rangle = \langle 1_{g,n,u,s} | P | 1_{g,n,u,s} \rangle \quad (20)$$

$$\langle 1_{g,n,u,s,\theta} | P | 0_{g,n,u,s,\theta} \rangle = 0. \quad (21)$$

The QEC properties of these θ -rotated gnu codes is invariant of θ . It is the distinguishability of these codes with respect to θ that makes them useful as probe states for classical field sensing.

D. Impact of errors on uncorrected symmetric states.

In the following we derive the QFI for shifted gnu states affected by either deletion errors or amplitude damping errors. The effect of dephasing errors on gnu codes is described in Ref. [7].

1. Deletion errors

The action of t deletion errors on any symmetric state, is equivalent to taking the partial trace $\text{tr}_t(\cdot)$ on the first t qubits. To discuss the action of deletion errors, it is often convenient to use the unnormalized Dicke states

$$|H_w^N\rangle = \sum_{\substack{\mathbf{x} \in \{0,1\}^N \\ \text{wt}(\mathbf{x})=w}} |x_1\rangle \otimes \cdots \otimes |x_N\rangle, \quad (22)$$

where $\text{wt}(\mathbf{x})$ denotes the Hamming weight of a binary string. Normalizing the basis states in (22) gives Dicke states $|D_w^N\rangle = |H_w^N\rangle / \sqrt{\binom{N}{w}}$. Then, Lemma 4 gives the partial trace of any symmetric state.

Lemma 4 (Impact of deletions). *Let N be a positive integer, and let v, w be integers such that $0 \leq v, w \leq N$. Let t be a positive integer where $t \leq N$. Let $|\psi\rangle = \sum_{w=0}^N a_w |D_w^N\rangle$, and for all $a = 0, \dots, t$, define*

$$|\psi\rangle_a = \sum_{w=a}^{N-t+a} a_w \frac{\sqrt{\binom{N-t}{w-a}}}{\sqrt{\binom{N}{w}}} |D_{w-a}^{N-t}\rangle. \quad (23)$$

Then

$$\text{tr}_t(|\psi\rangle\langle\psi|) = \sum_{a=0}^t \binom{t}{a} |\psi\rangle_a \langle\psi|_a. \quad (24)$$

Lemma 4 generalizes the result in [5, Lemma 5] where only shifted gnu codes were considered.

If $|\psi\rangle$ is a shifted gnu state, we have

$$|\psi\rangle_a = 2^{-n/2} \sum_{j=0}^n \sqrt{\binom{n}{j} \frac{\binom{N-t}{gj+g-a}}{\binom{N}{gj+g}}} |D_{gj+j-a}^{N-t}\rangle, \quad (25)$$

and hence its norm squared $n_a = \langle\psi_a|\psi_a\rangle$ is

$$n_a = 2^{-n} \sum_{j=0}^n \binom{n}{j} \frac{\binom{N-t}{gj+g-a}}{\binom{N}{gj+g}}, \quad (26)$$

and the variance of $|\psi_a\rangle/\sqrt{n_a}$ is

$$v_a = 2^{-n} \sum_{j=0}^n \binom{n}{j} \frac{\binom{N-t}{gj+g-a}}{n_a \binom{N}{gj+g}} (gj+s-a)^2 - \left(2^{-n} \sum_{j=0}^n \binom{n}{j} \frac{\binom{N-t}{gj+g-a}}{n_a \binom{N}{gj+g}} (gj+s-a) \right)^2. \quad (27)$$

Thus, we can determine the QFI for shifted gnu states.

Lemma 5. *The QFI of $|+_{g,n,u,s}\rangle$ after t deletions, when $g, n \geq t+1$, is $4 \sum_{a=0}^t n_a \binom{t}{a} v_a$.*

Proof. After t deletions, as long as $g, n \geq t+1$, the vectors $|\psi\rangle_a$ are pairwise orthogonal, and furthermore are supported on Dicke states of distinct weights modulo g . From Theorem 1, we can see that the SLDs of each of the states $|\psi\rangle_a/\sqrt{n_a}$ is pairwise orthogonal. This implies that the QFI of $|+_{g,n,u,s}\rangle$ after t deletions is a convex combination of the QFIs of the $|\psi\rangle_a/\sqrt{n_a}$, and hence is given by $4 \sum_{a=0}^t n_a \binom{t}{a} v_a$. \square

2. Amplitude damping errors

Amplitude damping (AD) errors are introduced by an AD channel \mathcal{A}_γ which has Kraus operators $A_0 = |0\rangle\langle 0| + \sqrt{1-\gamma}|1\rangle\langle 1|$ and $A_1 = \sqrt{\gamma}|0\rangle\langle 1|$. These Kraus operators model the relaxation of an excited state to the ground state with probability γ . We denote an amplitude damping channel on N qubits by $\mathcal{A}_{N,\gamma} = \mathcal{A}_\gamma^{\otimes N}$, which has the Kraus operators $A_{\mathbf{x}} = A_{x_1} \otimes \cdots \otimes A_{x_N}$ where $\mathbf{x} = (x_1, \dots, x_N) \in \{0,1\}^N$.

Given a subset P of $\{1, \dots, N\}$, we define an insertion channel Ins_P on an $N - |P|$ -qubit state to insert the pure state $|0\rangle^{\otimes |P|}$ in the positions labeled by P to result in an N qubit state. Insertion channels are discussed in more detail for instance in [32, 33]. Lemma 6 then expresses any symmetric state after amplitude damping in terms of insertions channels.

Lemma 6 (Impact of AD errors). *Let $|\psi\rangle = \sum_{w=0}^N a_w |D_w^N\rangle$ by any symmetric pure state. Now for any $x = 0, \dots, N$, define the subnormalized states*

$$|\phi_x\rangle = \sum_{w=x}^{N-x} a_w \sqrt{p_w(x)} |D_{w-x}^{N-x}\rangle, \quad (28)$$

where

$$p_w(x) = \binom{w}{x} \gamma^x (1-\gamma)^{w-x}. \quad (29)$$

Then

$$\mathcal{A}_{N,\gamma}(|\psi\rangle\langle\psi|) = \sum_{x=0}^N \frac{1}{\binom{N}{x}} \sum_{|P|=x} \text{Ins}_P(|\phi_x\rangle\langle\phi_x|). \quad (30)$$

We prove Lemma 6 in the appendix. Let $n_x = \langle\phi_x|\phi_x\rangle$, and let the variance of $|\phi_x\rangle/\sqrt{n_x}$ be

$$q_x = 2^{-n} \sum_{\substack{0 \leq k \leq n \\ x \leq gk \leq N-x}} \binom{n}{k} \frac{p_w(x)}{n_x} (gk+s-x)^2 - \left(2^{-n} \sum_{\substack{0 \leq k \leq n \\ x \leq gk \leq N-x}} \binom{n}{k} \frac{p_w(x)}{n_x} (gk+s-x) \right)^2 \quad (31)$$

Then, we obtain an upper bound on the QFI for shifted gnu states after AD errors.

Lemma 7. *The QFI of $|+_{g,n,u,s}\rangle$ after AD errors introduced by $\mathcal{A}_{N,\gamma}$ is at most $4 \sum_{x=0}^N n_x q_x$.*

Proof. The lemma follows directly from the convexity of the QFI with respect to the probe state, and the decomposition in Lemma 6. \square

IV. QUANTUM ERROR CORRECTION FOR PERMUTATION-INVARIANT CODES

A. Correcting t errors

Suppose that a noisy quantum channel \mathcal{N} has Kraus operators that act non-trivially on at most t qubits. Then any distance d permutation-invariant code can correct errors introduced by \mathcal{N} , provided that $d \geq 2t + 1$. Here, we outline a two stage quantum error correction procedure to correct these errors. Stage 1 projects the corrupted state onto the irreducible representations of the symmetric group S_N by measuring the total angular momentum of subsets of qubits. Stage 2 does further projections within the irreducible representations and finally performs a unitary to bring the state back to the codespace.

In Section IV A 1, after reviewing standard Young tableau, we describe how we can implement Stage 1 by measuring the total angular momentum of subsets of qubits as described in Section IV A 3.

1. Young diagrams and Young tableau

Consider Young diagrams [34, Page 29] comprising of N boxes arranged in two left-justified rows. We restrict our attention to Young diagrams with r_1 boxes on the first row and r_2 boxes on the second row where $r_1 \geq r_2$ and $r_1 + r_2 = N$.

$$(a) \quad (b) \quad (c) \quad (32)$$

In (32)(a), we depict a Young diagram with four boxes on the first row, and two boxes on the second row. Each Young diagram corresponds to an integer partition of N with two parts. A standard Young Tableau (SYT) is obtained by filling up the N boxes in a Young diagram with integers from 1 to N such that the integers strictly increase from left to right, and from top to bottom. Given a Young diagram, for instance in (32)(a), we give two examples of SYTs that can be obtained in (32)(b) and (32)(c) respectively. We can enumerate the number of

SYTs consistent with a given Young diagram using the hook-length formula [35, Corollary 7.21.6]. The hook-length formula states that the number of SYTs consistent with any Young diagram with N boxes is equal to $N!$ divided by the hook-length of each box. The hook-length of a given box is the total number of boxes in its hook, where the box's hook includes the box itself and all other boxes to its right and bottom.

$$(a) \quad (b) \quad (c) \quad (33)$$

In (33), we shade the hooks of the labelled cells. In (33)(a), (b) and (c), the hook-lengths are five, four and two respectively. From the hook-length formula, the number of SYTs corresponding to a Young diagram with two rows is

$$\frac{N!}{(N - r_1)!(r_1 + 1)!(r_1 - N + r_1 + 1)} = \binom{N}{r_1} \frac{2r_1 - N + 1}{r_1 + 1}. \quad (34)$$

Apart from SYTs, we also consider semistandard Young tableau (SSYT), where boxes are filled with integers that strictly increase from top to bottom and are non-decreasing from left to right. Here, we restrict our attention to SSYTs filled with the numbers 1 and 2. The number of such SSYTs obtainable from a Young diagram with two rows is

$$r_1 - r_2 + 1. \quad (35)$$

We list all SSYTs filled with the numbers 1 and 2 when $r_1 = 4$ and $r_2 = 2$ in (36) below.

$$(a) \quad (b) \quad (c) \quad (36)$$

From Schur-Weyl duality [36, Chapter 9.1] applied to quantum information theory [37, 38], we know that the N -qubit space $(\mathbb{C}^2)^{\otimes N}$ is isomorphic to

$$\bigoplus_D \mathcal{Q}^D \otimes \mathcal{P}^D, \quad (37)$$

where each D denotes a Young diagram with N boxes and two rows. For every Young diagram D , \mathcal{Q}^D is a space with basis elements labelled by all possible SYTs filled with integers 1 to N , and \mathcal{P}^D is a space with basis elements labelled by all possible SSYTs filled with integers 1 and 2. Since the basis of \mathcal{Q}^D is labeled by SYTs of shape D , we can write $\mathcal{Q}^D = \text{span}\{|\text{T}\rangle : \text{T is a SYT for } D\}$.

Since D always has two rows, we can represent it with the tuple (r_1, r_2) where r_1 and r_2 count the number of boxes in the first and second rows respectively. When $D = (N, 0)$, we can see from (34) and (35) that the dimension of $\mathcal{Q}^{(N,0)}$ is one, and the dimension of $\mathcal{P}^{(N,0)}$ is $N + 1$. In fact, $\mathcal{P}^{(N,0)}$ corresponds precisely to the symmetric subspace of an N -qubit symmetric state.

2. Symmetrizing lemma

When a channel acts identically and independently on every qubit, it always maps a pure symmetric state to a density matrix that is block diagonal on the spaces $\mathcal{Q}^D \otimes \mathcal{P}^D$ as given (37). For such block diagonal states, quantum error correction can proceed by projecting the density matrix onto one of the blocks labelled by D .

However the density matrices that we encounter in the quantum error correction of permutation-invariant codes do not necessarily have this block diagonal structure. In this scenario, such density matrices can always be made block diagonal in the Schur-Weyl basis by applying symmetrizing operations described by the quantum channel \mathcal{S} that randomly permutes qubits, and has Kraus operators $\{\frac{1}{\sqrt{N!}}P_\sigma : \sigma \in S_N\}$, where P_σ denotes an N -qubit matrix representation of a permutation operator that permutes qubit labels according to the permutation σ . In the following lemma, we prove that if we apply the symmetrizing channel, originally correctible errors remain correctible.

Lemma 8 (Symmetrizing lemma). *Let \mathcal{C} be any N -qubit permutation-invariant code of distance d . Let \mathcal{N} be any quantum channel with Kraus operators K of weight at most t . Then if $d \geq 2t + 1$, the channels \mathcal{N} and $\mathcal{S} \circ \mathcal{N}$ are both correctible with respect to \mathcal{C} .*

Proof. The channel \mathcal{N} is correctible, and hence satisfies the fundamental quantum error correction criterion [31]. To prove the lemma, we must show that the channel $\mathcal{S} \circ \mathcal{N}$ is also correctible.

Now, denote $\bar{K} = \{\frac{1}{\sqrt{N!}}P_\sigma A : \sigma \in S_N, A \in K\}$ as a set of Kraus operators for the quantum channel $\mathcal{S} \circ \mathcal{N}$. The Kraus operators in \bar{K} are correctible if and only if for every $\sigma, \tau \in S_N$ and $A, B \in K$, there exists a $g_{A,B,\sigma,\tau} \in \mathbb{C}$ such that

$$\Pi A^\dagger P_\sigma^\dagger P_\tau B \Pi = g_{A,B,\sigma,\tau} \Pi, \quad (38)$$

where Π the code projector for \mathcal{C} .

Since Π is a projector onto the symmetric subspace, for all $\sigma \in S_n$, we have that $P_\sigma \Pi = \Pi P_\sigma = \Pi$. Denoting $A_\sigma = P_\sigma A P_\sigma^\dagger$ and $B_\sigma = P_\sigma B P_\sigma^\dagger$, note that (38) is equivalent to

$$\Pi A_\sigma^\dagger B_\tau \Pi = g_{A,B,\sigma,\tau} \Pi. \quad (39)$$

Since A, B are operators with weight at most t , A_σ and B_τ must also be operators of weight at most t . Hence,

both A_σ and B_τ are linear combinations of Pauli operators of weight at most t . Namely,

$$A_\sigma = \sum_{P:|P|\leq t} a_{A,P,\sigma} P, \quad B_\tau = \sum_{P:|P|\leq t} b_{B,Q,\sigma} P, \quad (40)$$

where a_P and a_Q are real coefficients. From this, it follows that the left side of (39) is equivalent to

$$\Pi A_\sigma^\dagger B_\tau \Pi = \sum_{P,Q} a_{A,P,\sigma}^* b_{A,Q,\sigma} \Pi P Q \Pi. \quad (41)$$

From the Knill-Laflamme condition [31], since \mathcal{C} is a code of distance d , for every Pauli P and Q of weight at most t , there exists a $c_{P,Q} \in \mathbb{C}$ such that

$$\Pi P Q \Pi = c_{P,Q} \Pi. \quad (42)$$

Substituting (42) into the left side of (41), we can conclude that

$$\Pi A_\sigma^\dagger B_\tau \Pi = \sum_{P,Q} a_{A,P,\sigma}^* b_{A,Q,\sigma} c_{P,Q} \Pi. \quad (43)$$

This implies that

$$\Pi A^\dagger P_\sigma^\dagger P_\tau B \Pi = g_{A,B,\sigma,\tau} \Pi, \quad (44)$$

where

$$g_{A,B,\sigma,\tau} = \sum_{P,Q} a_{A,P,\sigma}^* b_{A,Q,\sigma} c_{P,Q}, \quad (45)$$

and this proves that $\mathcal{S} \circ \mathcal{N}$ is also correctible with respect to the code \mathcal{C} . \square

Lemma 8 gives us a hint of how we can perform quantum error correction on any permutation-invariant quantum code. Namely, if any correctible channel \mathcal{N} introduces errors on a permutation-invariant quantum code, we can project the state into the Schur-Weyl basis and still be able to correct the resultant errors. This is because a symmetrizing channel \mathcal{S} makes a quantum state block-diagonal in the Schur-Weyl basis, and Lemma 8 tells us that if \mathcal{N} is correctible, $\mathcal{S} \circ \mathcal{N}$ is also correctible. Section IV A 3 illustrates how we may project the state onto the diagonal blocks in the Schur-Weyl basis.

3. Syndrome extraction by measuring total angular momentum

Syndrome extraction for permutation-invariant codes proceeds by measuring the total angular momentum on nested subsets of qubits. The measurement results will reveal what Young diagram D and which corresponding SYT T we would have obtained. These measurements of total angular momentum occur in the sequentially coupled basis [39, 40], where subsets of qubits that we measure on are $[k] = \{1, \dots, k\}$, where $k = 1, \dots, N$. The

corresponding total angular momentum operators to be measured are $\hat{J}_{[1]}^2, \dots, \hat{J}_{[N]}^2$ ². where

$$\hat{J}_{[k]}^2 = (\hat{J}_{[k]}^x)^2 + (\hat{J}_{[k]}^y)^2 + (\hat{J}_{[k]}^z)^2, \quad (46)$$

and

$$\hat{J}_{[k]}^x = \frac{1}{2} \sum_{i=1}^k X_i, \quad \hat{J}_{[k]}^y = \frac{1}{2} \sum_{i=1}^k Y_i, \quad \hat{J}_{[k]}^z = \frac{1}{2} \sum_{i=1}^k Z_i. \quad (47)$$

The eigenvalues of the operators $\hat{J}_{[k]}^2$ are of the form $j_k(j_k + 1)$ where $2j_k$ are positive integers. After measurement, $\hat{J}_{[k]}^2$ gives an eigenvalue of $j_k(j_k + 1)$, and we can infer the total angular momentum number j_k . These total angular momentum numbers belong to the set

$$T_k = \{k/2 - j : j = 0, \dots, \lfloor k/2 \rfloor, k/2 - j \geq 0\}. \quad (48)$$

Since the total angular momentum operators $\hat{J}_{[k]}^2$ all commute, the order of measuring these operators does not affect the measurement outcomes. Hence we may measure $\hat{J}_{[k]}^2$ sequentially; that is we measure $\hat{J}_{[1]}^2$, followed by $\hat{J}_{[2]}^2$, and so on. Using the observed total angular momentum j_1, \dots, j_N , we construct SYTs corresponding to a Young diagram $D = (N/2 + j_N, N/2 - j_N)$ according to Algorithm 1. Algorithm 1 takes as input a quantum state ρ , uses the total angular momentums j_1, \dots, j_N of qubits in $[1], [2], \dots, [N]$ to iteratively construct a SYT \mathbb{T} by adding one labelled box at a time. Algorithm 1 outputs the resultant state $\rho_{\mathbb{T}}$, the SYT \mathbb{T} and $j_{\mathbb{T}} = j_N$.

Algorithm 1 Extract the SYT syndrome

```

1: procedure SYNDROMESYT( $\rho$ )
2:   Set  $i = 2$ , set  $\rho_{\mathbb{T}} = \rho$ .
3:   Set  $\mathbb{T}$  to be a SYT with one box on the first row filled with the number
   1, and no boxes on the second row.
4:   Set  $j, j_1 = 1/2$ .
5:   for  $k = 2$  to  $N$  do
6:     Measure observable  $S_k^2$  on qubits  $1, \dots, k$  of  $\rho_{\mathbb{T}}$ , and update  $\rho_{\mathbb{T}}$ .
7:     Set  $j_k(j_k + 1)$  as the measurement result, and find  $j_k$ .
8:     if  $j_k = j + 1/2$  then
9:       Update  $\mathbb{T}$ : create a box labelled by  $k$  to the first row's right.
10:      Set  $j \leftarrow j + 1/2$ .
11:     else  $j_k = j - 1/2$ 
12:       Update  $\mathbb{T}$ : create a box labelled by  $k$  to the second row's right.
13:       Set  $j \leftarrow j - 1/2$ .
14:     end if
15:     Set  $j_{\mathbb{T}} = j$ .
16:   end for.
17:   return  $(\rho_{\mathbb{T}}, \mathbb{T}, j_{\mathbb{T}})$ .
18: end procedure

```

Note that $j_{\mathbb{T}}$ denotes the total angular momentum of the N -qubits associated with the SYT \mathbb{T} . Combinatorially, for a SYT with r_1 and r_2 boxes on the first and second rows respectively, $j_{\mathbb{T}} = (r_1 - r_2)/2$.

After Algorithm 1 obtains a SYT \mathbb{T} , we know that $\rho_{\mathbb{T}}$ must have support within a subspace of

$$\mathcal{P}^{\mathbb{T}} = |\mathbb{T}\rangle \otimes \mathcal{P}^D. \quad (49)$$

We can enumerate the number of SSYTs to determine $|\mathcal{P}^{\mathbb{T}}|$; from (35), we find that

$$|\mathcal{P}^{\mathbb{T}}| = (N/2 + j_{\mathbb{T}}) - (N/2 - j_{\mathbb{T}}) + 1 = 2j_{\mathbb{T}} + 1. \quad (50)$$

This is sensible since $\mathcal{P}^{\mathbb{T}}$ corresponds to a space with total angular momentum $j_{\mathbb{T}}$ on all N qubits. Using information about the SYT \mathbb{T} , we can perform quantum error correction on the spaces $\mathcal{P}^{\mathbb{T}}$. Denoting $\Pi^{\mathbb{T}}$ as the projector onto $\mathcal{P}^{\mathbb{T}}$, we point out that $\Pi^{\mathbb{T}}$ commutes with the operator \hat{J}^z , because \hat{J}^z commutes with the $\hat{J}_{[k]}^2$. Hence, the eigenvectors of \hat{J}^z are also eigenvectors of $\Pi^{\mathbb{T}}$. In fact, we can write the projector $\Pi^{\mathbb{T}}$ as

$$\Pi^{\mathbb{T}} = \sum_{m=-j_{\mathbb{T}}}^{j_{\mathbb{T}}} |m_{\mathbb{T}}\rangle \langle m_{\mathbb{T}}|, \quad (51)$$

where $\{|m_{\mathbb{T}}\rangle : m = -j_{\mathbb{T}}, \dots, j_{\mathbb{T}}\}$ denotes an orthonormal basis of $\mathcal{P}^{\mathbb{T}}$ and

$$\hat{J}^z |m_{\mathbb{T}}\rangle = m |m_{\mathbb{T}}\rangle. \quad (52)$$

Here, the states $|m_{\mathbb{T}}\rangle$ are magnetic eigenstates of the operator \hat{J}^z . Note that when \mathbb{T} is the SYT with only one row, $|m_{\mathbb{T}}\rangle = |D_{m+j_{\mathbb{T}}}^N\rangle$ and $|m_{\mathbb{T}}\rangle$ is a Dicke state.

For any positive integer g , we can decompose the projector $\Pi^{\mathbb{T}}$ as

$$\Pi^{\mathbb{T}} = \sum_{a=0, \dots, g-1} \Pi_{\text{mod}, g, a}^{\mathbb{T}} \quad (53)$$

where

$$\Pi_{\text{mod}, g, a}^{\mathbb{T}} = \sum_{\substack{k \in \mathbb{Z} \\ -j_{\mathbb{T}} \leq gk + a - j_{\mathbb{T}} \leq j_{\mathbb{T}}}} |(gk + a - j_{\mathbb{T}})_{\mathbb{T}}\rangle \langle (gk + a - j_{\mathbb{T}})_{\mathbb{T}}|. \quad (54)$$

Here, we can see that the projector $\Pi_{\text{mod}, g, a}^{\mathbb{T}}$ projects onto the span of states $|m_{\mathbb{T}}\rangle$ where $\text{mod}(m + j_{\mathbb{T}}, g) = a$, that is, the space where magnetic quantum numbers plus $j_{\mathbb{T}}$ are equivalent to a modulo g for a particular SYT \mathbb{T} .

By defining the projector

$$Q_{g, a} = \sum_{\text{SYTs } \mathbb{T}} \Pi_{\text{mod}, g, a}^{\mathbb{T}}, \quad (55)$$

note that for any positive integer g , we have

$$\sum_{a=0}^{g-1} Q_{g, a} = I_N. \quad (56)$$

The projector $Q_{g, a}$ projects onto the span of states $|m_{\mathbb{T}}\rangle$ where $\text{mod}(m + j_{\mathbb{T}}, g) = a$ for any SYT \mathbb{T} .

² Note that throughout we have used the simplified notation for the total angular momentum of all spins as \hat{J}^z instead of $\hat{J}_{[N]}^z$.

Given a set of projectors $P = \{P_1, \dots, P_k\}$ such that $\sum_j P_j = I_N$ and an N -qubit density matrix to measure, let us denote the output state ρ' of a projective measurement on a density matrix ρ with respect to P using the notation

$$\rho' = \text{ProjMeas}(\rho, P). \quad (57)$$

An important algorithm that we use repeatedly is Algorithm 2 (**ModuloMeas**). Given fixed g , Algorithm 2 performs a projective measurement (the subroutine **ProjMeas**) on quantum state ρ according to the set of projectors $\{Q_{g,0}, \dots, Q_{g,g-1}\}$.

Algorithm 2 Modulo measurement

```

1: procedure MODULOMEAS( $\rho, g$ )
  ▷ Inputs:  $\rho$  is an  $N$ -qubit density matrix, and  $g$  a positive integer.
  ▷ Output:  $\rho'$ , an  $N$ -qubit state.
2:   Set  $\rho_1 = \text{ProjMeas}(\rho, \{Q_{g,a} : a = 0, \dots, g-1\})$ .
3:   if  $\rho_1 = Q_{g,a}\rho Q_{g,a}/\text{Tr}(Q_{g,a}\rho)$  then
4:     Set  $\rho' = \rho_1$ .
5:     Set  $a' = a$ .
6:   return  $(\rho', a')$ .
7: end if
8: end procedure

```

4. Further projections and recovery

When a channel's Kraus operators K_1, \dots, K_a are correctible, from Lemma 8, the operators $\Pi^\top K_1, \dots, \Pi^\top K_a$ must also be correctible for every SYT \top . From the Knill-Laflamme quantum error criterion [31], we know that \mathcal{P}^\top partitions into orthogonal correctible spaces and a single uncorrectible space. To describe the correctible subspace within \mathcal{P}^\top , we use the vectors $\Pi^\top K_i |j_L\rangle$, where $|j_L\rangle$ are logical codewords of the permutation-invariant code of dimension M and $j = 0, \dots, M-1$.

Next, for every $j = 0, \dots, M-1$, the Gram-Schmidt process [41, Section 0.6.4] takes as input the sequence of vectors

$$(\Pi^\top K_1 |j_L\rangle, \dots, \Pi^\top K_a |j_L\rangle), \quad (58)$$

and outputs the sequence of orthonormal vectors

$$(|\mathbf{v}_{1,j}^\top\rangle, \dots, |\mathbf{v}_{r_\top,j}^\top\rangle) \quad (59)$$

that span the same space \mathcal{A}_j^\top of dimension r_\top . From the Knill-Laflamme quantum error correction criterion, the spaces \mathcal{A}_j^\top and \mathcal{A}_k^\top are pairwise orthogonal for distinct j and k and both have dimension r_\top [31]. Hence

$$r_\top \leq |\mathcal{P}^\top|/M, \quad (60)$$

and r_\top is independent of the number of correctible Kraus operators A_1, \dots, A_a . Since $|\mathcal{P}^\top| = 2j_\top + 1$, the number of these correctible subspaces is at most $(2j_\top + 1)/M$, where M is the number of logical qubits the permutation-invariant code has.

From the sequence of vectors in (59), for $k = 1, \dots, r_\top$, we also define the spaces \mathcal{C}_k^\top spanned by the vectors $|\mathbf{v}_{k,0}^\top\rangle, \dots, |\mathbf{v}_{k,M-1}^\top\rangle$, and with corresponding projectors

$$\Pi_k^\top = \sum_{j=0}^{M-1} |\mathbf{v}_{k,j}^\top\rangle\langle\mathbf{v}_{k,j}^\top|. \quad (61)$$

Here, we interpret k as a label on the permutation-invariant code's correctible subspaces within \mathcal{P}^\top . From the Knill-Laflamme quantum error correction criterion, these spaces \mathcal{C}_k^\top and $\mathcal{C}_{k'}^\top$ are pairwise orthogonal for distinct k and k' .

To perform QEC after obtaining the syndrome \top , it suffices to execute the following steps that arise from the Knill-Laflamme QEC procedure [31].

1. First, we perform a projective measurement according to the projectors Π_k^\top for $k = 1, \dots, r_\top$.
2. If the obtained state is not in \mathcal{C}_k^\top for any k , then we have an uncorrectible error. Otherwise, the obtained state is in \mathcal{C}_k^\top for some $k = 1, \dots, r_\top$.
3. If the error is correctable, we perform a unitary operator that maps $|\mathbf{v}_{k,j}^\top\rangle$ to $|j_L\rangle$ for every $j = 0, \dots, M-1$. This completes the QEC procedure.

In contrast to this abstract procedure, we can also describe a more explicit implementation of an equivalent QEC procedure after obtaining the syndrome \top . For a permutation invariant code with logical codewords

$$|j_L\rangle = \sum_k a_k |D_k^N\rangle \quad (62)$$

for $j = 0, \dots, M-1$, we define corresponding \top -codes to have (subnormalized) logical codewords

$$|\text{code}_{j,\top}\rangle = \sum_k a_k |(k/2 - j_\top)_\top\rangle. \quad (63)$$

When the support of the permutation invariant code in the Dicke basis is appropriately restricted and when the SYT syndrome \top is correctible, the \top -code's logical codewords can be normalized. For simplicity, we continue the analysis assuming that $|\text{code}_{j,\top}\rangle$ are normalized vectors for correctible SYT syndromes \top .

We can obtain a \top -code using the following operations.

1. Apply a unitary W_\top , where for every $k = 1, \dots, r_\top$ and $j = 0, \dots, M-1$, we have

$$W_\top : |\mathbf{v}_{k,j}^\top\rangle \rightarrow |jr_\top + (k-1) - j_\top\rangle. \quad (64)$$

2. Next, we use Algorithm 2, **ModuloMeas**, to measure in the modulo magnetic quantum number basis. In particular, when the output state of the previous step is ρ_1 , and the output state of this step is ρ_2 , we set $(\rho_2, a) = \text{ModuloMeas}(\rho_1, r_\top)$. Here, $a = 0, \dots, r_\top - 1$ is what we call the syndrome outcome of the modulo measurement.

- Next, set $k = a + 1$. Using this value of k , we apply a unitary $V_{T,k}$ on ρ' , where

$$V_{T,k} : |j r_T + (k - 1) - j_T\rangle_T \rightarrow |\text{code}_{j,T}\rangle, \quad (65)$$

for all $j = 0, \dots, M - 1$. The state is now $\rho_3 = V_{T,k} \rho_2 V_{T,k}^\dagger$, which is in a T-code.

The final step is to map the T-code back to the original permutation-invariant code, using for instance, the quantum Schur transform.

- First we perform an inverse of the quantum Schur transform to map the states $|m_T\rangle$ in \mathcal{P}^T to computational basis states. The quantum Schur transform U_{schur} [37, 40, 42–45] is a unitary transformation which maps computational basis states to states of the form $|m_T\rangle$. Notably, to perform U_{schur} on N qubits to an accuracy of ϵ , it suffices to use $O(N^4 \log(N/\epsilon))$ gates [42] from the Boykin gateset [46]. Structurally, U_{schur} comprises of a cascading sequence of Clebsch-Gordan transformations [37]. Hence, we can perform U_{schur}^{-1} with a cascading sequence of inverse Clebsch-Gordan transformations using $O(N^4 \log(N/\epsilon))$ gates.
- Second, we want to perform a permutation amongst the computational basis states. Suppose that the syndrome SYT T with total angular momentum of j_T has been obtained. The objective here is to apply a unitary transformation Perm_T such that

$$\text{Perm}_T U_{\text{schur}}^{-1} |m_T\rangle = U_{\text{schur}}^{-1} |D_{m+j_T}^N\rangle, \quad (66)$$

and where $U_{\text{schur}}^{-1} |m_T\rangle$ and $U_{\text{schur}}^{-1} |D_{m+j_T}^N\rangle$ are both computational basis states. Since Perm_T permutes amongst computational basis states, it is a classical gate, and can be achieved using Toffolis, CNOTs and bit-flip gates.

- Third, we apply the quantum Schur transform U_{schur} , which takes the state to a subspace of the symmetric subspace.

When the logical codewords of the T-codes are normalized, this procedure recovers the original permutation-invariant codes. Algorithm 2 summarizes this general QEC procedure on permutation-invariant codes.

Algorithm 3 QEC for general errors

```

1: procedure QECGENERAL( $\rho, K_1, \dots, K_a$ )
    $\triangleright K_1, \dots, K_a$  are correctible errors.
2:   Execute SyndromeSYT on  $\rho$ .
3:   Let  $T$  be the obtained the SYT syndrome
4:   Let  $\rho_T$  be the obtained state.
5:   Set  $\rho_1 = W_T \rho W_T$ .
6:   Set  $(\rho_2, a) = \text{ModuloMeas}(\rho_1, r_T)$ .
7:   Set  $k = a + 1$ 
8:   Set  $\rho_3 = V_{T,k} \rho_2 V_{T,k}^\dagger$ .
9:   Map  $\rho_3$ , a T-code, to a permutation-invariant code. Set this state as  $\rho_4$ .
10:  return  $\rho_4$ .
11: end procedure

```

B. Teleportation based QEC

By consuming additional ancilla states, we can design a quantum error correction procedure for general errors that does not rely on the quantum Schur transform. The main idea is that we can bring our quantum state in the space \mathcal{P}^T to the symmetric subspace by state teleportation that consumes a single logical ancilla state [47, (7)]. For this idea to work, we restrict ourselves to shifted gnu codes with odd g and the following properties.

- Define the unitary map $X_{\text{schur}} : |m_T\rangle \rightarrow | -m_T\rangle$ for every $m = -j_T, \dots, j_T$ and SYT T . We need that X_{schur} implements the logical X gate on the T-codes for every correctible SYT T .
- Define the unitary $C_A X_B$ on two registers A and B such that for any SYTs S and T, the unitary $C_A X_B$ applies the map

$$|l_S\rangle |m_T\rangle \rightarrow |l_S\rangle X_{\text{schur}}^l |m_T\rangle. \quad (67)$$

Here, registers A and B can potentially have different numbers of qubits.

Next, we introduce a teleportation subroutine that takes an ancilla initialized as a shifted gnu code in register A and the state ρ that we want to teleport in register B. We assume that ρ is a T-code that corresponds to some shifted gnu code. The teleportation procedure entangles the registers and measures register B to teleport the register in B to the register in A. We furthermore require that both shifted gnu codes encode a single logical qubit, and have the same gap g that is also odd. We will also need to be able to implement Algorithm 2 (**ModuloMeas**).

Procedure Teleportation(ρ):

- Prepare $|+_L\rangle$ in a shifted gnu code in register A.
- Let ρ , a T-code, be in register B.
- Implement $C_A X_B$ on A and B respectively. This effectively implements the logical CNOT with control on register A and target on register B.
- On the state ρ_B in register B, we implement Algorithm 2 (**ModuloMeas**). Namely, we set $(\rho'_B, a) = \text{ModuloMeas}(\rho_B, 2g)$. The output state is $\rho'_A \otimes \rho'_B$. (This allows us to deduce the logical Z measurement outcome on the T-code in register B.)
- Suppose that ρ corresponds to a gnu code with shift s . Then set $\sigma = \text{mod}(a + j_T - s, 2g)$.
- If $\sigma = 0, \dots, (g-1)/2$ or $\sigma = 2g - (g-1)/2, \dots, 2g - 1$, then we declare that we obtained a logical 0 state on register B. Then we do nothing to register A.
- For all other values of σ , we declare that we obtained a logical 1 state on register B. Then we apply X_{schur} on register A, implementing the logical X correction on register A.

This teleportation subroutine is agnostic of which SYT syndrome the state ρ corresponds to, and how many qubits are in registers A and B. We can use the teleportation subroutine to teleport T-codes to permutation-invariant quantum codes. Section VI explains the physical implementation of steps in this teleportation subroutine.

With this teleportation subroutine, we can also implement QEC for general errors without employing quantum Schur transforms. Namely, instead of using quantum Schur transforms to bring T-codes to the symmetric subspace, we can directly teleport T-codes to the original permutation-invariant code in Step 9 of Algorithm 3.

C. Correcting deletion errors

When deletion errors occur on permutation-invariant quantum codes, the resultant state remains in the symmetric subspace, but on fewer qubits. If we accept having a quantum error corrected state with fewer qubits, we need not measure total angular momenta like we did in the previous section. Rather, we can use a much simpler QEC scheme.

Now suppose that t deletion errors occur on a permutation-invariant code that corrects at least t errors. Then, an initially N -qubit pure state $|\psi\rangle = \alpha|0_L\rangle + \beta|1_L\rangle$ in the codespace becomes an $(N - t)$ -qubit mixed state over the subnormalized states $|\psi\rangle_a = \alpha|0_L\rangle_a + \beta|1_L\rangle_a$ where $|0_L\rangle_a$ and $|1_L\rangle_a$ have the same normalizations and are defined by (23). Here, $a = 0, \dots, t$ is the syndrome associated with the deletion error that quantifies the amount of shift in the Dicke weights. When the permutation-invariant code is furthermore supported on Dicke states with distinct weights at least g apart with $g \geq t + 1$, the states $|\psi\rangle_a$ and $|\psi\rangle_{a'}$ are orthogonal for distinct a and a' .

Previously, Ref. [5] discusses how to perform QEC while also completely decoding the code to an unprotected state. Here, we will discuss how to perform QEC on the codespace without completely decoding the code, and thereby obtain a simpler QEC algorithm for deletion errors than that of [5].

1. To obtain a particular subnormalized state $|\psi\rangle_a$ along with the syndrome a , we can set $\rho_a = |\psi\rangle_a \langle \psi|_a / \langle \psi|_a | \psi\rangle_a$ and obtain $(\rho_a, a) = \text{ModuloMeas}(\rho, g)$.
2. We perform a non-unique unitary V_a that maps the normalized versions of the states $|0_L\rangle_a$ and $|1_L\rangle_a$ to $|0_L\rangle$ and $|1_L\rangle$ respectively. For us, it suffices to implement V_a using $5N$ geometric phase gates is described in Sec. VIC.

If the original permutation-invariant code is a shifted gnu code with shift $s \geq t$, the resultant permutation-invariant code is a shifted gnu code on t fewer qubits, and with a shift $s - a$. Algorithm 4 formalizes the

procedure for correcting deletions errors.

Algorithm 4 QEC for at most t deletion errors

- 1: **procedure** QEC_{DELETION}(ρ, t, g, n, s)
 - ▷ The code must be a shifted gnu code on N qubits with gap g and $g, n \geq t + 1$, and shift $s \geq t$.
 - 2: Set $(\rho_1, \sigma) = \text{ModuloMeas}(\rho, g)$.
 - 3: Set $a = \text{mod}(s - \sigma, g)$.
 - 4: Set $\rho' = V_a \rho_1 V_a^\dagger$.
 - 5: **return** ρ' , a shifted gnu code with the same g and n parameters as the original code, but on $N - t$ qubits and with shift $s - a$.
 - 6: **end procedure**
-

If we want to recover a permutation-invariant code with N qubits, we can apply the teleportation subroutine **Teleportation** after implementing Algorithm 4. For this to work, the permutation invariant code needs to satisfy the additional requirements of Algorithm 4.

V. INTEGRATING QEC INTO SENSING

In our scheme, we prepare a probe state $|+_{g,n,u,s}\rangle$ in a shifted gnu code with $N = gnu + s$ qubits. We consider two types of scenario with QEC. We discuss the first scenario in Section VA, where errors occur only during state-preparation, and the signal accumulation stage is error-free. We discuss the second scenario in Section VB, where deletion errors occur during the signal accumulation stage.

A. QEC before signal accumulation

Here, we assume that the only error-prone stages of the quantum sensor is during state preparation, before the signal arrives. This scenario is reasonable when state preparation takes a much longer time than the signal accumulation and measurement stage. If the preparation of the probe state takes too long, the probe state is prone to pick up errors, and therefore have poor precision in estimating the field unless we perform QEC. If the QEC procedure can be done quickly and with minimal errors, then the full power of the noiseless probe state can be recovered.

Here, we consider employing shifted gnu codes with appropriate values of g, n as probe states. Because such shifted gnu codes have a code distance of $\min\{g, n\}$, these codes can correct up to *any* t errors, provided that $t \leq (\min\{g, n\} - 1)/2$. One can implement the QEC procedure for instance using Algorithm 3. If the errors are deletion errors, we can employ the simpler Algorithm 4 and correct up to t deletion errors provided that $t \leq (\min\{g, n\} - 1)$.

Now, from Lemma 2, the QFI of using gnu codes is $g^2 n$. Hence if $t \leq (\min\{g, n\} - 1)/2$, we can perform QEC to recover this QFI of $g^2 n$. Hence, when $g = \Theta(N^\alpha)$ and $n = \Theta(N^{1-\alpha})$ where $\alpha \geq 1/2$, the maximum possible QFI for $t = \Omega(N^{1-\alpha})$ is given by the following theorem.

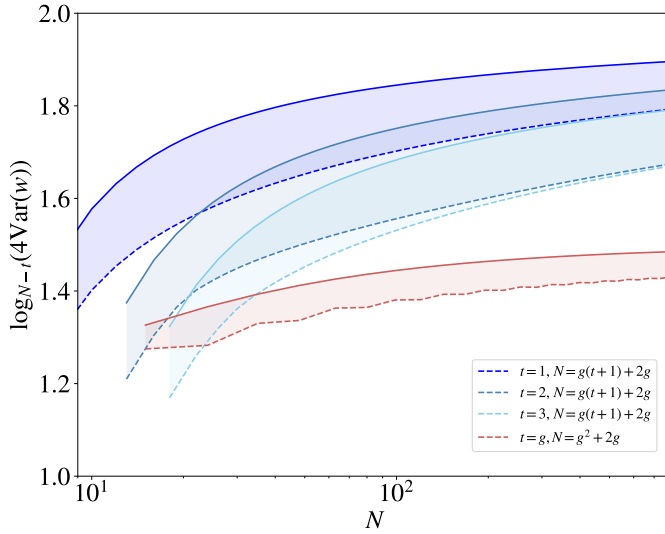


FIG. 4: Performance of shifted-gnu states when t deletions occur, with and without QEC. The solid and dashed lines correspond to the performance of shifted-gnu states with and without QEC respectively. Here t is either (1) constant, or (2) scales as the square root of the number of qubits N . The vertical axis quantifies the amount of QFI in log-scale. The values of the plots depicted are above 1 on the vertical axis, indicating a quantum advantage.

Theorem 9. *Let $\alpha \geq 1/2$, $g = \Theta(N^\alpha)$ and $n = \Theta(N^{1-\alpha})$. Then any $o(N^{1-\alpha})$ errors can be corrected on a corresponding shifted gnu code, and the corresponding QFI thereafter on θ for noiseless signal accumulation of U_θ on $|+_{g,n,u,s}\rangle$ is $g^2n = \Theta(N^{1+\alpha})$.*

Proof. For general errors, since $\alpha \geq 1/2$, the number of correctable errors is at most $(\min\{g, n\} - 1)/2 = \Theta(N^{1-\alpha})$. Hence any $o(N^{1-\alpha})$ errors are also correctable. From Lemma 2, we know that the QFI of $|+_{g,n,u,s}\rangle$ is g^2n . Since $\alpha \geq 1/2$, we have $g^2n = \Theta(N^{1+\alpha})$. \square

Consider Theorem 9 when $\alpha = 1/2$. Then, any $o(\sqrt{N})$ errors can be corrected and the QFI is $\Theta(N^{3/2})$.

B. During signal accumulation

We assume that the signal accumulates and deletion errors occur at a uniform rate and simultaneously. Now, consider non-negative numbers c and η . Let the signal strength per unit of time be $\theta = \Theta(N^{-c})$, so that in time τ , the unitary $U_{\theta\tau} = \exp(-i\theta\tau\hat{J}^z)$ acts on the probe state. In this section, we let $\Delta = \theta\tau$. Note that $c = 0$ corresponds to having very little prior information about the true value of θ . If we have used N classical sensors to estimate θ , then we can already know θ with mean square error (MSE) $\Theta(\sqrt{N})$, and take $c = 1/2$.

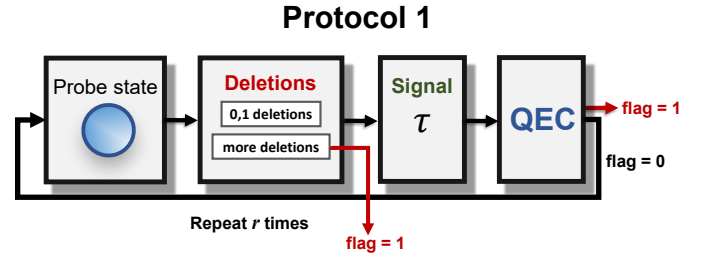


FIG. 5: Illustration of Protocol 1, which performs r rounds of QEC. Protocol 1 aborts if $\text{flag} = 1$ at any point. The QEC algorithm invoked is `QECsense` (see Algo. 5). Here $\tau = r^{-q}$ for fixed $q > 1$. After the r rounds of signal accumulation and QEC, measurements are performed in the plus-minus basis of the appropriated shifted gnu code. The appendix describes Protocol 1 algorithmically. We assume perfect and instantaneous QEC. The total duration of Protocol 1 is $r\tau$. Throughout the protocol, we ensure that the shift of the shifted gnu probe state satisfies $s = N/2 - gn/2 + o(g)$.

Let n_{del} be the expected number of deletions per unit time per qubit, and let $\eta = \log_N n_{\text{del}}N$. When deletion errors occur at a sublinear rate, we have $\eta < 1$. If deletion errors occur at a linear rate, we have $\eta = 1$.

Given fixed values of c and η , we introduce a QEC-enhanced protocol, Protocol 1 (see Fig. 5), for quantum sensing. Protocol 1 describes how one may perform QEC while deletions occur and the signal accumulates simultaneously. We invoke the algorithm `QECsense` to perform each QEC step in Protocol 1. Protocol 1 has r QEC steps, and the signal accumulates for time τ in between QEC steps. Throughout the protocol, QEC ensures that the shift of the shifted gnu probe state satisfies $s = N/2 - gn/2 + o(g)$. We set $q = -\log_r \tau$ so that $\tau = r^{-q}$. We call this duration of τ a *timestep*. We focus on asymptotic analysis, where $r = \Theta(N^\gamma)$ for some positive γ .

For each timestep, an average of $\Theta(N^{\eta-\gamma q})$ qubits is deleted from in $\Theta(N)$ qubits. When η and γ are constant, and whenever $q > \eta/\gamma$, this average number of deletions is $o(1)$ which approaches zero. When both r and q are sufficiently large, with probability approaching 1, we lose either no qubit or one qubit at each timestep, and the number of deletions follows a Poisson distribution. Consequently, it is natural to use permutation-invariant codes that correct at least a single deletion error in each timestep. We consider shifted gnu codes with $n = 3$ and $g = \Theta(N^\alpha)$ for $\alpha > 0$.

Ideally, Protocol 1 performs each QEC step perfectly and in negligible time. Protocol 1 fails whenever `QECsense` returns $\text{flag} = 1$ in any timestep, which occurs whenever at least 2 deletions occur in any timestep, and whenever `QECsense` returns $\text{flag} = 1$ in any timestep. Hence, Protocol 1 is a probabilistic quantum sensing algorithm with a heralded successful outcome.

Our QEC procedure `QECsense` (Algorithm 5) in Pro-

tolcol 1 specialized for quantum field sensing implements QEC that does not attempt to restore the qubits that have been deleted. Hence, during the operation of Protocol 1, the number of qubits invariably becomes fewer and fewer. Moreover `QECsense` does not attempt to correct the maximum number of errors. Rather, it only treats \hat{J}^z as an error, and corrects it away. Only the second and higher-order terms in the signal unitary are left after QEC. Since \hat{J}^z generates the signal, each operation of `QECsense` must degrade the signal. In fact, if r is too large, we would perform too much QEC and completely destroy the signal. Nonetheless, when r is finite, and τ is also appropriately chosen, we will show that by repeating Protocol 1 an appropriate number of times (this is Protocol 3, see Fig. 8) while updating our knowledge of the signal estimate in between rounds of Protocol 1, we can have a quantum advantage in field sensing, even when there is a linear rate of deletion errors.

Algorithm 5 Specialized QEC procedure for sensing with deletions

```

1: procedure QECsense( $\rho, g, n, u, s$ )
  ▷  $\rho$ : input state.
  ▷  $g, n, u, s$ : parameters for a shifted gnu code.
2:   Set  $(\rho_1, a) = \text{ModuloMeas}(\rho, g)$ 
3:   Set  $\sigma = \text{mod}(s - a, g)$ .
4:   Set  $s' = s - \sigma$ .
5:   For  $j = 0, 1$ , set  $|j_L\rangle = |j_{g,n,u,s'}\rangle$ .
6:   Define  $\Pi = |0_L\rangle\langle 0_L| + |1_L\rangle\langle 1_L|$ .
7:   For  $j = 0, 1$ , define  $|Q_j\rangle = \hat{J}^z|j_L\rangle - \langle j_L|\hat{J}^z|j_L\rangle|j_L\rangle$ .
8:   Set  $|q_j\rangle = |Q_{j,\sigma}\rangle/\sqrt{\langle Q_j|Q_j\rangle}$ .
9:   Define  $\Pi_1 = |q_0\rangle\langle q_0| + |q_1\rangle\langle q_1|$ .
10:  Set  $\rho_2 = \text{ProjMeas}(\rho_1, \{\Pi, \Pi_1, I - \Pi - \Pi_1\})$ .
11:  switch  $\rho_2$  do
12:    case  $\rho_2 = \Pi\rho_1\Pi/\text{Tr}(\Pi\rho_1\Pi)$ 
13:      Set syn = 0.
14:      Set flag = 0.
15:    case  $\rho_2 = \Pi_1\rho_1\Pi_1/\text{Tr}(\Pi_1\rho_1\Pi_1)$ 
16:      Apply unitary mapping  $|q_j\rangle$  to  $|j_L\rangle$  for  $j = 0, 1$ .
17:      Set syn = 1.
18:      Set flag = 0.
19:    case Otherwise
20:      Set syn = 2.
21:      Set flag = 1.
22:  return  $(\rho_2, s', \text{syn}, \text{flag})$ 
23: end procedure

```

Quantifying Protocol 1's performance requires much analysis. We begin by introducing the function

$$\begin{aligned} \phi_{n,j}(\Delta) = & e^{-i\Delta(N/2-s)} e^{ign\Delta/2} \\ & \times \left(\cos^n(g\Delta/2) + (-1)^j (-i)^n \sin^n(g\Delta/2) \right), \end{aligned} \quad (68)$$

so that we have Lemma 10 which we prove in Appendix F that calculates the probability amplitude of projecting $U_\Delta|j_L\rangle$ onto $|j_L\rangle$.

Lemma 10. *Let $|0_L\rangle$ and $|1_L\rangle$ be logical codewords of a shifted gnu code with parameters g, n, u and s . Then $\langle j_L|U_\Delta|j_L\rangle = \phi_{n,j}(\Delta)$ for $j = 0, 1$.*

Given any shifted gnu logical codeword $|0_L\rangle$ and $|1_L\rangle$,

we can define the vectors

$$|Q_0\rangle = \hat{J}^z|0_L\rangle - \langle 0_L|\hat{J}^z|0_L\rangle|0_L\rangle, \quad (69)$$

$$|Q_1\rangle = \hat{J}^z|1_L\rangle - \langle 1_L|\hat{J}^z|1_L\rangle|1_L\rangle, \quad (70)$$

and define $|q_j\rangle = |Q_j\rangle/\sqrt{\langle Q_j|Q_j\rangle}$. The vectors $|Q_j\rangle$ are orthogonal to $|j_L\rangle$ by construction. Note that

$$\langle Q_j|Q_j\rangle = \langle j_L|(\hat{J}^z)^2|j_L\rangle - \langle j_L|\hat{J}^z|j_L\rangle^2. \quad (71)$$

When $n \geq 3$ for a shifted gnu code, we have $\langle Q_0|Q_0\rangle = \langle Q_1|Q_1\rangle$, and in this case, it follows that

$$\langle Q_j|Q_j\rangle = \langle +_L|(\hat{J}^z)^2|+_L\rangle - \langle +_L|\hat{J}^z|+_L\rangle^2. \quad (72)$$

The quantity in (72) is the variance of a state with respect to the operator \hat{J}^z . Hence, from Lemma 2, we can see that

$$\langle Q_j|Q_j\rangle = g^2n/4. \quad (73)$$

Next Lemma 11 evaluates the probability of certain projections.

Lemma 11. *Let n be odd and ≥ 3 . Then*

$$\begin{aligned} |\langle q_j|U_\Delta|j_L\rangle|^2 = & n \left| \phi_{n,j}(\Delta) - e^{ig\Delta} \phi_{n-1,j\oplus 1}(\Delta) \right|^2 \\ = & \frac{n}{4} \sin^2 2x \left(\sin^{2n-4} x + \cos^{2n-4} x \right) \end{aligned} \quad (74)$$

$$= \frac{n(g\Delta)^2}{4} + O((g\Delta)^4), \quad (75)$$

where $x = g\Delta/2$.

Now Lemma 12 calculates the probability that each run of `QECsense` returns a failure flag, with `flag` = 1.

Lemma 12. *Let n be odd, let $\rho = |\psi\rangle\langle\psi|$ where $|\psi\rangle = a|0_L\rangle + b|1_L\rangle$ is a shifted gnu codestate. Let the input state to `QECsense` be $U_\Delta\rho U_\Delta^\dagger$. Let Π and Π_1 be as defined in `QECsense`. Let $x = g\Delta/2$. Then*

$$\|\Pi|\psi\rangle\|^2 = \cos^{2n} x + \sin^{2n} x, \quad (76)$$

$$\|\Pi_1|\psi\rangle\|^2 = \frac{n}{4} \sin^2 2x \left(\sin^{2n-4} x + \cos^{2n-4} x \right). \quad (77)$$

Also the probability that `flag` = 1 is p_{flag} where

$$p_{\text{flag}} = \sum_{k=2}^{n-2} \binom{n}{k} \cos^{2k} x \sin^{2n-2k} x. \quad (78)$$

From this, we can see that $p_{\text{flag}} = O(x^{2n-2})$.

Proof of Lemma 12. We consider input states to `QECsense` of the form $|\phi\rangle = U_\Delta|\psi\rangle$ where $|\psi\rangle = a|0_L\rangle + b|1_L\rangle$. Hence

$$p_{\text{flag}} = 1 - \|\Pi|\psi\rangle\|^2 - \|\Pi_1|\psi\rangle\|^2. \quad (79)$$

Let $x = g\Delta/2$. From Lemma 10, we can see that

$$\begin{aligned} & \|\Pi|\psi\rangle\|^2 \\ &= |a|0_L\rangle\langle 0_L|U_\Delta|0_L\rangle + b|1_L\rangle\langle 1_L|U_\Delta|1_L\rangle\|^2 \\ &= |a|^2|\phi_{n,0}(\Delta)|^2 + |b|^2|\phi_{n,1}(\Delta)|^2 \\ &= (|a|^2 + |b|^2)(\cos^{2n}x + \sin^{2n}x) \\ &= \cos^{2n}x + \sin^{2n}x. \end{aligned} \quad (80)$$

Similarly, using Lemma 11, we can see that

$$\begin{aligned} & \|\Pi_1|\psi\rangle\|^2 \\ &= |a|q_0\rangle\langle q_0|U_\Delta|0_L\rangle + b|q_1\rangle\langle q_1|U_\Delta|1_L\rangle\|^2 \\ &= |a|^2|\langle q_0|U_\Delta|0_L\rangle|^2 + |b|^2|\langle q_1|U_\Delta|1_L\rangle|^2 \\ &= (|a|^2 + |b|^2)\frac{n}{4}\sin^2 2x \left(\sin^{2n-4}x + \cos^{2n-4}x\right) \\ &= \frac{n}{4}\sin^2 2x \left(\sin^{2n-4}x + \cos^{2n-4}x\right). \end{aligned} \quad (81)$$

Now note that

$$\begin{aligned} & \cos^{2n}x + \sin^{2n}x + \frac{n}{4}\sin^2 2x \left(\sin^{2n-4}x + \cos^{2n-4}x\right) \\ &= \cos^{2n}x + \sin^{2n}x + n \left(\sin^{2n-2}x \cos^2x + \cos^{2n-2}x \sin^2x\right) \\ &= \sum_{k=0,1,n-1,n} \binom{n}{k} \cos^{2k}x \sin^{2n-2k}x \\ &= (\cos^2x + \sin^2x)^n - \sum_{k=2}^{n-2} \binom{n}{k} \cos^{2k}x \sin^{2n-2k}x \\ &= 1 - \sum_{k=2}^{n-2} \binom{n}{k} \cos^{2k}x \sin^{2n-2k}x. \end{aligned} \quad (82)$$

Hence the result follows. \square

From Lemma 13 we can determine the effective evolution on the codespace after the application of QECsense on $U_\Delta|\psi\rangle$ where $|\psi\rangle$ is a shifted gnu state with no deletions.

Lemma 13. *Let $|0_L\rangle$ and $|1_L\rangle$ be the logical codewords of a shifted gnu code, and let n be odd and ≥ 3 . Let Δ be a real number. Then*

$$\frac{\langle 1_L|U_\Delta|1_L\rangle}{\langle 0_L|U_\Delta|0_L\rangle} = e^{i\zeta_0}, \quad \frac{\langle q_1|U_\Delta|1_L\rangle}{\langle q_0|U_\Delta|0_L\rangle} = e^{i\zeta_1}, \quad (83)$$

where

$$\zeta_j = 2 \arctan \left((-1)^j i^{n-1} \tan^{n-2j}(g\Delta/2) \right). \quad (84)$$

From Lemma 13, we know that if QECsense has input state $|\psi\rangle = a|0_L\rangle + b|1_L\rangle$ and outputs $\text{flag} = 0$, the state output of QECsense is either $a|0_L\rangle + be^{i\zeta_0}|1_L\rangle$, or $a|0_L\rangle + be^{i\zeta_1}|1_L\rangle$, depending on whether QECsense initially projected $|\psi\rangle$ into the space supported by Π or Π_1 respectively. When $g\Delta/2$ is close to zero, we have the approximation

$$\zeta_j \approx 2(-1)^j i^{n-1} (g\Delta/2)^{n-2j}. \quad (85)$$

Since the probability of QECsense projecting onto the supports of Π and Π_1 are approximately 1 and $n(g\Delta/2)^2$ respectively, the expected accumulated phase is approximately

$$2(1-n)i^{n-1}(g\Delta/2)^n. \quad (86)$$

In the noiseless scenario, the accumulated phase would a magnitude of $\Delta = \tau\theta$. In contrast, with a successful run of QECsense, the expected accumulated phase has a magnitude of $(n-1)(g\tau\theta/2)^n$. If $g = \Delta^{-1+1/n}$, the expected accumulated phase in these two scenarios would be comparable. Otherwise, if $g \ll \Delta^{-1+1/n}$, then the accumulated phase for QECsense would be diminished as n becomes large. Hence, we choose n to be the smallest possible that allows the correction of a single error, which corresponds to $n = 3$.

The proof of Lemma 13 uses trigonometric identities.

Proof of Lemma 13. From Lemma 10 and (68), we can see that

$$\frac{\langle 1_L|U_\Delta|1_L\rangle}{\langle 0_L|U_\Delta|0_L\rangle} = \frac{\cos^n(g\Delta/2) - (-i)^n \sin^n(g\Delta/2)}{\cos^n(g\Delta/2) + (-i)^n \sin^n(g\Delta/2)}. \quad (87)$$

Since n is odd, (87) simplifies to

$$\frac{\langle 1_L|U_\Delta|1_L\rangle}{\langle 0_L|U_\Delta|0_L\rangle} = \frac{\cos^n(g\Delta/2) + i^n \sin^n(g\Delta/2)}{\cos^n(g\Delta/2) - i^n \sin^n(g\Delta/2)}. \quad (88)$$

Since n is odd, the absolute values of both the numerator and denominator in (88) are identical. Hence the quantity in (88) can be written as e^{ia} for some real number a . In fact, we can write the numerator and denominator in the form Re^{ib} and Re^{-ib} respectively for some positive number R , so that $a = 2b$. We proceed to determine the value of b using trigonometrical identities. If $\text{mod}(n, 4) = 1$, then

$$\frac{\langle 1_L|U_\Delta|1_L\rangle}{\langle 0_L|U_\Delta|0_L\rangle} = \frac{\cos^n(g\Delta/2) + i \sin^n(g\Delta/2)}{\cos^n(g\Delta/2) - i \sin^n(g\Delta/2)}. \quad (89)$$

and $\tan b = \tan^n(g\Delta/2)$. If $\text{mod}(n, 4) = 1$, then

$$\frac{\langle 1_L|U_\Delta|1_L\rangle}{\langle 0_L|U_\Delta|0_L\rangle} = \frac{\cos^n(g\Delta/2) + i \sin^n(g\Delta/2)}{\cos^n(g\Delta/2) - i \sin^n(g\Delta/2)}. \quad (90)$$

and $-\tan b = \tan^n(g\Delta/2)$. Hence we conclude that $\tan b = i^n \tan^n(g\Delta/2)$, and hence $b = \arctan(i^{n-1} \tan^n(g\Delta/2))$. By setting $\zeta_0 = 2b$ we get the first part of the lemma.

Next, note that

$$\frac{\langle q_1|U_\Delta|1_L\rangle}{\langle q_0|U_\Delta|0_L\rangle} = \frac{\langle Q_1|U_\Delta|1_L\rangle}{\langle Q_0|U_\Delta|0_L\rangle}. \quad (91)$$

For simplicity, let $x = g\Delta/2$. Using (F14) in Lemma (23) we get

$$\begin{aligned} \frac{\langle q_1|U_\Delta|1_L\rangle}{\langle q_0|U_\Delta|0_L\rangle} &= \frac{-i \cos^{n-1}x \sin x - i^{n-1} \sin^{n-1}x \cos x}{-i \cos^{n-1}x \sin x + i^{n-1} \sin^{n-1}x \cos x} \\ &= \frac{\cos^{n-2}x - i^n \sin^{n-2}x}{\cos^{n-2}x + i^n \sin^{n-2}x}. \end{aligned} \quad (92)$$

Hence $\frac{\langle q_1 | U_\Delta | 1_L \rangle}{\langle q_0 | U_\Delta | 0_L \rangle}$ is of the form $\frac{e^{-ic}}{e^{+ic}}$ where $i^{n-1} \tan c = \tan^{n-2} x$, and setting $\zeta_1 = -c$, we get the second result of the lemma. \square

The situation when we have a single deletion error is more complicated. A single deletion shifts the Dicke weights randomly either by 0 or 1. From (23), deleting a qubit from an initial N -qubit logical state $|\psi\rangle = a|0_L\rangle + be^{i\varphi}|1_L\rangle$ gives a probabilistic mixture of the (unnormalized) $(N-1)$ -qubit states

$$|\psi'_\sigma\rangle = a|0'_\sigma\rangle + be^{i\varphi}|1'_\sigma\rangle \quad (93)$$

where

$$|0'_\sigma\rangle = 2^{(-n+1)/2} \sum_{k \text{ even}} \sqrt{\binom{n}{k}} \sqrt{\frac{\binom{N-1}{gk+s-\sigma}}{\binom{N}{gk+s}}} |D_{gk+s-\sigma}\rangle \quad (94)$$

$$|1'_\sigma\rangle = 2^{(-n+1)/2} \sum_{k \text{ odd}} \sqrt{\binom{n}{k}} \sqrt{\frac{\binom{N-1}{gk+s-\sigma}}{\binom{N}{gk+s}}} |D_{gk+s-\sigma}\rangle. \quad (95)$$

Note that

$$\frac{\binom{N-1}{gk+s-\sigma}}{\binom{N}{gk+s}} = \begin{cases} 1 - (gk+s)/N, & \sigma = 0 \\ (gk+s)/N, & \sigma = 1 \end{cases} \quad (96)$$

$$= \begin{cases} 1/2 + (\lfloor gn/2 \rfloor - gk)/N, & \sigma = 0 \\ 1/2 - (\lfloor gn/2 \rfloor - gk)/N, & \sigma = 1. \end{cases} \quad (97)$$

The above form for the ratio of binomial coefficients allows us to approximate the states $|0'_\sigma\rangle$ and $|1'_\sigma\rangle$ in terms of the states

$$|0_\sigma\rangle = 2^{(-n+1)/2} \sum_{k \text{ even}} \sqrt{\binom{n}{k}} |D_{gk+s-\sigma}\rangle \quad (98)$$

$$|1_\sigma\rangle = 2^{(-n+1)/2} \sum_{k \text{ odd}} \sqrt{\binom{n}{k}} |D_{gk+s-\sigma}\rangle. \quad (99)$$

In our QEC algorithm, we wish to take the states $|\psi'_\sigma\rangle$ with an accumulated signal to the codespace spanned by $|0_\sigma\rangle$ and $|1_\sigma\rangle$.

Theorem 14 below quantifies the phase accumulated for a successful run of **QECsense** in terms of the real numbers $\phi_{t,j}$, where

$$\phi_{0,j} = \zeta_j, \quad j = 0, 1 \quad (100)$$

$$\phi_{1,j} = \arctan \frac{\text{Im}u_j}{\text{Re}u_j}, \quad (101)$$

where $u_0 = \frac{\langle 1_\sigma | U_\Delta | 1'_\sigma \rangle}{\langle 0_\sigma | U_\Delta | 0'_\sigma \rangle}$ and $u_1 = \frac{\langle q_{1,\sigma} | U_\Delta | 1'_\sigma \rangle}{\langle q_{0,\sigma} | U_\Delta | 0'_\sigma \rangle}$.

Theorem 14. *Let $|\psi\rangle = a|0_L\rangle + be^{i\varphi}|1_L\rangle$ where $a, b, \varphi \in \mathbb{R}$, and $|0_L\rangle$ and $|1_L\rangle$ are logical codewords of a shifted gnu*

*code on N qubits with parameters $g, n, u = (N-s)/gn$ and shift s . Let s satisfy the inequality, $N-s-gn/2 \geq N/4$ and $s+gn/2 \geq N/4$. Let n be odd and ≥ 3 . Let $t = 0, 1$, and let $\rho = U_\Delta \text{Tr}_t(|\psi\rangle\langle\psi|) U_\Delta^\dagger$ be the input state to **QECsense** for $\Delta \in \mathbb{R}$. Let*

$$(\rho_2, s', \text{syn}, \text{flag}) = \text{QECsense}(\rho, g, n, u, s). \quad (102)$$

*Then the probability that **QECsense** fails is $\Pr[\text{flag} = 1] = p_t$ where $p_0 = p_{\text{flag}}$ and*

$$p_1 \leq p_0 + \frac{2g^2n}{N^2}. \quad (103)$$

*Moreover when **QECsense** runs successfully, that is when $\text{flag} = 0$, then $\rho_2 = |\xi_{t,\text{syn}}\rangle\langle\xi_{t,\text{syn}}|$ is a shifted gnu state with shift s' where*

$$|\xi_{t,\text{syn}}\rangle = a_{t,\text{syn}}|0'_L\rangle + b_{t,\text{syn}}e^{i\varphi+i\phi_{t,\text{syn}}}|1'_L\rangle. \quad (104)$$

If $t = 0$, $|0'_L\rangle = |0_L\rangle$ and $|1'_L\rangle = |1_L\rangle$, and furthermore, $a_{0,0} = a_{0,1} = a, b_{0,0} = b_{0,1}$. If $t = 1$, $|0'_L\rangle = |0_\sigma\rangle$ and $|1'_L\rangle = |1_\sigma\rangle$ are the logical zero and one of a shifted gnu code on $N-1$ qubits, with parameters $g, n, u = (N-s')/gn$ and shift s' , where $\sigma = s - s'$.

Furthermore,

$$a_{1,\text{syn}} = \frac{a}{\sqrt{a^2 + b^2|u_{\text{syn}}|^2}}, \quad (105)$$

$$b_{1,\text{syn}} = \sqrt{1 - a_{1,\text{syn}}^2}, \quad (106)$$

$$\phi_{1,\text{syn}} = \arctan \frac{\text{Im}u_{\text{syn}}}{\text{Re}u_{\text{syn}}}. \quad (107)$$

The proof of Theorem 14 builds upon the results in Lemma 11 and Lemma 13. We prove this in the appendix.

The continuity of $\phi_{t,0}$, $\frac{d\phi_{t,0}}{d\theta}$, and u_j with respect to θ allows us to obtain the bounds

$$||u_{\text{syn}}| - 1| \leq \frac{3g\sqrt{n}}{N}, \quad (108)$$

$$|a_{1,j} - a| \leq \frac{12g\sqrt{n}}{N}, \quad (109)$$

$$|\phi_{1,0} - \zeta_0| \leq \frac{10g\sqrt{n}}{N} + \frac{98g^2n}{N^2}, \quad (110)$$

with the mild assumptions that $|\theta| \leq 1$, $gn\tau \leq 1/2$, $g\Delta/2 \leq \pi/6$ and $n \geq 3$. The above equations show that the effect of deleting a single qubit induces only mild perturbations proportional to $g\sqrt{n}/N$ in the relative amplitudes in the codespace, and also for $\phi_{1,1}$. The value of $\phi_{1,1}$ can potentially be very different from ζ_1 , depending on the actual parameters of Protocol 1, and also of the magnitude of θ , and hence we do not make an approximation of $\phi_{1,1}$ to ζ .

Moreover, for $n = 3$, we prove that

$$\left| \zeta_0 + \frac{(g\tau\theta)^3}{8} \right| \leq 52|g\tau\theta|^5 \quad (111)$$

$$|\zeta_1 - g\tau\theta| \leq \frac{3}{16}|g\tau\theta|^3. \quad (112)$$

Using the techniques of calculus, we prove the results (108), (109), (110), (111) and (112) in Appendix I.

From (111) and (112), we also have

$$\frac{d}{d\theta}\zeta_0 \approx -\frac{3}{8}g^3\tau^3\theta^2, \quad \frac{d}{d\theta}\zeta_1 \approx g\tau. \quad (113)$$

Furthermore, when $n = 3$ we have

$$\left| \phi_{1,0} + \frac{(g\tau\theta)^3}{8} \right| \leq \frac{10g\sqrt{3}}{N} + \frac{294g^2n}{N^2} + 52|g\tau\theta|^2, \quad (114)$$

$$\frac{d}{d\theta}\phi_{1,0} \approx -\frac{3g^3\tau^3\theta^2}{8}, \quad (115)$$

and in Appendix J we show that when $s = N/2 - gn/2 + o(g)$, we have

$$\phi_{1,1} \approx 4\sqrt{2}g\tau\theta, \quad (116)$$

$$\frac{d}{d\theta}\phi_{1,1} \approx 4\sqrt{2}g\tau. \quad (117)$$

This shows that $\phi_{1,1}$ is not a good approximation of ζ_1 . Rather, $\phi_{1,1}$ is directly proportional to ζ_1 to a good approximation, albeit with a constant of proportionality that is $4\sqrt{2}$.

Let $r_{t,j}$ count the number of timesteps where the number of deletions is t and where $\mathbf{syn} = j$. Then, the total phase that accumulates during a successful run of Protocol 1 depends is

$$\Phi = \sum_{t=0}^1 \sum_{j=0}^1 r_{t,j} \phi_{t,j}. \quad (118)$$

The total phase Φ is a random variable, because $r_{t,j}$ are random variables. Next consider Φ as a function of θ . Then Lemma 15, which we prove in Appendix B, gives the FI of θ that we can extract from Protocol 1.

Lemma 15. *Let Φ be a continuous function of θ , and let $|\psi(\Phi)\rangle = \frac{\cos\phi|a_0\rangle + e^{i\Phi}\sin\phi|a_1\rangle}{\sqrt{2}}$ where $|a_0\rangle$ and $|a_1\rangle$ be orthonormal vectors. Let $|a_+\rangle = \frac{1}{\sqrt{2}}(|a_0\rangle + |a_1\rangle)$ and $|a_-\rangle = \frac{1}{\sqrt{2}}(|a_0\rangle - |a_1\rangle)$. Then the FI of θ by performing projective measurements on $|\psi(\Phi)\rangle$ with respect to the projectors $|a_+\rangle\langle a_+|$ and $|a_-\rangle\langle a_-|$ when $\phi = \pi/4$ is $(\frac{d\Phi}{d\theta})^2$. In general the FI is*

$$F = \frac{\sin^2 2\phi \sin^2 \Phi}{(1 - \sin^2 2\phi \cos^2 \Phi)} \left(\frac{\partial \Phi}{\partial \theta} \right)^2. \quad (119)$$

The state at the end of a successful run of Protocol 1 has the form $a|0_L\rangle + be^{i\Phi}|1_L\rangle$, where $a = \cos\phi$ and $b = \sin\phi$. Denote the FI of Protocol 1 as F_{P1} . If Protocol 1 fails with $\mathbf{flag} = 1$, we declare $F_{P1} = 0$. In our calculation of F_{P1} when $\mathbf{flag} = 0$, we use information about only the phase Φ and not the amplitude a . This simplifies the derivation of the FI's precise analytical form.

When $\phi = \pi/4 + \epsilon$, we have $\sin 2\phi = \sin(\pi/2 + 2\epsilon) = \sin(\pi/2)\cos(2\epsilon) + \sin(2\epsilon)\cos(\pi/2) = \cos(2\epsilon)$. When $\epsilon = 0$,

the prefactor $f = \frac{\sin^2 2\phi \sin^2 \Phi}{(1 - \sin^2 2\phi \cos^2 \Phi)}$ is $f = \sin^2 \Phi / (1 - \cos^2 \Phi) = 1$. Let $\delta_\phi > 0$. When $|\epsilon| \leq \delta_\phi$, it follows that $|\cos(2\epsilon) - (1 - 4\epsilon^2)| \leq \frac{16}{3}\delta_\phi^4$. Hence, for small δ_ϕ and small Φ , we have

$$\left| F_{P1} - (1 - 4\delta_\phi^2 \sin^{-2} \Phi) \left(\frac{\partial \Phi}{\partial \theta} \right)^2 \right| \leq \frac{16\delta_\phi}{3} \left(\frac{\partial \Phi}{\partial \theta} \right)^2. \quad (120)$$

By taking derivatives on both sides of (118), we find

$$\frac{\partial \Phi}{\partial \theta} = \sum_{t=0}^1 \sum_{j=0}^1 r_{t,j} \frac{\partial \phi_{t,j}}{\partial \theta}. \quad (121)$$

We are now ready to quantify the performance of Protocol 1 in Theorem 16.

Theorem 16. *Let the total number of qubits during the execution of Protocol 1 be between $N/2$ and N , and let $\tau = o(1/N)$. With probability $1 - \delta$ where $\delta \leq rp_{\mathbf{flag}} + r\frac{2g^2n}{N^2} + rn_{\text{del}}N\tau$, Protocol 1 can run successfully, that is, there is no timestep where $\mathbf{flag} = 1$. Furthermore, when $n = 3$ and for small g/N , the expected FI of Protocol 1 is*

$$\mathbb{E}[F_{P1}] \approx \frac{37}{64}r^2g^6\tau^6\theta^4. \quad (122)$$

Proof of Theorem 16. Protocol 1 constitutes of running r repetitions of QECsense. From Theorem 14, each round of QECsense fails with probability at most $p_{\mathbf{flag}} + \frac{2g^2n}{N^2}$. Hence by the union bound, the probability of Protocol 1 failing on at least one instance of QECsense is at most $rp_{\mathbf{flag}} + r\frac{2g^2n}{N^2}$.

Another way for Protocol 1 to fail is to have at least 2 deletion errors in any timestep. For constant rate n_{del} of deletion per qubit per unit time, and for $\tau = o(1/N)$, and when the number of qubits in each timestep at most N , the number of deletions per time step to a good approximation follows a Poisson distribution with expectation approximately given by λ . Since the total number of qubits is between $N/2$ and N , we have $n_{\text{del}}N\tau/2 \leq \lambda \leq n_{\text{del}}N\tau$. For each timestep, the probability of having at least two deletions is at most $1 - e^{-\lambda} - \lambda e^{-\lambda} \leq \lambda^2/2$ for small λ . Hence the failure probability from having too many deletions during the protocol is at most $rn_{\text{del}}N\tau$. Hence the total failure probability of Protocol 1 is at most $rp_{\mathbf{flag}} + r\frac{2g^2n}{N^2} + rn_{\text{del}}N\tau$.

Now conditioned on Protocol 1 not failing, the number of deletions in each timestep $s = 1, \dots, r$ is Bernoulli random variable X_s , taking a value of either 0 or 1. If the number of deletions at timestep s is Poisson random variable with expected number λ_s , then $\Pr[X_s = 0] = \frac{1}{1 + \lambda_s}$ and $\Pr[X_s = 1] = \frac{\lambda_s}{1 + \lambda_s}$. Since the total number of qubits is between $N/2$ and N , we have $n_{\text{del}}\tau N/2 \leq \lambda_s \leq n_{\text{del}}\tau N$. This leads to the bound $\frac{1}{1 + n_{\text{del}}\tau N} \leq \Pr[X_s = 0] \leq \frac{1}{1 + n_{\text{del}}\tau N/2}$. Now for $x \in [0, 1]$

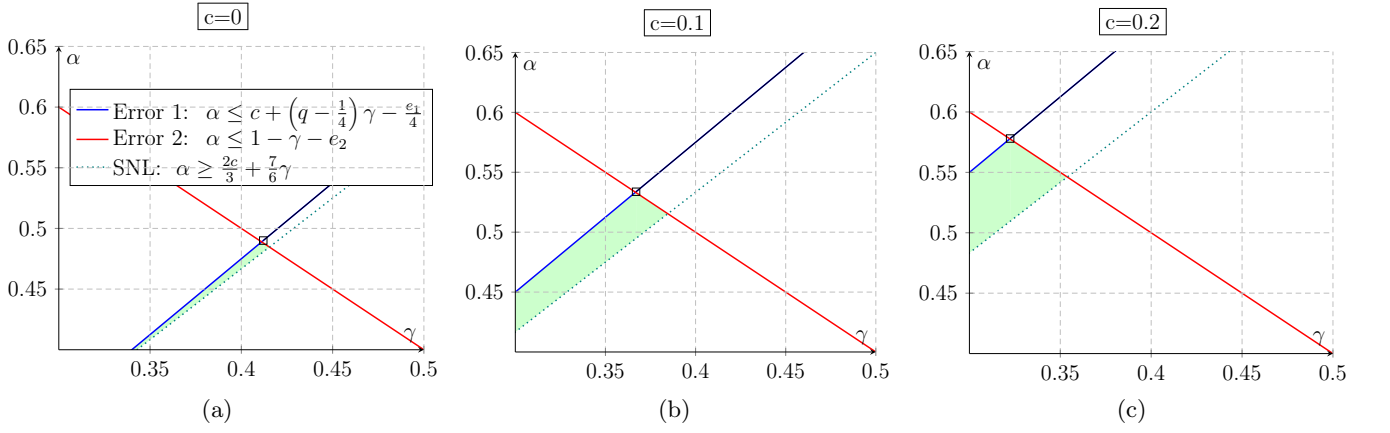


FIG. 6: Here, we consider a linear rate of deletion errors with $\eta = 1$, a signal per unit time $\theta = \Theta(N^{-c})$, and r timesteps, each of duration r^{-q} with $q = 3/2$. The error parameters are $e_1 = e_2 = 0.1$. The shaded region shows the parameters where $r = \Theta(N^\gamma)$ rounds of QEC while sensing using shifted gnu codes with $g = \Theta(N^\alpha)$ has a quantum advantage beating the shot noise limit (SNL). For $q = 3/2$, when our scheme beats the SNL, our scheme also beats the repeated GHZ state scheme. The black squares give the values of α and γ that maximize the FI of Protocol 1

we have $1 - x \leq 1/(1+x) \leq 1 - x/2$. Hence $1 - n_{\text{del}}\tau N \leq \Pr[X_s = 0] \leq 1 - n_{\text{del}}\tau N/4$ and $n_{\text{del}}\tau N/4 \leq \Pr[X_s = 1] \leq n_{\text{del}}\tau N$. Now let $r_1 = \sum_{s=1}^r X_s$, and let $r_0 = r - r_1$. Now denote $p_s = \mathbb{E}[X_s]$, so we have $n_{\text{del}}\tau N/4 \leq p_s \leq n_{\text{del}}\tau N$. Then r_1 is a Poisson binomial random variable with mean $\mu_{r_1} = \sum_{s=1}^r p_s$ and variance $v_{r_1} = \sum_{s=1}^r (1 - p_s)p_s$. Hence $rn_{\text{del}}\tau N/4 \leq \mu_{r_1} \leq rn_{\text{del}}\tau N$ and $rn_{\text{del}}\tau N/4 - rn_{\text{del}}^2\tau^2N^2 \leq v_{r_1} \leq rn_{\text{del}}\tau N - rn_{\text{del}}^2\tau^2N^2/16$. Hence

$$\frac{rn_{\text{del}}\tau N}{4} \leq \mathbb{E}[r_1] \leq rn_{\text{del}}\tau N \quad (123)$$

$$\frac{r^2n_{\text{del}}^2\tau^2N^2}{16} \leq \mathbb{E}[r_1^2] \leq r^2n_{\text{del}}^2\tau^2N^2 + rn_{\text{del}}\tau N. \quad (124)$$

Since the variance of r_0 is the same as the variance of r_1 , and using the fact that $1 - \frac{n_{\text{del}}\tau N}{4} \leq 1$, we have

$$r(1 - n_{\text{del}}\tau N) \leq \mathbb{E}[r_0] \leq r \quad (125)$$

$$r^2 - 2r^2n_{\text{del}}\tau N \leq \mathbb{E}[r_0^2] \leq r^2 + rn_{\text{del}}\tau N. \quad (126)$$

This means that for $\tau = o(1/N)$, for some positive constants $c_1 \in [1/4, 1]$, we have

$$\mathbb{E}[r_0] \approx r^2 \quad (127)$$

$$\mathbb{E}[r_0^2] \approx r^2 \quad (128)$$

$$\mathbb{E}[r_1] \approx c_1rn_{\text{del}}\tau N \quad (129)$$

$$\mathbb{E}[r_1^2] \approx c_1^2r^2n_{\text{del}}^2\tau^2N^2 + c_1rn_{\text{del}}\tau N. \quad (130)$$

Now let Y_s be a Bernoulli random variable that is equal to 0 when QECsense projects according to Π and equal to 1 when QECsense projects according to Π_1 . To leading order in τ and g/N we have $\mathbb{E}[Y_s] \approx p'$ where $p' = ng^2\tau^2\theta^2/4$.

Then let us define

$$r_{0,0} = \sum_{s=1}^r (1 - X_s)(1 - Y_s) \quad (131)$$

$$r_{1,0} = \sum_{s=1}^r X_s(1 - Y_s) \quad (132)$$

$$r_{0,1} = \sum_{s=1}^r (1 - X_s)Y_s \quad (133)$$

$$r_{1,1} = \sum_{s=1}^r X_sY_s. \quad (134)$$

Now let

$$p_{s,0,0} = \Pr[(1 - X_s)(1 - Y_s) = 1] \quad (135)$$

$$p_{s,1,0} = \Pr[X_s(1 - Y_s) = 1] \quad (136)$$

$$p_{s,0,1} = \Pr[(1 - X_s)Y_s = 1] \quad (137)$$

$$p_{s,1,1} = \Pr[X_sY_s = 1]. \quad (138)$$

Then we have

$$p_{s,0,0} \approx (1 - p_s)(1 - p') \quad (139)$$

$$p_{s,1,0} \approx p_s(1 - p') \quad (140)$$

$$p_{s,0,1} \approx (1 - p_s)p' \quad (141)$$

$$p_{s,1,1} \approx p_sp'. \quad (142)$$

Using the fact that $r_{t,j}$ are Poisson binomial random variables along with the proximity of p' and p_s to zero, we

get

$$\mathbb{E}[r_{0,0}] \approx r \quad (143)$$

$$\mathbb{E}[r_{0,0}^2] \approx r^2 \quad (144)$$

$$\mathbb{E}[r_{1,0}] \approx c_1 r n_{\text{del}} \tau N \quad (145)$$

$$\mathbb{E}[r_{1,0}^2] \approx c_1^2 r^2 n_{\text{del}}^2 \tau^2 N^2 + c_1 r n_{\text{del}} \tau N \quad (146)$$

$$\mathbb{E}[r_{0,1}] \approx r p' \quad (147)$$

$$\mathbb{E}[r_{0,1}^2] \approx r^2 (p')^2 + r p' \quad (148)$$

$$\mathbb{E}[r_{1,1}] \approx c_1 r n_{\text{del}} \tau N p' \quad (149)$$

$$\mathbb{E}[r_{1,1}^2] \approx c_1^2 r^2 n_{\text{del}}^2 \tau^2 N^2 (p')^2 + c_1 r n_{\text{del}} \tau N p'. \quad (150)$$

With our notation, we can write the total phase as $\Phi = r_{0,0}\zeta_0 + r_{0,1}\zeta_1 + r_{1,0}\phi_{1,0}$, and note that

$$\frac{\partial \Phi}{\partial \theta} \approx -(r_{0,0} + r_{1,0}) \frac{3}{8} g^3 \tau^3 \theta^2 + (r_{0,1} + r_{1,1} 4\sqrt{2}) g \tau, \quad (151)$$

and

$$\begin{aligned} \left(\frac{\partial \Phi}{\partial \theta} \right)^2 &\approx \frac{9}{64} (r_{0,0} + r_{1,0})^2 g^6 \tau^6 \theta^4 \\ &\quad - \frac{3}{4} (r_{0,0} + r_{1,0}) (r_{0,1} + r_{1,1} 4\sqrt{2}) g^4 \tau^4 \theta^2 \\ &\quad + (r_{0,1} + r_{1,1} 4\sqrt{2})^2 g^2 \tau^2. \end{aligned} \quad (152)$$

We want to evaluate the $\mathbb{E}[(\frac{\partial \Phi}{\partial \theta})^2]$. For this, we need to evaluate $\mathbb{E}[(r_{0,0} + r_{1,0})^2]$, $\mathbb{E}[(r_{0,0} + r_{1,0})(r_{0,1} + r_{1,1} 4\sqrt{2})]$, and $\mathbb{E}[(r_{0,1} + r_{1,1} 4\sqrt{2})^2]$. By the linearity of the expectation and the independence of the random variables $r_{0,0}$ and $r_{1,0}$, we have

$$\mathbb{E}[(r_{0,0} + r_{1,0})^2] = \mathbb{E}[r_{0,0}^2] + 2\mathbb{E}[r_{0,0}]\mathbb{E}[r_{1,0}] + \mathbb{E}[r_{1,0}^2]. \quad (153)$$

Next, $r_{t,0}$ and $r_{t,1}$ are dependent random variables, in the sense that $r_{t,0} = r_t - r_{t,1}$. From the linearity of the expectation and the independence of the random variables r_t and $r_{t,j}$, we get

$$\begin{aligned} &\mathbb{E}[(r_{0,0} + r_{1,0})(r_{0,1} + 4\sqrt{2}r_{1,1})] \\ &= \mathbb{E}[r_{0,0}r_{0,1}] + 4\sqrt{2}\mathbb{E}[r_{0,0}r_{1,1}] + \mathbb{E}[r_{1,0}r_{0,1}] + 4\sqrt{2}\mathbb{E}[r_{1,0}r_{1,1}] \\ &= \mathbb{E}[r_0]\mathbb{E}[r_{0,1}] - \mathbb{E}[r_{0,1}^2] + 4\sqrt{2}\mathbb{E}[r_{0,0}]\mathbb{E}[r_{1,1}] \\ &\quad + \mathbb{E}[r_{1,0}]\mathbb{E}[r_{0,1}] + 4\sqrt{2}\mathbb{E}[r_1]\mathbb{E}[r_{1,1}] - 4\sqrt{2}\mathbb{E}[r_{1,1}^2]. \end{aligned} \quad (154)$$

Also,

$$\mathbb{E}[(r_{0,1} + r_{1,1})^2] = \mathbb{E}[r_{0,1}^2] + 2\mathbb{E}[r_{0,1}]\mathbb{E}[r_{1,1}] + \mathbb{E}[r_{1,1}^2]. \quad (155)$$

To leading order in τ , we have

$$\mathbb{E}[r_{0,1}] \approx \mathbb{E}[r_0] n g^2 \tau^2 \theta^2 / 4 \quad (156)$$

$$\mathbb{E}[r_{1,1}] \approx \mathbb{E}[r_1] n g^2 \tau^2 \theta^2 / 4, \quad (157)$$

and

$$\mathbb{E}(r_{0,0}) \approx \mathbb{E}[r_0], \quad \mathbb{E}(r_{1,0}) \approx \mathbb{E}[r_1]. \quad (158)$$

Hence

$$\begin{aligned} &\mathbb{E}[(r_{0,0} + r_{1,0})^2] \\ &\approx r^2 (1 + 2c_1 n_{\text{del}} \tau N + c_1^2 n_{\text{del}}^2 \tau^2 N^2) + c_1 r n_{\text{del}} \tau N \end{aligned} \quad (159)$$

For $\tau N = o(1)$, this becomes

$$\mathbb{E}[(r_{0,0} + r_{1,0})^2] \approx r^2. \quad (160)$$

Using the same idea, we also get

$$\mathbb{E}[(r_{0,1} + r_{1,1})^2] \approx \mathbb{E}[r_{0,1}^2] \approx r^2 (p')^2 + r(p'), \quad (161)$$

and

$$\mathbb{E}[(r_{0,0} + r_{1,0})(r_{0,1} + 4\sqrt{2}r_{1,1})] \approx \mathbb{E}[r_{0,0}]\mathbb{E}[r_{0,1}] \approx r^2 p'. \quad (162)$$

Hence

$$\begin{aligned} \mathbb{E} \left[\left(\frac{\partial \Phi}{\partial \theta} \right)^2 \right] &\approx \frac{9}{64} r^2 g^6 \tau^6 \theta^4 - \frac{9}{16} r^2 g^6 \tau^6 \theta^4 + r^2 g^6 \tau^6 \theta^4 \\ &= \frac{37}{64} r^2 g^6 \tau^6 \theta^4. \end{aligned} \quad (163)$$

Consider the prefactor $f = \frac{\sin^2 2\phi \sin^2 \Phi}{(1 - \sin^2 2\phi \cos^2 \Phi)}$ as a function of ϕ . Let p denote the actual prefactor on the FI for Protocol 1. We like to obtain an upper bound on $|p - 1|$, since 1 denotes the ideal prefactor when the angle is $\pi/4$. Let ϕ denote the actual angle after the implementation of Protocol 1. Hence $|p - 1| = |f(\phi) - f(\pi/4)|$. From (120), when $|\phi - \pi/4| \leq \delta_\phi$, we have $|f(\phi) - f(\pi/4)| \leq 16\delta_\phi/3$.

Next we obtain an upper bound on δ_ϕ . Note that a is a function of ϕ , namely, $a = \cos \phi$. Hence $\phi = \arccos a$. We have $\frac{d\phi}{da} = -1/\sqrt{1-a^2}$. Hence when $|a - \pi/4| \leq \delta_a$, it follows that $|\phi - \pi/4| \leq 2\delta_a/\sqrt{3}$, if the minimum a is $1/\sqrt{4}$. Hence $|f(\phi) - f(\pi/4)| \leq 32\delta_a/3\sqrt{3} \leq 7\delta_a$. Hence, a successful run of Protocol 1 gives a Fisher information of

$$(1 \pm 7\delta_\phi) \left(\frac{d\Phi}{d\theta} \right)^2. \quad (164)$$

Since we keep doing QEC to keep the shift of the shifted gnu code to satisfy $s = N/2 - gn/2 + o(g)$, we can guarantee that δ_ϕ is very close to zero. Hence F_{P_1} is very close to $\left(\frac{d\Phi}{d\theta} \right)^2$ and we get the result. \square

Therefore, when $n = 3$, we have

$$\mathbb{E}[F_{P_1}] = \Theta(N^{6\alpha - 4c + (2-6q)\gamma}). \quad (165)$$

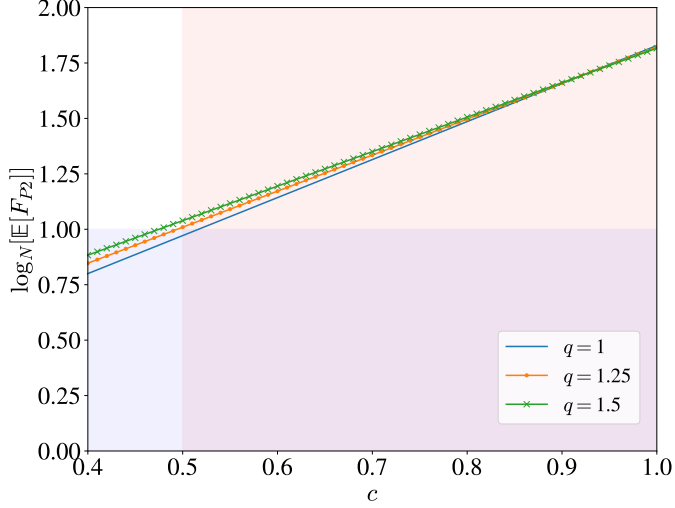


FIG. 7: Logarithm of Protocol 2's FI of θ against the parameter c , where from prior knowledge, the MSE of prior estimates on θ is $\Theta(N^{-c})$. For instance, using classical sensing techniques, we may get $c = 1/2$. When the lines are above 1, Protocol 1 has quantum advantage, i.e., we outperform the SNL. In Protocol 1, we set $e_1 = e_2 = 0$.

We like to compare the performance of our scheme with that of using copies of GHZ states, because GHZ states are optimal for field sensing in the noiseless setting. To make a fair comparison, note that the duration of Protocol 1 is $rr^{-q} = \Theta(N^{\gamma(-q+1)})$. Hence, the expected number of deletions on N qubits in this duration is $n_{\text{del}}Nrr^{-q} = \Theta(N^{\eta+\gamma(1-q)})$. Now, even a single deletion error can render a GHZ state completely classical, so with $\Theta(N^{\eta+\gamma(1-q)})$ deletions on N qubits, we would like to make $\Theta(N^{\min\{\eta+\gamma(1-q), 1\}})$ copies of GHZ states on N qubits to ensure that with high probability, a constant number of such GHZ states will have no deletions. The number of qubits for each such GHZ state is $\Theta(N^{\max\{1-\eta-\gamma(1-q), 0\}})$, where we consider the maximization with 0 because we cannot use fewer than a constant number of qubits for each GHZ state. The FI from such a protocol is

$$\begin{aligned} F_{\text{GHZ}} &= \Theta(N^{\max\{2(1-\eta+(q-1)\gamma), 0\}})\Theta(N^{2\gamma(-q+1)}) \\ &= \Theta(N^{\max\{2-2\eta, -2\gamma(q-1)\}}). \end{aligned} \quad (166)$$

When $q \geq 1$ and $\eta \in [0, 1]$, this simplifies to

$$F_{\text{GHZ}} = \Theta(N^{2-2\eta}). \quad (167)$$

When N is large, we can determine the optimal values of α and γ that maximize $\mathbb{E}[F_{\text{P1}}]$ while keeping certain errors small. These errors are:

1. Type 1 error: the probability that in r rounds of implementing `QECsense`, there is at least one instance where `flag` = 1. We define this error to be $\epsilon_1 = \Theta(N^{-e_1})$. Here $\epsilon_1 = \Theta(r(g(\theta/r^q))^4)$. Hence

$$\gamma + 4(\alpha - c - q\gamma) = -e_1. \quad (168)$$

2. Type 2 error: the deviation of the final output state after r rounds with $t = 0$ versus the r -round ideal state in terms of the 1-norm. We define this error to be $\epsilon_2 = \Theta(N^{-e_2})$. Here $\epsilon_2 = \Theta(rq/N)$.

$$\gamma + \alpha - 1 = -e_2. \quad (169)$$

We optimize our protocol's performance with respect to α and γ according to the following linear program.

$$\begin{aligned} \text{maximize} \quad & 6\alpha - 4c + (2 - 6q)\gamma \\ \alpha, \gamma \geq & 0 \end{aligned} \quad (170a)$$

$$\text{subject to} \quad \alpha \leq c + \left(q - \frac{1}{4}\right)\gamma - \frac{e_1}{4}, \quad (170b)$$

$$\alpha \leq 1 - \gamma - e_2, \quad (170c)$$

$$\alpha \geq \frac{2c}{3} + \left(q - \frac{1}{3}\right)\gamma + \frac{1}{2} - \frac{q}{3}, \quad (170d)$$

$$\alpha \geq \frac{2c - \eta}{3} + \left(q - \frac{1}{3}\right)\gamma. \quad (170e)$$

Here, positive numbers e_1 and e_2 are error parameters. When (170b) and (170c) hold, the failure probability of our protocol is small for large N .

We would also like to know when Protocol 1 has a FI on θ that outperforms both the shot noise limit (SNL) and that of a repeated GHZ state protocol. When (170d) holds, our protocol outperforms the shot noise limit (SNL), where the SNL quantifies the ultimate performance of all classical estimation strategies. When (170e) holds, our protocol outperforms the repeated GHZ state strategy. Note that whenever

$$q \leq \frac{3}{2} + \eta, \quad (171)$$

having inequality (170d) to hold implies that (170e) also holds.

Now let `Polytope` be the set of (α, γ) for which all the inequalities (170b), (170c), (170d) and (170e) are satisfied. Theorem 17 implies that any (α, γ) that lies within the interior of `Polytope` allows Protocol 1 to succeed with high probability and be a competitive solution for QEC-enhanced sensing.

Theorem 17. *Let $c, e_1, e_2 > 0$ and $q \geq 1$. Let α, γ be positive numbers such that (α, γ) satisfy the inequalities (170d) and (170e) strictly, and also satisfy (170b) and (170c) (not necessarily strictly). Let the conditions required by Theorem 14 and Theorem 16 hold. Then Protocol 1 that uses shifted gnu codes with parameters as given in Theorem 14 with $n = 3$ and parameters (α, γ) asymptotically outperforms the shot noise limit and the repeated GHZ state strategy with vanishing failure probability for large N . Moreover, the corresponding expected FI on θ obtained by Protocol 1 is asymptotically $\Theta(N^{6\alpha - 4c + (2 - 6q)\gamma})$.*

Proof. First, we establish inequalities that guarantees that Protocol 1 will succeed. Second, we establish in-

equalities guarantee that Protocol 1 has a quantum advantage. Rearranging (168) and (169), we get

$$\alpha = c + \left(q - \frac{1}{4}\right)\gamma - \frac{e_1}{4}, \quad (172)$$

$$\alpha = 1 - \gamma - e_2. \quad (173)$$

We use the expected FI of Protocol 1 as calculated in Theorem 16. For Protocol 1 to have an asymptotic quantum advantage, that is, to beat the SNL, we need $\mathbb{E}[F_{P1}] \geq \Theta(N)\Theta(N^{2-2q})$, which is equivalent to

$$\alpha \geq \frac{2c}{3} + \left(q - \frac{1}{3}\right)\gamma + \frac{1}{2} - \frac{q}{3}. \quad (174)$$

Next, note that from (167), we can see that Protocol 1 has a FI that is larger than the FI when multiple GHZ states are used, when $\mathbb{E}[F_{P1}] \geq \Theta(N^{2(1-\eta-(q-1)\gamma)})$ which is equivalent to

$$\alpha \geq \frac{2c+1-\eta}{3} + \frac{(q+1)\gamma}{3}. \quad (175)$$

□

Theorem 17 implies that solving the linear program as specified in (170a), (170b), (170c), (170d), and (170e) allows us to find the optimal parameters α and γ for Protocol 1.

To understand the implications of Theorem 17, we consider some parameter regimes where Protocol 1 can have a good performance. Consider a linear number of deletions per unit time, so $\eta = 1$. Consider $q = 3/2$ so that the time elapsed per timestep is $r^{-3/2}$. We consider three scenarios where we have an increasing amount of information about θ , including the case where there is minimal prior information about the signal, so $c = 0$, and where $c = 0.1$ and $c = 0.2$. We set the error parameters as $e_1 = e_2 = 0.1$. We plot the corresponding feasible regions of Polytope in Fig. 6.

Now we define Protocol 2 to be the repetition of Protocol 1 r^{q-1} times. Protocol 2 therefore requires r^{q-1} repeated initializations of the shifted gnu probe state. For Protocol 2, the total amount of time used for sensing is 1, because each run of Protocol 1 takes r^{1-q} time. Let the FI of Protocol 2 be F_{P2} . Then the expected FI of θ for Protocol 2 is

$$\mathbb{E}[F_{P2}] = r^{q-1}(1 - f_1)\mathbb{E}[F_{P1}], \quad (176)$$

where f_{P1} denotes the failure probability of each run of Protocol 1. By Theorem 16, Since the failure probability f_1 is vanishing, we have that $\mathbb{E}[F_{P2}] \approx r^{q-1}\mathbb{E}[F_{P1}]$.

Now we assume that $\eta = 1$ which corresponds to a linear rate of deletions per unit time. Also for every round of Protocol 1, we consider using

$$\gamma = \frac{-4c + e_1 - 4e_2 + 4}{4q + 3}, \quad (177)$$

along with

$$\alpha = \frac{4c + 4q - 1 - e_1 - 4e_2q + e_2}{4q + 3}. \quad (178)$$

Note that (177) and (178) satisfy the inequalities (170b) and (170c) with equality. Correspondingly $\mathbb{E}[F_{P2}]$ with this value of (α, γ) after r^{q-1} repeats of Protocol 1 is

$$\begin{aligned} \mathbb{E}[F_{P2}] &\approx r^{q-1}\mathbb{E}[F_{P1}] = \Theta(N^{\gamma(q-1)+(6\alpha-4c+(2-6q)\gamma)}) \\ &= \Theta(N^{\frac{4c(q+2)-5e_1(q+1)-2(e_2-1)(2q-1)}{4q+3}}). \end{aligned} \quad (179)$$

In Fig. 7, we plot $\log_N(\mathbb{E}[F_{P2}])$ versus c with α and γ given by (177) and (178). Here, c indicates the extent of our prior knowledge of the true value of θ . In the plot, we set $q = 1, 1.25, 1.5$, and the plot shows that increasing q increases the FI of Protocol 2. However, increasing q also makes Protocol 1 harder to implement practically, because each timestep becomes increasingly short. For illustration, let us consider choosing $q = 3/2$. In this scenario, we have

$$\log_N(\mathbb{E}[F_{P2}]) \approx \frac{4 + 14c - 25e_1/2 - 4e_2}{9}. \quad (180)$$

We like to emphasize that we can always have prior knowledge of c , for example by using classical resources. The largest c that we can attain from estimating θ first using N classical probe states is $c = 1/2$. Using this prior classical information, the maximum $\mathbb{E}[F_{P2}]$ can approach $\Theta(N^{3/2})$. If we repeat this process, we can iteratively boost the FI at the expense by iteratively improving the prior precision of the phase that we wish to estimate. Protocol 3 implements this idea.

Protocol 3:

1. Use N classical sensors to estimate θ with mean-square error $\Theta(N^{-2c_1})$, where $c_1 = 1/2$.
2. Use Protocol 2 to estimate θ setting $c = c_1$. The FI is $\Theta(N^{2c_2})$ and hence by the quantum Cramér Rao bound, the mean-square error of θ is $\Theta(N^{-2c_2})$.
3. Set k to be a constant positive integer. For $j = 2, \dots, k$, Use Protocol 2 to estimate θ with $c = c_j$. The FI is $\Theta(N^{2c_{j+1}})$ and the mean-square error is $\Theta(N^{-2c_{j+1}})$.

From Fig. 7 and (180), we can see that after k repeats of Protocol 2, the FI of θ keeps increasing and gets close to, but does not reach the Heisenberg limit (because of the positive values of the error parameters e_1 and e_2). We define Protocol 3 to be the repeat of Protocol 2 by k times in this manner. In fact, as we let e_1 and e_2 approach zero, from (180), we can see that we can approach the Heisenberg limit for phase estimation when k is a large constant.

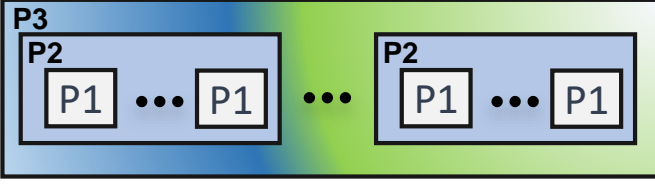


FIG. 8: Our protocol for quantum sensing with QEC has a nested structure. Protocol 3 comprises of k repeats of Protocol 2, and Protocol 2 comprises of r^{q-1} repeats of Protocol 1. In each instance of Protocol 1, a fresh shifted gnu probe is used. Each instance of Protocol 2 requires an update on the mean-square error of the phase, based on the previous run of Protocol 2. Protocol 3 contains enough repeats of Protocol 2, so that we can approach the Heisenberg limit for phase estimation to the limits as to what is allowed by the error parameters e_1 and e_2 .

VI. QUANTUM CONTROL

Here we describe how to implement many of the operations used for QEC with symmetric probes using quantum control of the spins together with a bosonic mode.

A. Measurement of \hat{J}^2

Measurement of total spin angular momentum involves measuring $\hat{J}^x + \hat{J}^y + \hat{J}^z = \hat{J}^2$ with eigenvalues $j(j+1)$. While \hat{J}^2 is clearly a Hermitian operator and in principle measurable, the actual physical construction of such an observable is not so straightforward. One possibility is to leverage recent results which show that singlet/triplet measurements on pairs of qubits can efficiently simulate universal quantum computation, or **STP = BQP** [48, 49]. Once the number of pairwise qubit measurements becomes polynomially large compared to J^2 , the accuracy converges exponentially.

Another way to measure \hat{J}^2 is to couple the spins to an ancillary bosonic mode and measure that. Consider the following Hamiltonian which generates a displacement of the position quadrature of the mode dependent on the total angular momentum

$$\hat{H} = \hat{H}_0 + \hat{H}_d. \quad (181)$$

Here the free Hamiltonian of the mode is $\hat{H}_0 = \omega_0 \hat{a}^\dagger \hat{a}$ and the interaction term is

$$\hat{H}_d = \gamma_d (\hat{a}^\dagger + \hat{a}) \hat{J}^2. \quad (182)$$

where the mode creation and annihilation operators satisfy canonical commutation relations $[\hat{a}, \hat{a}^\dagger] = 1$. In some physical systems it may be more natural for the mode to couple to the second moment of a particular component of spin, as in $\hat{H}'_d = \gamma_d (\hat{a}^\dagger + \hat{a}) \hat{J}^{z^2}$. In such a case one

could approximate evolution by \hat{H} via a Trotterized expansion by a product of short time evolutions generated by \hat{H}'_d and conjugated by collective spin rotations around the \hat{x} and \hat{y} directions.

In the simplest protocol, one begins with the mode prepared in the vacuum state, i.e. the coherent state $|\alpha = 0\rangle$. Consider an initial spin state written as a superposition of basis states $\{|j, \mathbb{T}, m\rangle\}$, where j is the total angular momentum, \mathbb{T} is a SYT, and m is an eigenvalue of \hat{J}^z (equivalently an SSYT). After evolving the joint system according to \hat{H} for a time t , the joint state in the frame rotating at the bare mode frequency ω_0 is

$$\begin{aligned} e^{-iHt} |\psi(0)\rangle &= e^{-iHt} \sum_{j, \mathbb{T}, m} c_{j, \mathbb{T}, m} |j, \mathbb{T}, m\rangle \otimes |\alpha = 0\rangle \\ &= \sum_{j, \Lambda, M} c_{j, \mathbb{T}, m} |j, \mathbb{T}, m\rangle |\alpha = \gamma_d t j(j+1)\rangle. \end{aligned} \quad (183)$$

The effect is the mode state becomes a displaced coherent state with the magnitude of displacement proportional to $j(j+1)$. The mode quadrature can then be measured by heterodyne measurement and a projective measurement of \hat{J}^2 is obtained provided the standard deviation of the coherent state is less than the minimum spacing between displacements, i.e. $1/2 \ll \gamma_d t$. In fact, thanks to the quadratic scaling of the eigenvalues of \hat{J}^2 , if we assume that the initial spin state is dominated by components near maximum $j = n/2$, which is true if e.g. only a constant number of amplitude damping or deletion errors occur, then the criterion for a projective measurement is $1/2 \ll \gamma_d t n$.

This primitive can be applied to compute the total angular momentum of any subset of spins and hence to project onto an SYT.

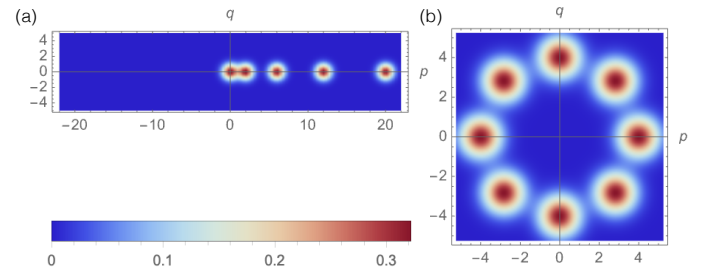


FIG. 9: Observables on spins mapped to quadratures of a bosonic mode as illustrated by plots of the Wigner distribution. (a) Measurement of \hat{J}^2 . The mode is prepared in the vacuum $|\alpha = 0\rangle$ and displaced by evolution generated by \hat{H}_d (Eq. 182) providing projection onto j eigenspaces. Here $\gamma_d t = 1$, and $j \in \{0, 1, 2, 3, 4\}$. (b) Modular measurement of \hat{J}^z . The mode is prepared in $|\alpha = 4\rangle$ and rotated by evolution generated by \hat{H}_r (Eq. 184) providing projection onto $M \bmod g$ eigenspaces. Here $\gamma_r t = 2\pi/g$ with $g = 8$.

B. Modular measurement of \hat{J}^z .

The measurement of \hat{J}^z modulo a constant g can be done as follows. We focus on the measurement in the symmetric subspace spanned by Dicke states but the argument follows for measurement in any SYT. Define the Dicke space on N spins as $\mathcal{H} = \text{span}_{\mathbb{C}}\{|D_w^N\rangle\}_{w=0}^N$. In order to do the error detection for probe states using the gnu code, we need to perform a non-destructive measurement of the operator $\hat{J}^z + \frac{N}{2}\mathbf{1}$ modulo $g \in \mathbb{Z}_{N+1}$. That is we want a projector onto the eigensubspaces $\{\mathcal{H}_p\}_{p=0}^{g-1}$ where $\mathcal{H}_p = \text{span}_{\mathbb{C}}\{|D_w^N\rangle; w \bmod g = p\}$. One way to do this is to employ a dispersive coupling between a bosonic mode and the spins of the type

$$\hat{H}_r = \gamma_r \hat{J}^z \hat{a}^\dagger \hat{a}. \quad (184)$$

If we start with the bosonic mode prepared in the coherent state $|\alpha\rangle$, with $2\pi|\alpha|^2 \gg g$, and allow the interaction to take place over a time $\tau = 2\pi/(g\gamma_r)$, then in the frame rotating at ω_0

$$e^{-iH_{\text{rot}}\tau}|J, M\rangle \otimes |\alpha\rangle = |J, M\rangle \otimes |\alpha e^{-i2\pi M/g}\rangle, \quad (185)$$

i.e. the initial phase space distribution with radius $|\alpha|^2$ and standard deviation $1/\sqrt{2}$ is mapped to g different equiangular rotations in the complex plane. Using balanced homodyne detection [50] we can measure the quadratures of the output bosonic field, and because we chose $2\pi|\alpha|^2 \gg g$, the distributions for different s will be distinguishable, hence we project onto the eigenspaces \mathcal{H}_p in a non-destructive way.

C. Geometric phase gates and unitary synthesis on Dicke states

Several of the primitive operations for QEC and measurement with symmetric probe states can be realized using dispersive geometric phase gates (GPGs) [51]. We assume a dispersive coupling of the spins to a single bosonic mode with creation and annihilation operators satisfying the commutation relations $[\hat{a}, \hat{a}^\dagger] = 1$:

$$V = ga^\dagger a \hat{J}^z. \quad (186)$$

The GPG makes use of two basic operators, the displacement operator $D(\alpha) = e^{\alpha a^\dagger - \alpha^* a}$ and the rotation operator $R(\theta) = e^{i\theta a^\dagger a}$ which satisfy the relations: $D(\beta)D(\alpha) = e^{i\Im(\beta\alpha^*)}D(\alpha + \beta)$, and $R(\theta)D(\alpha)R(-\theta) = D(\alpha e^{i\theta})$. Furthermore, we have the relations for an operator A acting on a system other than the mode,

$$D(\alpha e^{i\theta A}) = R(\theta A)D(\alpha)R(-\theta A), \quad (187)$$

where $R(\theta A) = e^{i\theta A \otimes a^\dagger a}$. For our purposes the rotation operator will be generated by the dispersive coupling over

a time t : $R(-\theta J^z) = e^{-iVt}$ for $\theta = gt$. Putting these primitives together, one can realize an evolution which performs a closed loop in the mode phase space:

$$\begin{aligned} U_{\text{GPG}}(\theta, \phi, \chi) &= D(-\beta)R(\theta J^z)D(-\alpha)R(-\theta J^z) \\ &\quad \times D(\beta)R(\theta J^z)D(\alpha)R(-\theta J^z) \\ &= e^{-i2\chi \sin(\theta J^z + \phi)} \end{aligned} \quad (188)$$

where $\phi = \arg(\alpha) - \arg(\beta)$ and $\chi = |\alpha\beta|$. After this gate, the spins and mode are disentangled from each other, and notably the gate works irrespective of the initial state of the mode.

State preparation of gnu codes can be done using the protocol given in Ref. [27]. Specifically, the mapping $|D_0^N\rangle \rightarrow \sum_w a_w |D_w^N\rangle$ can be performed using N GPGs via the following sequence:

$$\left[\prod_{s=1}^{N-1} e^{i\beta_s J^y} U_{\text{GPG}}(\theta_s, \phi_s, \chi_s) \right] e^{-i\frac{\pi}{2} J^y} U_{\text{GPG}}\left(\frac{\pi}{2}, 0, \frac{\pi}{4}\right) e^{i\frac{\pi}{2} J^y}$$

where the angles $\{\beta_s, \theta_s, \phi_s, \chi_s\}_{s=1}^{N-1}$ can be found by efficient classical optimization. The overall complexity is N GPGs.

Consider the problem of a subspace mapping, *i.e.* the unitary synthesis of k state mappings $\{|a_j\rangle \rightarrow |b_j\rangle\}_{j=1}^k$, where the set $S_a = \{|a_j\rangle\}$ is orthonormal as is $S_b = \{|b_j\rangle\}$, but the sets are not necessarily mutually orthogonal. As shown in Ref. [52], it suffices to use k instances of the following composition: a unitary state synthesis mapping, followed by the phasing on a particular state (here a Dicke state), followed by an inverse state mapping. Phasing of a Dicke state is achieved using $N/2$ GPGs [27]. Hence the overall cost of k dimensional subspace mapping is $\lceil 5Nk/2 \rceil$ GPGs. In the case $k = N + 1$ we have full unitary synthesis over the Dicke subspace.

D. Operations for teleportation

The requisite operations for teleportation are described in Sec. IV B. Since we have already described how to prepare the state $|+L\rangle$ and to perform the modular measurement of \hat{J}^z , the remaining requirement is to implement the controlled not gate $C_A X_B$ between an ancilla system A and the register system B the latter of which has undergone error and been projected onto a SYT T. Recall the action of X_{schur} on an eigenstate of \hat{J}^z in an SYT labeled T is to reverse the sign on the eigenstates of \hat{J}^z . We use the following definition, which is a bit flip up to a phase i :

$$X_{\text{schur}}|m_T\rangle = i|-m_T\rangle.$$

This can be realized using $X_{\text{schur}} = i \prod_{j=1}^M X_j$, since then $X_{\text{schur}}^\dagger \hat{J}^z X_{\text{schur}} = -\hat{J}^z$. The phase i can be accounted for in the readout step.

To see how to construct the required controlled not gate, we first consider the simple case of a single ancilla qubit coupled to the cavity mode via the interaction $W = g|1\rangle\langle 1|\hat{a}^\dagger\hat{a}$. Over a time $t = \pi/g$ this generates the dispersive rotation $e^{-iWt} = R(-\pi|1\rangle\langle 1|) = R(\pi|1\rangle\langle 1|)$. From Eq.(187) notice that the composite pulse sequence produces

$$D(\beta/2)R(\pi|1\rangle\langle 1|)D(-\beta/2)R(-\pi|1\rangle\langle 1|) = \begin{aligned} &|0\rangle\langle 0| \otimes \mathbf{1} \\ &+ |1\rangle\langle 1| \otimes D(\beta). \end{aligned}$$

We need to extend this gate to one that performs a displacement depending on a logical state. To do so we define the controlled displacement operator $\Lambda_1(D(\beta))$ by its action on the logical subspace of an encoded qubit:

$$\Lambda_1(D(\beta))(c_0|0_L\rangle + c_1|1_L\rangle) \otimes |\psi_{\text{mode}}\rangle = c_0|0_L\rangle \otimes |\psi_{\text{mode}}\rangle + c_1|1_L\rangle \otimes D(\beta)|\psi_{\text{mode}}\rangle \quad (189)$$

where $|\psi_{\text{mode}}\rangle$ is an arbitrary state of the bosonic mode. Similarly, we define a controlled GPG by the action:

$$\Lambda_1(U_{\text{GPG}}(\theta, \phi, \chi))(c_0|0_L\rangle + c_1|1_L\rangle) \otimes |\psi_{\text{mode}}\rangle = c_0|0_L\rangle \otimes |\psi_{\text{mode}}\rangle + c_1|1_L\rangle \otimes U_{\text{GPG}}(\theta, \phi, \chi)|\psi_{\text{mode}}\rangle. \quad (190)$$

Now let the ancilla **A** be an N qubit s -shifted gnu logical state $|+L\rangle_A = \frac{1}{\sqrt{2}}(|0_L\rangle_A + |1_L\rangle_A)$ with g odd and s even. Then $|0_L\rangle_A(|1_L\rangle_A)$ is a superposition of Dicke states with even(odd) Hamming weights. Extending the dispersive interaction over all the spins of **A**, where the notation $|1_j\rangle_A$ indicates state $|1\rangle$ of the j -th qubit in **A**, we have

$$W = g\left(\sum_{j=1}^N |1_j\rangle_A \langle 1_j| \right) \hat{a}^\dagger \hat{a}. \quad (191)$$

Again choosing a time $t = \pi/g$ the controlled displacement operator is realized by the sequence:

$$\Lambda_1(D(\beta)) = D(\beta/2)e^{-iWt}D(-\beta/2)e^{-iWt}, \quad (192)$$

which follows because all Dicke state components of logical zero(one) generate a phase space rotation by an even(odd) multiple of 2π . Now take the register **B** to be an $M \leq N$ qubit state. The controlled displacement operator can be inserted into the decomposition in Eq.(188) to realize a GPG on register **B** controlled by **A**:

$$\Lambda_1(U_{\text{GPG}}(\theta, \phi, \chi)) = \Lambda_1(D(-\beta))R(\theta J_{\mathbf{B}}^z)\Lambda_1(D(-\alpha)) \times R(-\theta J_{\mathbf{B}}^z)\Lambda_1(D(\beta))R(\theta J_{\mathbf{B}}^z) \times \Lambda_1(D(\alpha))R(-\theta J_{\mathbf{B}}^z). \quad (193)$$

Here the dispersive rotation operators on register **B** are generated by the interaction V from Eq. (186) acting only on that register and not on **A**. It is easily verified that

$$U_{\text{GPG}}(\theta = \pi, \phi = -\frac{\pi}{2}(1+M \bmod 4), \chi = \frac{\pi}{4}) = i \prod_{j=1}^M Z_j.$$

The controlled not is then constructed as

$$C_{\mathbf{A}}X_{\mathbf{B}} = e^{-i\frac{\pi}{2}J_{\mathbf{B}}^y}\Lambda_1(U_{\text{GPG}}(\pi, -\frac{\pi(1+M \bmod 4)}{2}, \frac{\pi}{4}))e^{i\frac{\pi}{2}J_{\mathbf{B}}^y}. \quad (194)$$

E. Realizing the SLD projectors

In order to achieve the precision given by the QFI, the optimal observable is given by the SLD L which as shown in Sec. A has two eigenvectors

$$\frac{|b_1\rangle \pm i|b_2\rangle}{\sqrt{2}} = \frac{|\psi\rangle \pm i|\bar{b}_2\rangle}{\sqrt{2}},$$

with eigenvalues $\pm 2v_\psi$. This can be realized by (1) performing any unitary extension of the mapping: $\frac{|b_1\rangle \pm i|b_2\rangle}{\sqrt{2}} \rightarrow |D_0^N\rangle$ (2). measuring \hat{J}^z with outcome m , and (3) weighting the result with $2v_\psi$ for the outcome $m = -N/2$ and $-2v_\psi$ otherwise. The state synthesis mapping can be done using N GPGs as described in Sec. VIC.

VII. DISCUSSIONS

This paper has three main contributions. First, we complete the theory of QEC for permutation-invariant codes. Second, we prove that by applying QEC on appropriate shifted gnu states while a noisy signal accumulates, we can nonetheless have a substantial quantum advantage in quantum sensors that do phase estimation. The noise is modelled by a linear rate of deletion errors, and the quantum advantage can in an asymptotic limit, approach the Heisenberg limit. Third, we elucidate near-term implementations of all of the algorithms that we discussed in this paper, thereby making near-term QEC and near-term QEC-enhanced quantum sensing a compelling possibility.

Our first key contribution is our introduction of a general theory of how explicit QEC procedures can be performed on *any* permutation-invariant quantum code. We unravel deep connections between our QEC theory and the representation theory of symmetric groups and Schur-Weyl duality. Namely, we show that QEC can be done by measuring total angular momentum on consecutive pairs of qubits, and labelling the syndrome with standard Young tableau. After this, we can apply geometric phase gates which act in the same way on the orthogonal spaces labelled by the standard Young tableau. QEC is greatly simplified with deletion errors. One only requires operations within the symmetric subspace, and measurements in the modulo Dicke basis.

Our second key contribution is Protocol 3 (Fig. 8), which can be used for quantum field-sensing in the face of a linear-rate of deletion errors. With appropriate prior information about the phase to be estimated, we can amplify this prior information, obtain a quantum advantage in quantum sensing.

Our third contribution is our description of how quantum control techniques can be used to implement the algorithms that we discussed in this paper.

In contrast to many other works on QEC-enhanced quantum sensing which do not consider QEC that can

correct away any part of signal, we relax this restriction. We also allow the noise to possibly act in the same space as the signal. By working in this paradigm, and by consider QEC on symmetric states, we are able to show a result that is markedly different from prior work. Namely, we show that even with a linear rate of deletions, we can approach the Heisenberg limit using quantum sensors. We are able to achieve this by finding the appropriate rates of QEC, because we do find that an excessive amount of QEC degrades the signal, so we only perform as much QEC as is necessary. We thereby offer a different perspective on the topic of QEC-enhanced quantum sensing.

There are many interesting avenues for future work. An immediate next step is to optimize our protocol for a finite number of qubits, which we leave as a problem for

future work. It is also interesting to extend our results to the simultaneous estimation of all three components of classical fields, using recent developments in multiparameter quantum metrology [53, 54].

VIII. ACKNOWLEDGEMENTS

Y.O. acknowledges support from EPSRC (Grant No. EP/W028115/1). Y.O. also acknowledges the Quantum Engineering Programme grant NRF2021-QEP2-01-P06, and the NUS startup grants (R-263-000-E32-133 and R-263-000-E32-731). G.K.B. acknowledges support from the Australian Research Council Centre of Excellence for Engineered Quantum Systems (Grant No. CE 170100009).

-
- [1] D. W. Leung, M. A. Nielsen, I. L. Chuang, and Y. Yamamoto, Approximate quantum error correction can lead to better codes, *Physical Review A* **56**, 2567 (1997).
 - [2] Y. Wu, S. Kolkowitz, S. Puri, and J. D. Thompson, Erasure conversion for fault-tolerant quantum computing in alkaline earth rydberg atom arrays, *Nature Communications* **13**, 4657 (2022).
 - [3] J. Leahy, D. Touchette, and P. Yao, Quantum insertion-deletion channels, arXiv preprint arXiv:1901.00984 (2019).
 - [4] M. Hagiwara and A. Nakayama, A four-qubits code that is a quantum deletion error-correcting code with the optimal length, in *IEEE International Symposium on Information Theory, ISIT 2020, Los Angeles, CA, USA, June 21-26, 2020* (IEEE, 2020) pp. 1870–1874.
 - [5] Y. Ouyang, Permutation-invariant quantum coding for quantum deletion channels, in *2021 IEEE International Symposium on Information Theory (ISIT)* (2021) pp. 1499–1503.
 - [6] M. Oszmaniec, R. Augusiak, C. Gogolin, J. Kolodynski, A. Acin, and M. Lewenstein, Random bosonic states for robust quantum metrology, *Physical Review X* **6**, 041044 (2016).
 - [7] Y. Ouyang, N. Shettell, and D. Markham, Robust quantum metrology with explicit symmetric states, *IEEE Transactions on Information Theory* **68**, 1809 (2022).
 - [8] Y. Ouyang and N. Rengaswamy, Describing quantum metrology with erasure errors using weight distributions of classical codes, *Phys. Rev. A* **107**, 022620 (2023).
 - [9] R. Demkowicz-Dobrzański, J. Kołodyński, and M. Guţă, The elusive heisenberg limit in quantum-enhanced metrology, *Nature Communications* **3**, 10.1038/ncomms2067 (2012).
 - [10] W. Dür, M. Skotiniotis, F. Froewis, and B. Kraus, Improved quantum metrology using quantum error correction, *Physical Review Letters* **112**, 080801 (2014).
 - [11] G. Arrad, Y. Vinkler, D. Aharonov, and A. Retzker, Increasing sensing resolution with error correction, *Physical review letters* **112**, 150801 (2014).
 - [12] E. M. Kessler, I. Lovchinsky, A. O. Sushkov, and M. D. Lukin, Quantum error correction for metrology, *Physical review letters* **112**, 150802 (2014).
 - [13] T. Unden, P. Balasubramanian, D. Louzon, Y. Vinkler, M. B. Plenio, M. Markham, D. Twitchen, A. Stacey, I. Lovchinsky, A. O. Sushkov, *et al.*, Quantum metrology enhanced by repetitive quantum error correction, *Physical review letters* **116**, 230502 (2016).
 - [14] Y. Matsuzaki and S. Benjamin, Magnetic-field sensing with quantum error detection under the effect of energy relaxation, *Physical Review A* **95**, 032303 (2017).
 - [15] S. Zhou, M. Zhang, J. Preskill, and L. Jiang, Achieving the heisenberg limit in quantum metrology using quantum error correction, *Nature Communications* **9**, 78 (2018).
 - [16] D. Layden, S. Zhou, P. Cappellaro, and L. Jiang, Ancilla-free quantum error correction codes for quantum metrology, *Physical review letters* **122**, 040502 (2019).
 - [17] W. Górecki, S. Zhou, L. Jiang, and R. Demkowicz-Dobrzański, Optimal probes and error-correction schemes in multi-parameter quantum metrology, *Quantum* **4**, 288 (2020).
 - [18] S. Zhou and L. Jiang, Optimal approximate quantum error correction for quantum metrology, *Physical Review Research* **2**, 013235 (2020).
 - [19] N. Shettell, W. J. Munro, D. Markham, and K. Nemoto, Practical limits of error correction for quantum metrology, *New Journal of Physics* **23**, 043038 (2021).
 - [20] R. Demkowicz-Dobrzański, J. Czajkowski, and P. Sekatski, Adaptive quantum metrology under general markovian noise, *Phys. Rev. X* **7**, 041009 (2017).
 - [21] M. B. Ruskai, Pauli Exchange Errors in Quantum Computation, *Physical Review Letters* **85**, 194 (2000).
 - [22] H. Pollatsek and M. B. Ruskai, Permutationally invariant codes for quantum error correction, *Linear Algebra and its Applications* **392**, 255 (2004).
 - [23] Y. Ouyang, Permutation-invariant quantum codes, *Physical Review A* **90**, 062317 (2014), 1302.3247.
 - [24] Y. Ouyang and J. Fitzsimons, Permutation-invariant codes encoding more than one qubit, *Physical Review A* **93**, 042340 (2016).
 - [25] Y. Ouyang, Permutation-invariant qudit codes from polynomials, *Linear Algebra and its Applications* **532**, 43 (2017).

- [26] Y. Ouyang and R. Chao, Permutation-invariant constant-excitation quantum codes for amplitude damping, *IEEE Transactions on Information Theory* **66**, 2921 (2019).
- [27] M. T. Johnsson, N. R. Mukty, D. Burgarth, T. Volz, and G. K. Brennen, Geometric pathway to scalable quantum sensing, *Physical Review Letters* **125**, 190403 (2020).
- [28] J. S. Sidhu and P. Kok, Geometric perspective on quantum parameter estimation, *AVS Quantum Science* **2**, 014701 (2020).
- [29] R. Movassagh and Y. Ouyang, Constructing quantum codes from any classical code and their embedding in ground space of local hamiltonians, arXiv preprint arXiv:2012.01453 (2020).
- [30] Y. Ouyang, Quantum storage in quantum ferromagnets, *Phys. Rev. B* **103**, 144417 (2021).
- [31] E. Knill and R. Laflamme, Theory of quantum error-correcting codes, *Physical Review A* **55**, 900 (1997).
- [32] T. Shibayama and M. Hagiwara, Permutation-invariant quantum codes for deletion errors, in *2021 IEEE International Symposium on Information Theory (ISIT)* (2021) pp. 1493–1498.
- [33] T. Shibayama and Y. Ouyang, The equivalence between correctability of deletions and insertions of separable states in quantum codes, in *2021 IEEE Information Theory Workshop (ITW)* (IEEE, 2021) pp. 1–6.
- [34] R. P. Stanley, *Enumerative Combinatorics: volume 1*, Vol. 1 (Cambridge University Press, 1997).
- [35] R. P. Stanley, *Enumerative Combinatorics: volume 2*, Vol. 2 (Cambridge University Press, 1999).
- [36] R. Goodman and N. R. Wallach, *Representations and invariants of the classical groups* (Cambridge University Press, 2000).
- [37] D. Bacon, I. L. Chuang, and A. W. Harrow, Efficient quantum circuits for Schur and Clebsch-Gordan transforms, *Physical Review Letters* **97**, 170502 (2006).
- [38] A. W. Harrow, The church of the symmetric subspace, arXiv preprint arXiv:1308.6595 (2013).
- [39] S. P. Jordan, Permutational quantum computing, *Quantum Info. Comput.* **10**, 470–497 (2010).
- [40] V. Havlíček and S. Strelchuk, Quantum schur sampling circuits can be strongly simulated, *Phys. Rev. Lett.* **121**, 060505 (2018).
- [41] R. A. Horn and C. R. Johnson, *Matrix analysis* (Cambridge university press, 2012).
- [42] W. M. Kirby and F. W. Strauch, A practical quantum algorithm for the schur transform, *Quantum Information & Computation* **18**, 0721 (2019).
- [43] H. Krovi, An efficient high dimensional quantum Schur transform, *Quantum* **3**, 122 (2019).
- [44] V. Havlíček, S. Strelchuk, and K. Temme, Classical algorithm for quantum su(2) schur sampling, *Phys. Rev. A* **99**, 062336 (2019).
- [45] E. Pearce-Crump, A multigraph approach for performing the quantum schur transform, arXiv preprint arXiv:2204.10694 (2022).
- [46] P. O. Boykin, T. Mor, M. Pulver, V. Roychowdhury, and F. Vatan, On universal and fault-tolerant quantum computing: a novel basis and a new constructive proof of universality for Shor’s basis, in *Foundations of Computer Science, 1999. 40th Annual Symposium on* (1999) pp. 486–494.
- [47] X. Zhou, D. W. Leung, and I. L. Chuang, Methodology for quantum logic gate construction, *Physical Review A* **62**, 052316 (2000).
- [48] T. Rudolph and S. S. Virmani, Relational quantum computing using only maximally mixed initial qubit states (2023), arXiv:2107.03239 [quant-ph].
- [49] M. H. Freedman, M. B. Hastings, and M. Shokrian Zini, Symmetry Protected Quantum Computation, *Quantum* **5**, 554 (2021).
- [50] M. O. Scully and M. S. Zubairy, *Quantum Optics* (Cambridge University Press, 1997).
- [51] X. Wang and P. Zanardi, Simulation of many-body interactions by conditional geometric phases, *Phys. Rev. A* **65**, 032327 (2002).
- [52] S. T. Merkel, G. Brennen, P. S. Jessen, and I. H. Deutsch, Constructing general unitary maps from state preparations, *Phys. Rev. A* **80**, 023424 (2009).
- [53] J. S. Sidhu, Y. Ouyang, E. T. Campbell, and P. Kok, Tight bounds on the simultaneous estimation of incompatible parameters, *Phys. Rev. X* **11**, 011028 (2021).
- [54] M. Hayashi and Y. Ouyang, Tight Cramér-Rao type bounds for multiparameter quantum metrology through conic programming, arXiv preprint arXiv:2209.05218 (2022).
- [55] G. Tóth and I. Apellaniz, Quantum metrology from a quantum information science perspective, *Journal of Physics A: Mathematical and Theoretical* **47**, 424006 (2014).

Appendix A: Optimal measurements for symmetric states

Here, we derive the optimal SLD for field sensing when pure symmetric states are used.

Proof of Theorem 1. Now

$$\hat{J}^z |D_w^N\rangle = (N/2 - w) |D_w^N\rangle. \quad (\text{A1})$$

Hence, for $|\psi\rangle = \sum_w a_w |D_w^N\rangle$, we have

$$\begin{aligned} \hat{J}^z |\psi\rangle &= \sum_w a_w (N/2 - w) |D_w^N\rangle \\ &= (N/2) |\psi\rangle - \sum_w w a_w |D_w^N\rangle. \end{aligned} \quad (\text{A2})$$

For us, $\rho_\theta = |\psi\rangle\langle\psi|$ is a pure state. Hence a feasible solution of L to (3) is $L = 2i(|\psi\rangle\langle\psi| \hat{J}^z - \hat{J}^z |\psi\rangle\langle\psi|)$ [55]. Using (A2), we can express L as

$$\begin{aligned} L &= 2i|\psi\rangle\langle\psi| \left((N/2) - \sum_{w'} w' a_{w'}^* \langle D_{w'}^N | \right) \\ &\quad - 2i \left((N/2) |\psi\rangle - \sum_w w a_w |D_w^N\rangle \right) \langle\psi| \\ &= -2i \sum_{w'} w' a_{w'}^* |\psi\rangle \langle D_{w'}^N | + 2i \sum_w w a_w |D_w^N\rangle \langle\psi| \\ &= i \sum_{w, w'} a_w a_{w'}^* |D_w\rangle \langle D_{w'}| (2w - 2w'). \end{aligned} \quad (\text{A3})$$

Note the simple identity

$$(u+i)(v-i) - (u-i)(v+i) = 2i(v-u). \quad (\text{A4})$$

This implies that by setting $a(u) = u + i$, we have that

$$a(u)a(v)^* - a(u)^*a(v) = 2i(v - u). \quad (\text{A5})$$

for real u and v . Using (A5) in (A3), we get

$$\begin{aligned} L &= \sum_{w,w'} a_w a_{w'}^* a(w) a(w')^* |D_w^N\rangle \langle D_{w'}^N| \\ &\quad - \sum_{w,w'} a_w a_{w'}^* a(w)^* a(w') |D_w^N\rangle \langle D_{w'}^N|. \end{aligned} \quad (\text{A6})$$

Let

$$|v_1\rangle = \sum_w a_w(w + i) |D_w^N\rangle, \quad (\text{A7})$$

$$|v_2\rangle = \sum_w a_w(w - i) |D_w^N\rangle. \quad (\text{A8})$$

Substituting the definitions of $|v_1\rangle$ and $|v_2\rangle$, we find

$$L = |v_1\rangle \langle v_1| - |v_2\rangle \langle v_2|. \quad (\text{A9})$$

While $|v_1\rangle$ and $|v_2\rangle$ are not necessarily orthogonal, the vector

$$|v_2'\rangle = |v_2\rangle - \frac{\langle v_1 | v_2 \rangle}{\langle v_1 | v_1 \rangle} |v_1\rangle \quad (\text{A10})$$

is orthogonal to $|v_1\rangle$. Now $|v_1\rangle$ and $|v_2'\rangle$ lie in the span of $|b_1\rangle$ and $|b_2\rangle$ where

$$|b_1\rangle = \sum_w a_w |D_w^N\rangle \quad (\text{A11})$$

$$|b_2\rangle = \sum_w w a_w |D_w^N\rangle. \quad (\text{A12})$$

By definition $\langle b_1 | b_1 \rangle = 1$. Using Gram-Schmidt we see that

$$\begin{aligned} |b_2'\rangle &= |b_2\rangle - \frac{|b_1\rangle \langle b_1 | b_2 \rangle}{\langle b_1 | b_1 \rangle} \\ &= |b_2\rangle - m_1 |b_1\rangle. \end{aligned} \quad (\text{A13})$$

Hence $|b_2\rangle = |b_2'\rangle + m_1 |b_1\rangle$. Also note that

$$\begin{aligned} \langle b_2' | b_2' \rangle &= \langle b_2 | b_2 \rangle - m_1 \langle b_2 | b_1 \rangle - m_1 \langle b_1 | b_2 \rangle + m_1^2 \langle b_1 | b_1 \rangle \\ &= m_2 - m_1^2 = v_\psi. \end{aligned} \quad (\text{A14})$$

Now let $|\bar{b}_2\rangle = |b_2'\rangle / \sqrt{\langle b_2' | b_2' \rangle}$ so that $\{|b_1\rangle, |\bar{b}_2\rangle\}$ is an orthonormal basis. In this orthonormal basis, we can write

$$\begin{aligned} |v_1\rangle &= i|b_1\rangle + |b_2\rangle \\ &= i|b_1\rangle + |b_2'\rangle + m_1 |b_1\rangle \\ &= (m_1 + i)|b_1\rangle + \sqrt{v_\psi} |\bar{b}_2\rangle \end{aligned} \quad (\text{A15})$$

Similarly, we get

$$\begin{aligned} |v_2\rangle &= i|b_1\rangle + |b_2\rangle \\ &= i|b_1\rangle + |b_2'\rangle + m_1 |b_1\rangle \\ &= (m_1 - i)|b_1\rangle + \sqrt{v_\psi} |\bar{b}_2\rangle \end{aligned} \quad (\text{A16})$$

Hence on the orthonormal basis $\{|b_1\rangle, |\bar{b}_2\rangle\}$, the SLD is an effective size two matrix

$$\begin{aligned} M &= \begin{pmatrix} |m_1 + i|^2 & (m_1 + i)\sqrt{v_\psi} \\ (m_1 - i)\sqrt{v_\psi} & v_\psi \end{pmatrix} \\ &\quad - \begin{pmatrix} |m_1 - i|^2 & (m_1 - i)\sqrt{v_\psi} \\ (m_1 + i)\sqrt{v_\psi} & v_\psi \end{pmatrix} \\ &= 2\sqrt{v_\psi} \begin{pmatrix} 0 & -i \\ i & 0 \end{pmatrix}. \end{aligned} \quad (\text{A17})$$

Thus the eigenvalues of the SLD operator are given by $\pm 2v_\psi$ with corresponding eigenvectors

$$\frac{|b_1\rangle \pm i|\bar{b}_2\rangle}{\sqrt{2}} = \frac{|\psi\rangle \pm i|\bar{b}_2\rangle}{\sqrt{2}}. \quad (\text{A18})$$

□

Appendix B: Calculations on Fisher Information

Here, we evaluate a lower bound on the FI from measurement in the plus-minus code basis for a shifted gnu code, after U_θ applies on $|+_{g,n,u,s}\rangle$.

Proof of Theorem 3. Recall that the FI is

$$I(\theta) = \frac{1}{p_+} \left(\frac{dp_+}{d\theta} \right)^2 + \frac{1}{p_-} \left(\frac{dp_-}{d\theta} \right)^2. \quad (\text{B1})$$

For any shifted gnu code,

$$\begin{aligned} p_+ &= \langle +_L | U_\theta | +_L \rangle \langle +_L | U_\theta^\dagger | +_L \rangle \\ &= |\langle +_L | U_\theta | +_L \rangle|^2 \\ &= \left| 2^{-n} \sum_{k=0}^n \binom{n}{k} e^{-2igk\theta} \right|^2 \\ &= 2^{-2n} ((1 + e^{-2ig\theta})(1 + e^{+2ig\theta}))^n \\ &= 2^{-2n} (2 + 2\cos(2g\theta))^n \\ &= \left(\frac{1}{2} + \frac{1}{2} \cos(2g\theta) \right)^n \\ &= \cos^{2n}(g\theta). \end{aligned} \quad (\text{B2})$$

Similarly,

$$\begin{aligned} p_- &= \langle -_L | U_\theta | +_L \rangle \langle +_L | U_\theta^\dagger | -_L \rangle \\ &= |\langle -_L | U_\theta | +_L \rangle|^2 \\ &= \left| 2^{-n} \sum_{k=0}^n \binom{n}{k} (-1)^k e^{-2igk\theta} \right|^2 \\ &= 2^{-2n} ((1 + e^{-2ig\theta - \pi i})(1 + e^{+2ig\theta + \pi i}))^n \\ &= 2^{-2n} (2 + 2\cos(2g\theta + \pi))^n \\ &= \left(\frac{1}{2} - \frac{1}{2} \cos(2g\theta) \right)^n \\ &= \sin^{2n}(g\theta). \end{aligned} \quad (\text{B3})$$

It follows that

$$\frac{\partial p_+}{\partial \theta} = -2gn \cos^{2n-1}(g\theta) \sin(g\theta), \quad (\text{B4})$$

$$\frac{\partial p_-}{\partial \theta} = 2gn \sin^{2n-1}(g\theta) \cos(g\theta). \quad (\text{B5})$$

Hence

$$\frac{\left(\frac{\partial p_+}{\partial \theta}\right)^2}{p_+} = 4g^2 n^2 \sin^2(g\theta) \cos^{2n-2}(g\theta) \quad (\text{B6})$$

and

$$\frac{\left(\frac{\partial p_-}{\partial \theta}\right)^2}{p_-} = 4g^2 n^2 \cos^2(g\theta) \sin^{2n-2}(g\theta). \quad (\text{B7})$$

The sum of the terms in (B6) and (B7) is the FI. \square

Proof of Lemma 15. Let us define \bar{U}_Φ , so that

$$\bar{U}_\Phi |a_+\rangle = \frac{|a_0\rangle + e^{i\Phi} |a_1\rangle}{\sqrt{2}} \quad (\text{B8})$$

$$\bar{U}_\Phi |a_-\rangle = \frac{|a_0\rangle - e^{i\Phi} |a_1\rangle}{\sqrt{2}}. \quad (\text{B9})$$

Note that $|\psi(\Phi)\rangle\langle\psi(\Phi)| = \bar{U}_\Phi |a_+\rangle\langle a_+| \bar{U}_\Phi^\dagger$. Hence we find that

$$\begin{aligned} \text{tr}|a_+\rangle\langle a_+|\psi(\Phi)\rangle\langle\psi(\Phi)| &= \langle a_+|\bar{U}_\Phi|a_+\rangle\langle a_+|\bar{U}_\Phi^\dagger|a_+\rangle \\ &= |\langle a_+|\bar{U}_\Phi|a_+\rangle|^2 \end{aligned} \quad (\text{B10})$$

$$\begin{aligned} \text{tr}|a_-\rangle\langle a_-|\psi(\Phi)\rangle\langle\psi(\Phi)| &= \langle a_-|\bar{U}_\Phi|a_+\rangle\langle a_+|\bar{U}_\Phi^\dagger|a_-\rangle \\ &= |\langle a_-|\bar{U}_\Phi|a_+\rangle|^2. \end{aligned} \quad (\text{B11})$$

The FI from measurement corresponding to the projectors $|a_+\rangle\langle a_+|$ and $|a_-\rangle\langle a_-|$ is

$$I(\theta) = \frac{1}{p_+} \left(\frac{\partial p_+}{\partial \theta}\right)^2 + \frac{1}{p_-} \left(\frac{\partial p_-}{\partial \theta}\right)^2, \quad (\text{B12})$$

where

$$\begin{aligned} p_+ &= \langle a_+|\bar{U}_\Phi|a_+\rangle\langle a_+|\bar{U}_\Phi^\dagger|a_+\rangle \\ p_- &= \langle a_-|\bar{U}_\Phi|a_-\rangle\langle a_-|\bar{U}_\Phi^\dagger|a_-\rangle. \end{aligned} \quad (\text{B13})$$

Note that when $\phi = \pi/4$, $p_+ = \cos^2(\Phi/2)$ and $p_- = \sin^2(\Phi/2)$. Hence $\frac{\partial p_\pm}{\partial \theta} = \mp \sin(\Phi/2) \cos(\Phi/2) \frac{d\Phi}{d\theta}$ and it follows that

$$\frac{1}{p_+} \left(\frac{\partial p_+}{\partial \theta}\right)^2 = \left(\frac{\partial \Phi}{\partial \theta}\right)^2 \sin^2(\Phi/2) \quad (\text{B14})$$

$$\frac{1}{p_-} \left(\frac{\partial p_-}{\partial \theta}\right)^2 = \left(\frac{\partial \Phi}{\partial \theta}\right)^2 \cos^2(\Phi/2). \quad (\text{B15})$$

Adding these two terms above gives the FI.

Now let us consider the case for general ϕ . Then

$$\begin{aligned} p_+ &= \frac{1}{2}(\cos \phi + \sin \phi e^{i\Phi})(\cos \phi + \sin \phi e^{-i\Phi}) \\ &= \frac{1}{2}(1 + \sin \phi \cos \phi (e^{i\Phi} + e^{-i\Phi})) \\ &= \frac{1}{2}(1 + \sin 2\phi \cos \Phi). \end{aligned} \quad (\text{B16})$$

We also have

$$\begin{aligned} p_- &= \frac{1}{2}(\cos \phi - \sin \phi e^{i\Phi})(\cos \phi - \sin \phi e^{-i\Phi}) \\ &= \frac{1}{2}(1 - \sin \phi \cos \phi (e^{i\Phi} + e^{-i\Phi})) \\ &= \frac{1}{2}(1 - \sin 2\phi \cos \Phi). \end{aligned} \quad (\text{B17})$$

Hence it follows that

$$\frac{\partial}{\partial \theta} p_\pm = \mp \frac{1}{2} \sin 2\phi \sin \Phi \frac{\partial \Phi}{\partial \theta}. \quad (\text{B18})$$

Therefore the FI is

$$\begin{aligned} &\frac{\frac{1}{4} \sin^2 2\phi \sin^2 \Phi \left(\frac{\partial \Phi}{\partial \theta}\right)^2}{\frac{1}{2}(1 + \sin 2\phi \cos \Phi)} + \frac{\frac{1}{4} \sin^2 2\phi \sin^2 \Phi \left(\frac{\partial \Phi}{\partial \theta}\right)^2}{\frac{1}{2}(1 - \sin 2\phi \cos \Phi)} \\ &= \frac{\sin^2 2\phi \sin^2 \Phi \left(\frac{\partial \Phi}{\partial \theta}\right)^2}{2(1 + \sin 2\phi \cos \Phi)} + \frac{\sin^2 2\phi \sin^2 \Phi \left(\frac{\partial \Phi}{\partial \theta}\right)^2}{2(1 - \sin 2\phi \cos \Phi)} \\ &= \frac{1}{2} \sin^2 2\phi \sin^2 \Phi \left(\frac{\partial \Phi}{\partial \theta}\right)^2 \frac{1 - \sin 2\phi \cos \Phi + 1 + \sin 2\phi \cos \Phi}{1 - \sin^2 2\phi \cos^2 \Phi} \\ &= \frac{\sin^2 2\phi \sin^2 \Phi \left(\frac{\partial \Phi}{\partial \theta}\right)^2}{1 - \sin^2 2\phi \cos^2 \Phi}. \end{aligned} \quad (\text{B19})$$

This gives the result. \square

Appendix C: Deletions

Here we like to evaluate what happens to an arbitrary symmetric state after t deletions occur.

Proof of Lemma 4. Recall that the input state before deletions is $|\psi\rangle = \sum_w a_w |D_w^N\rangle$ in the Dicke basis. We can alternatively write $|\psi\rangle = \sum_w \bar{a}_w |H_w^N\rangle$ where $\bar{a}_w = a_w / \sqrt{\binom{N}{w}}$.

We first note determine the domain of the summation index in the Vandermonde decomposition

$$|H_w^N\rangle = \sum_a |H_a^t\rangle \otimes |H_{w-a}^{N-t}\rangle. \quad (\text{C1})$$

Note that we must have $0 \leq a \leq t$ and $0 \leq w-a \leq N-t$. Together, these inequalities are equivalent to $\max\{0, t+w-N\} \leq a \leq \min\{w, t\}$. Hence it follows that

$$|H_w^N\rangle = \sum_{a \in A_w} |H_a^t\rangle \otimes |H_{w-a}^{N-t}\rangle, \quad (\text{C2})$$

where

$$A_w = \{a : 0, t + w - N \leq a \leq w, t\}. \quad (\text{C3})$$

Applying the definition of the partial trace and its linearity, we see that $\text{tr}_t(|\psi\rangle\langle\psi|)$ is equal to

$$\sum_{\mathbf{x} \in \{0,1\}^t} \sum_{w,v=0}^N \bar{a}_w \bar{a}_v^* \left(\langle \mathbf{x} | \otimes I^{\otimes N-t} \right) |H_w^N\rangle \langle H_v^N| \times \left(|\mathbf{x}\rangle \otimes I^{\otimes N-t} \right). \quad (\text{C4})$$

Using (C2), we find that $|H_w^N\rangle \langle H_v^N|$ is equal to

$$\sum_{a \in A_w} \sum_{b \in A_v} |H_a^t\rangle \langle H_b^t| \otimes |H_{w-a}^{N-t}\rangle \langle H_{v-b}^{N-t}|. \quad (\text{C5})$$

Hence we find that $\text{tr}_t(|\psi\rangle\langle\psi|)$ is equal to

$$\sum_{\mathbf{x} \in \{0,1\}^t} \sum_{w,v=0}^N \sum_{\substack{a \in A_w \\ b \in A_v}} \bar{a}_w \bar{a}_v^* \langle \mathbf{x} | H_a^t \rangle \langle H_b^t | \mathbf{x} \rangle |H_{w-a}^{N-t}\rangle \langle H_{v-b}^{N-t}|. \quad (\text{C6})$$

Now note that $\langle \mathbf{x} | H_a^t \rangle = 1$ when the Hamming weight of \mathbf{x} is equal to a , and $\langle \mathbf{x} | H_a^t \rangle = 0$ otherwise. Hence for non-trivial contributions to the above sum, we must have $a = b$. Using these facts and moving the summation over \mathbf{x} inside, we find that $\text{tr}_t(|\psi\rangle\langle\psi|)$ equals to

$$\sum_{a=0}^t \binom{t}{a} \sum_{w,v=0}^N \bar{a}_w \bar{a}_v^* \delta[a \in A_w] \delta[a \in A_v] |H_{w-a}^{N-t}\rangle \langle H_{v-a}^{N-t}|. \quad (\text{C7})$$

Hence

$$\text{tr}_t(|\psi\rangle\langle\psi|) = \sum_{a=0}^t \binom{t}{a} |\phi_a\rangle \langle \phi_a|, \quad (\text{C8})$$

where

$$\begin{aligned} |\phi_a\rangle &= \sum_w \delta[a \in A_w] \bar{a}_w |H_{w-a}^{N-t}\rangle \\ &= \sum_{w=a}^{N-t+a} \bar{a}_w |H_{w-a}^{N-t}\rangle \\ &= \sum_{w=a}^{N-t+a} \bar{a}_w \sqrt{\binom{N-t}{w-a}} |D_{w-a}^{N-t}\rangle \\ &= \sum_{w=a}^{N-t+a} a_w \frac{\sqrt{\binom{N-t}{w-a}}}{\sqrt{\binom{N}{w}}} |D_{w-a}^{N-t}\rangle. \end{aligned} \quad (\text{C9})$$

Since $|\phi_a\rangle = |\psi\rangle_a$, the result follows. \square

Appendix D: Amplitude damping errors

Here, we study what happens after amplitude damping errors afflict a pure symmetric state.

Proof of Lemma 6. For non-negative integer x such that $x \leq N$, let $(\mathbf{1}^x, \mathbf{0}^{N-x})$ denote a length N binary vector that has its first x bits equal to 1 and the remaining bits equal to 0. Let $\mathbf{1}^x$ denote a ones vector of length x and $\mathbf{0}^{N-x}$ be a zeros vector of length $N - x$. Then

$$\begin{aligned} &A_{(\mathbf{1}^x, \mathbf{0}^{N-x})} |H_w^N\rangle \\ &= \sum_{j=0}^x (A_{\mathbf{1}^x} |H_j^N\rangle) \otimes (A_{\mathbf{0}^{N-x}} |H_{w-j}^{N-x}\rangle) \\ &= (A_{\mathbf{1}^x} |H_x^N\rangle) \otimes (A_{\mathbf{0}^{N-x}} |H_{w-x}^{N-x}\rangle) \\ &= (\gamma^{x/2} |H_0^N\rangle) \otimes ((1-\gamma)^{(w-x)/2} |H_{w-x}^{N-x}\rangle) \\ &= \sqrt{q_w(x)} |0\rangle^{\otimes x} \otimes |H_{w-x}^{N-x}\rangle, \end{aligned} \quad (\text{D1})$$

where $q_w(x) = \gamma^x (1-\gamma)^{w-x}$. From this it follows that

$$\begin{aligned} A_{(\mathbf{1}^x, \mathbf{0}^{N-x})} |D_w^N\rangle &= \frac{1}{\sqrt{\binom{N}{w}}} A_{(\mathbf{1}^x, \mathbf{0}^{N-x})} |H_w^N\rangle \\ &= \frac{\sqrt{q_w(x)}}{\sqrt{\binom{N}{w}}} |0\rangle^{\otimes x} \otimes |H_{w-x}^{N-x}\rangle \\ &= \sqrt{\frac{\binom{N-x}{w-x}}{\binom{N}{w}}} \sqrt{q_w(x)} |0\rangle^{\otimes x} \otimes |D_{w-x}^{N-x}\rangle \\ &= \sqrt{\frac{\binom{w}{x}}{\binom{N}{x}}} \sqrt{q_w(x)} |0\rangle^{\otimes x} \otimes |D_{w-x}^{N-x}\rangle \\ &= \sqrt{\frac{p_w(x)}{\binom{N}{x}}} |0\rangle^{\otimes x} \otimes |D_{w-x}^{N-x}\rangle. \end{aligned} \quad (\text{D2})$$

When $x > w$ we trivially have $A_{(\mathbf{1}^x, \mathbf{0}^{N-x})} |D_w^N\rangle = 0$. Since $\binom{w}{x} = 0$ and $p_w(x) = 0$ whenever $x > w$, for all $x = 0, 1, \dots, N$, we have

$$A_{(\mathbf{1}^x, \mathbf{0}^{N-x})} |D_w^N\rangle = \sqrt{\frac{p_w(x)}{\binom{N}{x}}} |0\rangle^{\otimes x} \otimes |D_{w-x}^{N-x}\rangle. \quad (\text{D3})$$

Hence,

$$\begin{aligned} &\mathcal{A}_{N,\gamma}(|D_w^N\rangle \langle D_{w'}^N|) \\ &= \sum_{x=0}^N \sum_{|P|=x} \frac{\sqrt{p_w(x) p_{w'}(x)}}{\binom{N}{x}} \text{Ins}_P(|D_w^N\rangle \langle D_{w'}^N|). \end{aligned} \quad (\text{D4})$$

Hence,

$$\begin{aligned}
& \mathcal{A}_{N,\gamma}(|\psi\rangle\langle\psi|) \\
&= \sum_{w,w'=0}^N a_w a_{w'}^* \mathcal{A}_{N,\gamma}(|D_w^N\rangle\langle D_{w'}^N|) \\
&= \sum_{w,w'=0}^N a_w a_{w'}^* \sum_{x=0}^N \sum_{|P|=x} \frac{\sqrt{p_w(x)p_{w'}(x)}}{\binom{N}{x}} \text{Ins}_P(|D_w^N\rangle\langle D_{w'}^N|).
\end{aligned} \tag{D5}$$

Exchanging the orders of the summations, the lemma follows after substituting the definition of $|\phi_x\rangle$. \square

Appendix E: Binomial identities

In this section, let $S(n, s)$ denote the Stirling number of the second kind, and denote $k_{(j)}$ as the falling factorial $k \dots (k - j + 1)$. Next, we have the following lemma.

Lemma 18 ([23, Lemma 1]). *Let n and s be non-negative integers. If $s < n$, then*

$$\sum_{k \text{ even}} \binom{n}{k} k^s = \sum_{k \text{ odd}} \binom{n}{k} k^s. \tag{E1}$$

Here we extend the above lemma for larger s .

Lemma 19. *Let n and s be non-negative integers. Let $s \geq n$. When n is even, then*

$$\sum_{k \text{ even}} \binom{n}{k} k^s + S(s, n)n! = \sum_{k \text{ odd}} \binom{n}{k} k^s. \tag{E2}$$

When n is odd, then

$$\sum_{k \text{ even}} \binom{n}{k} k^s = \sum_{k \text{ odd}} \binom{n}{k} k^s + S(s, n)n!. \tag{E3}$$

Proof. The main idea is to use the identity $k^s = \sum_{j=0}^s S(s, j)k_{(j)}$. Next we note that whenever k is a non-negative integer and if $k \leq n$, then $k_{(j)} = 0$ for all $j > n$. Hence in this situation, $k^s = \sum_{j=0}^n S(s, j)k_{(j)}$. Note that

$$\begin{aligned}
\sum_{k \text{ even}} \binom{n}{k} k^s &= \sum_{k \text{ even}} \binom{n}{k} \sum_{j=0}^n S(s, j)k_{(j)} \\
&= \sum_{j=0}^n S(s, j) \sum_{k \text{ even}} \binom{n}{k} k_{(j)}
\end{aligned} \tag{E4}$$

When n is even, we can use Lemma 18 to get

$$\begin{aligned}
\sum_{k \text{ even}} \binom{n}{k} k^s &= S(s, n)n! + \sum_{j=0}^{n-1} S(s, j) \sum_{k \text{ even}} \binom{n}{k} k_{(j)} \\
&= S(s, n)n! + \sum_{j=0}^{n-1} S(s, j) \sum_{k \text{ odd}} \binom{n}{k} k_{(j)} \\
&= S(s, n)n! + \sum_{k \text{ odd}} \binom{n}{k} k^s.
\end{aligned} \tag{E5}$$

Similarly, when n is odd, we get

$$\sum_{k \text{ odd}} \binom{n}{k} k^s = S(s, n)n! + \sum_{k \text{ even}} \binom{n}{k} k^s. \tag{E6}$$

\square

Lemma 20. *Let n, s be non-negative integers, and let $s < n$. Let y be a real number. Let $y' = y/2$. Then*

$$\begin{aligned}
& \sum_{k \text{ even}} \binom{n}{k} k_{(s)} e^{iky} \\
&= n_{(s)} e^{iy'(n+s)} 2^{n-s-1} (\cos^{n-s} y' + (-1)^n i^{n-s} \sin^{n-s} y'),
\end{aligned} \tag{E7}$$

and

$$\begin{aligned}
& \sum_{k \text{ odd}} \binom{n}{k} k_{(s)} e^{iky} \\
&= n_{(s)} e^{iy'(n+s)} 2^{n-s-1} (\cos^{n-s} y' - (-1)^n i^{n-s} \sin^{n-s} y').
\end{aligned} \tag{E8}$$

Proof. To prove this lemma, we use the method of generating functions. Consider the generating function $f(x) = (1+x)^n$. Expanding $f(x)$ as a power series in x using the binomial theorem, we see that

$$f(x) = \sum_{k=0}^n \binom{n}{k} x^k. \tag{E9}$$

Then by taking s formal derivatives of $f(x)$ with respect to x , we get that for all non-negative integers n' such that $s < n$, we have

$$\begin{aligned}
\frac{d^s f(x)}{dx^s} &= n_{(s)} (1+x)^{n-s} \\
&= \sum_{k=0}^n \binom{n}{k} k_{(s)} x^{k-s} \\
&= \sum_{k=0}^n \binom{n}{k} k_{(s)} x^{k-s}.
\end{aligned} \tag{E10}$$

Next, we make the substitution $x = e^{iy}$ to get

$$\begin{aligned}
n_s (1 + e^{iy})^{n-s} &= \sum_{k=0}^n \binom{n}{k} k_{(s)} (e^{iy})^{k-s} \\
&= \sum_{k=0}^n \binom{n}{k} k_{(s)} e^{i(k-s)y}.
\end{aligned} \tag{E11}$$

Rearranging the terms in the above equation, we get

$$\sum_{k=0}^n \binom{n}{k} k_{(s)} e^{iky} = n_{(s)} (1 + e^{iy})^{n-s} e^{isy}. \tag{E12}$$

We can also make the substitution $x = -e^{iy}$ to get

$$\sum_{k=0}^n \binom{n}{k} k_{(s)} e^{iky} (-1)^k = n_{(s)} (1 - e^{iy})^{n-s} e^{isy} (-1)^s. \quad (\text{E13})$$

By the method of generating functions, it follows that

$$\begin{aligned} & \sum_{k \text{ even}} \binom{n}{k} k_{(s)} e^{iky} (-1)^k \\ &= \frac{1}{2} \left(\sum_{k=0}^n \binom{n}{k} k_{(s)} e^{iky} + \sum_{k=0}^n \binom{n}{k} k_{(s)} e^{iky} (-1)^k \right), \end{aligned} \quad (\text{E14})$$

and

$$\begin{aligned} & \sum_{k \text{ odd}} \binom{n}{k} k_{(s)} e^{iky} (-1)^k \\ &= \frac{1}{2} \left(\sum_{k=0}^n \binom{n}{k} k_{(s)} e^{iky} - \sum_{k=0}^n \binom{n}{k} k_{(s)} e^{iky} (-1)^k \right). \end{aligned} \quad (\text{E15})$$

Hence

$$\begin{aligned} & \sum_{k \text{ even}} \binom{n}{k} k_{(s)} e^{iky} (-1)^k \\ &= \frac{n_{(s)} ((1 + e^{iy})^{n-s} e^{isy} + (1 - e^{iy})^{n-s} e^{isy} (-1)^s)}{2} \end{aligned} \quad (\text{E16})$$

and

$$\begin{aligned} & \sum_{k \text{ odd}} \binom{n}{k} k_{(s)} e^{iky} (-1)^k \\ &= \frac{n_{(s)} ((1 + e^{iy})^{n-s} e^{isy} - (1 - e^{iy})^{n-s} e^{isy} (-1)^s)}{2}. \end{aligned} \quad (\text{E17})$$

Next we use the fact that

$$\begin{aligned} & \frac{(1 + e^{iy})^{n-s} \pm (-1)^s (1 - e^{iy})^{n-s}}{2} \\ &= e^{iy(n-s)/2} 2^{n-s-1} (\cos^{n-s}(y/2) \pm (-1)^s (-i)^{n-s} \sin^{n-s}(y/2)) \end{aligned} \quad (\text{E18})$$

to get the result. \square

Next we evaluate binomial sums weighted by the product of monomials and exponentials.

Lemma 21. *Let n and s be non-negative integers where $s < n$. Let y be a real number and let $y' = y/2$. Then*

$$\begin{aligned} & 2^{-n+1} \sum_{k \text{ even}} \binom{n}{k} k^s e^{iky} \\ &= 2^{-j} \sum_{j=0}^s S(s, j) n_{(j)} e^{i(n+j)y'} \\ & \quad \times (\cos^{n-j} y' + (-1)^j (-i)^{n-j} \sin^{n-j} y') \end{aligned} \quad (\text{E19})$$

and

$$\begin{aligned} & 2^{-n+1} \sum_{k \text{ odd}} \binom{n}{k} k^s e^{iky} \\ &= 2^{-j} \sum_{j=0}^s S(s, j) n_{(j)} e^{i(n+j)y'} \\ & \quad \times (\cos^{n-j} y' - (-1)^j (-i)^{n-j} \sin^{n-j} y'). \end{aligned} \quad (\text{E20})$$

For example, we have for $s = 0$,

$$\begin{aligned} & 2^{-n+1} \sum_{k \text{ even}} \binom{n}{k} e^{iky} \\ &= e^{iny'} (\cos^n y' + (-i)^n \sin^n y'), \end{aligned} \quad (\text{E21})$$

$$\begin{aligned} & 2^{-n+1} \sum_{k \text{ odd}} \binom{n}{k} e^{iky} \\ &= e^{iny'} (\cos^n y' - (-i)^n \sin^n y'). \end{aligned} \quad (\text{E22})$$

When $s = 1$ we have

$$\begin{aligned} & 2^{-n+1} \sum_{k \text{ even}} \binom{n}{k} k e^{iky} \\ &= 2^{-1} n e^{i(n+1)y'} (\cos^{n-1} y' - (-i)^{n-1} \sin^{n-1} y') \\ & 2^{-n+1} \sum_{k \text{ odd}} \binom{n}{k} k e^{iky} \\ &= 2^{-1} n e^{i(n+1)y'} (\cos^{n-1} y' + (-i)^{n-1} \sin^{n-1} y'). \end{aligned} \quad (\text{E23})$$

When $s = 2$ we have the following

$$\begin{aligned} & 2^{-n+1} \sum_{k \text{ even}} \binom{n}{k} k^2 e^{iky} \\ &= 2^{-1} n e^{i(n+1)y'} (\cos^{n-1} y' - (-i)^{n-1} \sin^{n-1} y') \\ & \quad + 2^{-2} n(n-1) e^{i(n+2)y'} (\cos^{n-1} y' + (-i)^{n-2} \sin^{n-2} y') \\ & 2^{-n+1} \sum_{k \text{ odd}} \binom{n}{k} k^2 e^{iky} \\ &= 2^{-1} n e^{i(n+1)y'} (\cos^{n-1} y' + (-i)^{n-1} \sin^{n-1} y') \\ & \quad + 2^{-2} n(n-1) e^{i(n+2)y'} (\cos^{n-1} y' - (-i)^{n-2} \sin^{n-2} y'). \end{aligned} \quad (\text{E24})$$

Proof of Lemma 21. We can express monomials x^n in terms of falling factorials:

$$x^n = \sum_{k=0}^n S(n, k) x_{(k)}. \quad (\text{E25})$$

Hence we see that

$$\begin{aligned} & 2^{-n+1} \sum_{k \text{ even}} \binom{n}{k} k^s e^{iky} \\ &= 2^{-n+1} \sum_{k \text{ even}} \binom{n}{k} \left(\sum_{j=0}^s S(s, j) k_{(j)} \right) e^{iky} \\ &= 2^{-n+1} \sum_{j=0}^s S(s, j) \sum_{k \text{ even}} \binom{n}{k} k_{(j)}. \end{aligned} \quad (\text{E26})$$

Using Lemma 20 gives the first result. Similarly, we use Lemma 20 to get the second result. \square

Next we generalize Lemma 21 to include binomial sums weighted by exponentials and higher power monomials.

Lemma 22. *Let n and s be non-negative integers. Let y be a real number and let $y' = y/2$. When n is even,*

$$\begin{aligned} & 2^{-n+1} \sum_{k \text{ even}} \binom{n}{k} k^s e^{iky} \\ &= \frac{S(s, n) n! e^{iny}}{2^{n-1}} + \sum_{j=0}^{n-1} S(s, j) \frac{n^{(j)}}{2^j} e^{iy'(n+j)} \\ & \quad \times (\cos^{n-j} y' + (-1)^n i^{n-j} \sin^{n-j} y') \end{aligned} \quad (\text{E27})$$

and

$$\begin{aligned} & 2^{-n+1} \sum_{k \text{ odd}} \binom{n}{k} k^s e^{iky} \\ &= \sum_{j=0}^{n-1} S(s, j) \frac{n^{(j)}}{2^j} e^{iy'(n+j)} (\cos^{n-j} y' - (-1)^n i^{n-j} \sin^{n-j} y'). \end{aligned} \quad (\text{E28})$$

When n is odd,

$$\begin{aligned} & 2^{-n+1} \sum_{k \text{ even}} \binom{n}{k} k^s e^{iky} \\ &= \sum_{j=0}^{n-1} S(s, j) \frac{n^{(j)}}{2^j} e^{iy'(n+j)} (\cos^{n-j} y' + (-1)^n i^{n-j} \sin^{n-j} y') \end{aligned} \quad (\text{E29})$$

and

$$\begin{aligned} & 2^{-n+1} \sum_{k \text{ odd}} \binom{n}{k} k^s e^{iky} \\ &= \frac{S(s, n) n! e^{iny}}{2^{n-1}} + \sum_{j=0}^{n-1} S(s, j) \frac{n^{(j)}}{2^j} e^{iy'(n+j)} \\ & \quad \times (\cos^{n-j} y' - (-1)^n i^{n-j} \sin^{n-j} y'). \end{aligned} \quad (\text{E30})$$

Proof. Note that for non-negative integer k with $k \leq n$, and for non-negative integer s , we can always write $k^s = \sum_{j=0}^n S(s, j) k^{(j)}$. Hence when n is even,

$$\begin{aligned} & \sum_{k \text{ even}} \binom{n}{k} k^s e^{iky} \\ &= \sum_{k \text{ even}} \sum_{j=0}^n S(s, j) k^{(j)} \binom{n}{k} e^{iky} \\ &= \sum_{j=0}^n S(s, j) \sum_{k \text{ even}} k^{(j)} \binom{n}{k} e^{iky} \\ &= S(s, n) n! e^{iny} + \sum_{j=0}^{n-1} S(s, j) \sum_{k \text{ even}} k^{(j)} \binom{n}{k} e^{iky}. \end{aligned} \quad (\text{E31})$$

When n is even,

$$\begin{aligned} & \sum_{k \text{ odd}} \binom{n}{k} k^s e^{iky} \\ &= \sum_{k \text{ odd}} \sum_{j=0}^n S(s, j) k^{(j)} \binom{n}{k} e^{iky} \\ &= \sum_{j=0}^n S(s, j) \sum_{k \text{ odd}} k^{(j)} \binom{n}{k} e^{iky} \\ &= \sum_{j=0}^{n-1} S(s, j) \sum_{k \text{ odd}} k^{(j)} \binom{n}{k} e^{iky}. \end{aligned} \quad (\text{E32})$$

Next we use Lemma 20 with (E31) and (E32) to get the first result. Similarly when n is odd,

$$\begin{aligned} & \sum_{k \text{ odd}} \binom{n}{k} k^s e^{iky} \\ &= \sum_{k \text{ odd}} \sum_{j=0}^n S(s, j) k^{(j)} \binom{n}{k} e^{iky} \\ &= \sum_{j=0}^n S(s, j) \sum_{k \text{ odd}} k^{(j)} \binom{n}{k} e^{iky} \\ &= S(s, n) n! e^{iny} + \sum_{j=0}^{n-1} S(s, j) \sum_{k \text{ odd}} k^{(j)} \binom{n}{k} e^{iky}, \end{aligned} \quad (\text{E33})$$

and we use Lemma 20 to get the second result. \square

Appendix F: Sandwiches of shifted gnu logical states

In this section we evaluate sandwiches of shifted gnu logical states, which are expressions of the form $\langle j_L | A | j_L \rangle$ where $|j_L\rangle$ are logical codewords of shifted gnu logical states and A is an appropriately sized complex matrix. We begin by considering $\langle j_L | \hat{J}^z | j_L \rangle$ and $\langle j_L | (\hat{J}^z)^2 | j_L \rangle$. We make a mild assumption that $n \geq 3$. We note that

$$\langle 0_L | \hat{J}^z | 0_L \rangle = (N/2 - s) - 2^{-n+1} \sum_{j \text{ even}} \binom{n}{j} gj, \quad (\text{F1})$$

$$\langle 1_L | \hat{J}^z | 1_L \rangle = (N/2 - s) - 2^{-n+1} \sum_{j \text{ odd}} \binom{n}{j} gj. \quad (\text{F2})$$

Now $\sum_{j=0}^n j \binom{n}{j} = 2^{n-1} n$. Whenever $n \geq 2$, we have $2^{-n+1} \sum_{j \text{ odd}} \binom{n}{j} j = 2^{-n+1} \sum_{j \text{ even}} \binom{n}{j} j = \frac{n}{2}$. Hence

$$\langle 0_L | \hat{J}^z | 0_L \rangle = \langle 1_L | \hat{J}^z | 1_L \rangle = N/2 - s - gn/2. \quad (\text{F3})$$

Now $\sum_{j=0}^n j^2 \binom{n}{j} = 2^{n-2} n(n+1)$. When $n \geq 3$, $2^{-n+1} \sum_{j \text{ odd}} j^2 \binom{n}{j} = 2^{-n+1} \sum_{j \text{ even}} j^2 \binom{n}{j} = n(n+1)/4$.

Next, we evaluate the following.

$$\begin{aligned}
& \langle 0_L | (\hat{J}^z)^2 | 0_L \rangle \\
&= 2^{-n+1} \sum_{j \text{ even}} \binom{n}{j} (N/2 - (gj + s))^2, \\
&= 2^{-n+1} \sum_{j \text{ even}} \binom{n}{j} (N^2/4 - N(gj + s) + (gj + s)^2) \\
&= 2^{-n+1} \sum_{j \text{ even}} \binom{n}{j} (N^2/4 - N(gj + s) + (g^2j^2 + 2gjs + s^2)) \\
&= 2^{-n+1} \sum_{j \text{ even}} \binom{n}{j} ((N/2 - s)^2 + (2s - N)gj + g^2j^2) \\
&= (N/2 - s)^2 + \frac{(2s - N)gn}{2} + \frac{g^2n(n+1)}{4}. \quad (\text{F4})
\end{aligned}$$

Similarly,

$$\langle 1_L | (\hat{J}^z)^2 | 1_L \rangle = (N/2 - s)^2 + \frac{(2s - N)gn}{2} + \frac{g^2n(n+1)}{4}. \quad (\text{F5})$$

Now we prove Lemma 10, which involves evaluating the quantities $\langle 0_L | U_\Delta | 0_L \rangle$ and $\langle 1_L | U_\Delta | 1_L \rangle$.

Proof of Lemma 10. Now $\hat{J}^z | D_w^N \rangle = (N/2 - w) | D_w^N \rangle$. Hence

$$\begin{aligned}
U_\Delta | D_w^N \rangle &= \sum_w a_w \exp(-i\Delta(N/2 - w)) | D_w^N \rangle \\
&= e^{-i\Delta N/2} \sum_w a_w e^{i\Delta w} | D_w^N \rangle. \quad (\text{F6})
\end{aligned}$$

Using (F6) and the definition of logical codewords for shifted gnu codes with shift s , we see that

$$\langle 0_L | U_\Delta | 0_L \rangle = e^{-i\Delta N/2} 2^{-n+1} \sum_{\substack{0 \leq k \leq n \\ k \text{ even}}} \binom{n}{k} e^{i(gk+s)\Delta}, \quad (\text{F7})$$

$$\langle 1_L | U_\Delta | 1_L \rangle = e^{-i\Delta N/2} 2^{-n+1} \sum_{\substack{0 \leq k \leq n \\ k \text{ odd}}} \binom{n}{k} e^{i(gk+s)\Delta}. \quad (\text{F8})$$

Note that

$$\begin{aligned}
& \sum_{k \text{ even}} \binom{n}{k} e^{igk\Delta} \\
&= \frac{(1 + e^{ig\Delta})^n + (1 - e^{ig\Delta})^n}{2} \\
&= \frac{(2e^{ig\Delta/2} \cos(g\Delta/2))^n + (-2ie^{ig\Delta/2} \sin(g\Delta/2))^n}{2} \\
&= 2^{n-1} e^{ign\Delta/2} (\cos^n(g\Delta/2) + (-i)^n \sin(g\Delta/2)). \quad (\text{F9})
\end{aligned}$$

Similarly,

$$\begin{aligned}
& \sum_{k \text{ odd}} \binom{n}{k} e^{igk\Delta} \\
&= \frac{(1 + e^{ig\Delta})^n - (1 - e^{ig\Delta})^n}{2} \\
&= 2^{n-1} e^{ign\Delta/2} (\cos^n(g\Delta/2) - (-i)^n \sin(g\Delta/2)). \quad (\text{F10})
\end{aligned}$$

Hence

$$\frac{\langle 0_L | U_\Delta | 0_L \rangle}{e^{-i\Delta(N/2-s)} e^{ign\Delta/2}} = \cos^n(g\Delta/2) + (-i)^n \sin(g\Delta/2). \quad (\text{F11})$$

Similarly,

$$\frac{\langle 1_L | U_\Delta | 1_L \rangle}{e^{-i\Delta(N/2-s)} e^{ign\Delta/2}} = \cos^n(g\Delta/2) - (-i)^n \sin(g\Delta/2). \quad (\text{F12})$$

The result follows. \square

Here, Lemma 23 evaluates $\langle Q_j | U_\Delta | j_L \rangle$ for shifted gnu codes with $n \geq 3$.

Lemma 23. *Let $|0_L\rangle$ and $|1_L\rangle$ be logical codewords of a shifted gnu code where $n \geq 3$. Then,*

$$\langle Q_j | U_\Delta | j_L \rangle = \frac{gn}{2} \left(\phi_{n,j}(\Delta) - e^{ig\Delta} \phi_{n-1,j\oplus 1}(\Delta) \right). \quad (\text{F13})$$

Furthermore, if n is odd, then we have

$$\begin{aligned}
\frac{2}{gn} \langle Q_j | U_\Delta | j_L \rangle &= e^{-i\Delta(N/2-s)} e^{inx} \left(-i \cos^{n-1} x \sin x \right. \\
&\quad \left. + i^{n-1} (-1)^j \sin^{n-1} x \cos x \right), \quad (\text{F14})
\end{aligned}$$

where $x = g\Delta/2$.

Proof of Lemma 23. Consider $\langle Q_j | U_\Delta | j_L \rangle$ for $j = 0, 1$. We apply $\frac{\partial}{\partial \Delta} U_\Delta = (-i\hat{J}^z) U_\Delta$ together with the definitions of $|Q_j\rangle$ and find that

$$\begin{aligned}
\langle Q_j | U_\Delta | j_L \rangle &= \langle j_L | \hat{J}^z U_\Delta | j_L \rangle - \langle j_L | U_\Delta | j_L \rangle \langle j_L | \hat{J}^z | j_L \rangle \\
&= i \frac{\partial}{\partial \Delta} \langle j_L | U_\Delta | j_L \rangle - \langle j_L | U_\Delta | j_L \rangle \langle j_L | \hat{J}^z | j_L \rangle. \quad (\text{F15})
\end{aligned}$$

Using Lemma 10 and (F3), we can write

$$\langle Q_j | U_\Delta | j_L \rangle = i \frac{\partial}{\partial \Delta} \phi_{n,j}(\Delta) - \phi_{n,j}(\Delta) (N/2 - s - gn/2). \quad (\text{F16})$$

Next, note the recursion relation

$$\frac{\partial}{\partial \Delta} \phi_{n,j}(\Delta) = -i \left(\frac{N}{2} - s \right) \phi_{n,j}(\Delta) + \frac{ign}{2} e^{ig\Delta} \phi_{n-1,j\oplus 1}(\Delta), \quad (\text{F17})$$

where $0 \oplus 1 = 1$ and $1 \oplus 1 = 0$. Hence,

$$\begin{aligned}
\langle Q_j | U_\Delta | j_L \rangle &= \left(\left(\frac{N}{2} - s \right) \phi_{n,j}(\Delta) - \frac{gn}{2} e^{ig\Delta} \phi_{n-1,j\oplus 1}(\Delta) \right) \\
&\quad - \phi_{n,j}(\Delta) (N/2 - s - gn/2), \quad (\text{F18})
\end{aligned}$$

and simplifying this, the first result follows.

Now let $x = g\Delta/2$, and note that

$$\begin{aligned} \cos x - e^{ix} &= -i \sin x, \\ -i \sin x + e^{ix} &= \cos x. \end{aligned} \quad (\text{F19})$$

Now we evaluate $\phi_{n,j}(\Delta) - e^{ig\Delta}\phi_{n-1,j\oplus 1}(\Delta)$. Note that

$$\begin{aligned} & e^{i\Delta(N/2-s)} e^{-inx} \left(\phi_{n,j}(\Delta) - e^{ig\Delta}\phi_{n-1,j\oplus 1}(\Delta) \right) \\ &= (\cos^n x + (-1)^j (-i)^n \sin^n x) \\ & \quad - e^{-ix} e^{2ix} (\cos^{n-1} x - (-1)^{1-j} (-i)^{n-1} \sin^{n-1} x) \\ &= \cos^{n-1} x (\cos x - e^{ix}) \\ & \quad + (-1)^j (-i)^{n-1} \sin^{n-1} x ((-i) \sin x + e^{ix}). \end{aligned} \quad (\text{F20})$$

Hence when n is odd, $(-i)^{n-1} = i^{n-1}$ and the result follows. \square

Proof of Lemma 11. Using (73), we get

$$\langle q_j | U_\Delta | j_L \rangle = \frac{2}{g\sqrt{n}} \langle Q_j | U_\Delta | j_L \rangle. \quad (\text{F21})$$

To simplify notation, let $x = g\Delta/2$. Since n is odd, we use (F13) in Lemma 23 to get

$$\begin{aligned} & |\langle q_j | U_\Delta | j_L \rangle| \\ &= \sqrt{n} \left| \phi_{n,j}(\Delta) - e^{ig\Delta}\phi_{n-1,j\oplus 1}(\Delta) \right| \\ &= \sqrt{n} \left| -i \cos^{n-1} x \sin x + i^{n-1} (-1)^j \sin^{n-1} x \cos x \right| \\ &= \sqrt{n} \sqrt{\sin^{2n-2} x \cos^2 x + \cos^{2n-2} x \sin^2 x} \\ &= \frac{\sqrt{n}}{2} |\sin 2x| \sqrt{\sin^{2n-4} x + \cos^{2n-4} x}. \end{aligned} \quad (\text{F22})$$

Hence the result follows. \square

Appendix G: Simple projections of $|Q_j\rangle$

Here we evaluate $\langle Q_j | v \rangle$ for various choices of $|v\rangle$. Recall the definition $|Q_j\rangle = \hat{J}_z |j_L\rangle - \langle j_L | \hat{J}_z |j_L\rangle |j_L\rangle$, where $|j_L\rangle$ is a logical codeword of a shifted gnu code.

Then we have

$$\begin{aligned} \langle Q_j | \hat{J}_z |j_L\rangle &= \langle j_L | \hat{J}_z \hat{J}_z |j_L\rangle - \langle j_L | \hat{J}_z |j_L\rangle \langle j_L | \hat{J}_z |j_L\rangle \\ &= \langle j_L | (\hat{J}_z)^2 |j_L\rangle - \langle j_L | \hat{J}_z |j_L\rangle \langle j_L | \hat{J}_z |j_L\rangle. \end{aligned} \quad (\text{G1})$$

From (F3) and (F4), we get

$$\begin{aligned} \langle Q_j | \hat{J}_z |j_L\rangle &= \langle j_L | \hat{J}_z \hat{J}_z |j_L\rangle - \langle j_L | \hat{J}_z |j_L\rangle \langle j_L | \hat{J}_z |j_L\rangle \\ &= (N/2 - s)^2 + \frac{(2s - N)gn}{2} + \frac{g^2 n(n+1)}{4} \\ & \quad - (N/2 - s - gn/2)^2 \\ &= \frac{g^2 n}{4}. \end{aligned} \quad (\text{G2})$$

Appendix H: Proof of Theorem 14

Proof of Theorem 14. The first step is to obtain an upper bound on p_0 and p_1 . We note from Lemma 12 that $p_0 = p_{\text{flag}}$. Hence it remains to bound p_1 . We achieve this by approximating the state with a single deletion as a shifted gnu state. Note that a single deletion error shifts the Dicke weights by a random number $\sigma = s - s'$, where σ could be 0 or 1. From (23), deleting a qubit from our N -qubit logical state $|\psi\rangle = a|0_L\rangle + be^{i\varphi}|1_L\rangle$ gives a probabilistic mixture of the (unnormalized) $(N-1)$ -qubit states

$$|\psi'_\sigma\rangle = a|0'_\sigma\rangle + be^{i\varphi}|1'_\sigma\rangle \quad (\text{H1})$$

where

$$|0'_\sigma\rangle = 2^{(-n+1)/2} \sum_{k \text{ even}} \sqrt{\binom{n}{k}} \sqrt{\frac{\binom{N-1}{gk+s-\sigma}}{\binom{N}{gk+s}}} |D_{gk+s-\sigma}\rangle \quad (\text{H2})$$

$$|1'_\sigma\rangle = 2^{(-n+1)/2} \sum_{k \text{ odd}} \sqrt{\binom{n}{k}} \sqrt{\frac{\binom{N-1}{gk+s-\sigma}}{\binom{N}{gk+s}}} |D_{gk+s-\sigma}\rangle. \quad (\text{H3})$$

Note that

$$\frac{\binom{N-1}{gk+s-\sigma}}{\binom{N}{gk+s}} = \begin{cases} 1 - (gk+s)/N & , \quad \sigma = 0 \\ (gk+s)/N & , \quad \sigma = 1 \end{cases}. \quad (\text{H4})$$

The above form for the ratio of binomial coefficients allows us to approximate the states $|0'_\sigma\rangle$ and $|1'_\sigma\rangle$ in terms of the states

$$|0_\sigma\rangle = 2^{(-n+1)/2} \sum_{k \text{ even}} \sqrt{\binom{n}{k}} |D_{gk+s-\sigma}\rangle \quad (\text{H5})$$

$$|1_\sigma\rangle = 2^{(-n+1)/2} \sum_{k \text{ odd}} \sqrt{\binom{n}{k}} |D_{gk+s-\sigma}\rangle. \quad (\text{H6})$$

From the properties of binomial sums,

$$\langle 0'_\sigma | 0'_\sigma \rangle = 1 - \frac{s}{N} - \frac{gn}{2N}, \quad \langle 1'_\sigma | 1'_\sigma \rangle = \frac{s}{N} + \frac{gn}{2N}. \quad (\text{H7})$$

This is because

$$\begin{aligned} \langle 0'_\sigma | 0'_\sigma \rangle &= 1 - \frac{s}{N} - 2^{-n+1} \sum_{k \text{ even}} \binom{n}{k} \frac{gk}{N} \\ &= 1 - \frac{s}{N} - \frac{gn}{2N}, \end{aligned} \quad (\text{H8})$$

and

$$\langle 1'_\sigma | 1'_\sigma \rangle = \frac{s}{N} + \frac{gn}{2N}. \quad (\text{H9})$$

To leading order in g/N , we have

$$|0'_\sigma\rangle \approx \sqrt{1 - s/N} |0_\sigma\rangle, \quad |1'_\sigma\rangle \approx \sqrt{s/N} |1_\sigma\rangle. \quad (\text{H10})$$

Now let $x_k = gn/2N - gk/N$. To calculate the leading order correction, we can appeal to the binomial theorem to get

$$\begin{aligned}\sqrt{1+x_k/z} &= \sum_{j \geq 0} \binom{1/2}{j} (x_k)^j \\ &= 1 + \frac{x_k/z}{2} - \frac{x_k^2/z^2}{8} + O(x_k^3),\end{aligned}\quad (\text{H11})$$

where $\binom{1/2}{j} = (1/2)_{(j)}/j!$ and $(1/2)_{(j)} = (1/2)(1/2 - 1) \dots (1/2 - j + 1)$ denotes the falling factorial. Using the formula for the remainder term in the series expansion of $\sqrt{1+x_k/z}$ for $z > 0$, we find that

$$\left| \sqrt{1+x_k/z} - (1+x_k/2z+x_k^2/8z^2) \right| \leq |x_k/z|^3/32. \quad (\text{H12})$$

Defining $|\epsilon_{j,\sigma}\rangle = |j'_\sigma\rangle - \sqrt{z_j}|j_\sigma\rangle$ where $z_j = (\delta_{j,0} - (-1)^j(s/N - gn/2N))$, we can express $|j'_\sigma\rangle$ as a perturbation of $\sqrt{z_\sigma}|j_\sigma\rangle$. Then

$$\begin{aligned}\langle \epsilon_{j,\sigma} | \epsilon_{j,\sigma} \rangle &= (\langle j'_\sigma | - \sqrt{z_j} \langle j_\sigma |) (|j'_\sigma\rangle - \sqrt{z_j} |j_\sigma\rangle) \\ &= \langle j'_\sigma | j'_\sigma \rangle + z_j \langle j_\sigma | j_\sigma \rangle - 2\sqrt{z_j} \langle j_\sigma | j'_\sigma \rangle \\ &= 2z_j - 2\sqrt{z_j} \langle j_\sigma | j'_\sigma \rangle.\end{aligned}\quad (\text{H13})$$

Then

$$\begin{aligned}\langle \epsilon_{0,\sigma} | \epsilon_{0,\sigma} \rangle &= 2z_0 - 2\sqrt{z_0} 2^{-n+1} \sum_{k \text{ even}} \binom{n}{k} \sqrt{z_0 + x_k} \\ &= 2z_0 \left(1 - 2^{-n+1} \sum_{k \text{ even}} \binom{n}{k} \sqrt{1 + \frac{x_k}{z_0}} \right) \\ &= 2z_0 \left(1 - 2^{-n+1} \sum_{k \text{ even}} \binom{n}{k} \left(1 + \frac{x_k}{2z_0} - \frac{x_k^2}{8z_0^2} + \frac{x_k^3}{16z_0^3} + \dots \right) \right) \\ &= \frac{2^{-n+1}}{4z_0} \sum_{k \text{ even}} \binom{n}{k} x_k^2 - \frac{2^{-n+1}}{8z_0^2} \sum_{k \text{ even}} \binom{n}{k} x_k^3 + \dots\end{aligned}\quad (\text{H14})$$

From the Taylor's theorem with remainder, and using $|x_k/z_0| \leq \frac{gn}{2Nz_0}$ we know that

$$\begin{aligned}\left| \langle \epsilon_{0,\sigma} | \epsilon_{0,\sigma} \rangle - \frac{2^{-n+1}}{4z_0} \sum_{k \text{ even}} \binom{n}{k} x_k^2 \right| \\ \leq 2z_0 \frac{g^3 n^3}{32(8N^3 z_0^3)} = \frac{g^3 n^3}{128N^3 z_0^2}.\end{aligned}\quad (\text{H15})$$

Since $x_k = gn/(2N) - (g/N)k$, we have $x_k^2 =$

$g^2 n^2/(4N^2) - (g^2 n)k/N^2 + (g^2/N^2)k^2$. We see that

$$\begin{aligned}2^{-n+1} \sum_{k \text{ even}} \binom{n}{k} x_k^2 \\ = \frac{g^2 n^2}{4N^2} - \frac{g^2 n}{N^2} \binom{n}{2} + \frac{g^2}{N^2} \binom{n(n+1)}{4} \\ = \frac{g^2 n}{4N^2}.\end{aligned}\quad (\text{H16})$$

Since $x_k = gn/(2N) - (g/N)k$, we have

$$\begin{aligned}x_k^3 &= \frac{g^3 n^3}{8N^3} - 3\frac{g^2 n^2}{4N^2} \frac{gk}{N} + 3\frac{gn}{2N} \frac{g^2 k^2}{N^2} - \frac{g^3 k^3}{N^3} \\ &= \frac{g^3 n^3}{8N^3} - \frac{3g^3 n^2}{4N^3} k + 3\frac{3g^3 n}{2N^3} k^2 - \frac{g^3}{N^3} k^3.\end{aligned}\quad (\text{H17})$$

Now $\sum_{k=0}^n \binom{n}{k} k^3 =$. Hence from Lemma 19, for odd n , we have

$$\sum_{k \text{ odd}} \binom{n}{k} k^3 = 2^n n^2 (n+3)/16 - S(3, n)n!/2, \quad (\text{H18})$$

$$\sum_{k \text{ even}} \binom{n}{k} k^3 = 2^n n^2 (n+3)/16 + S(3, n)n!/2. \quad (\text{H19})$$

Hence

$$2^{-n+1} \sum_{k \text{ odd}} \binom{n}{k} k^3 = \frac{n^2(n+3)}{8} - S(3, n)n!, \quad (\text{H20})$$

$$2^{-n+1} \sum_{k \text{ even}} \binom{n}{k} k^3 = \frac{n^2(n+3)}{8} + S(3, n)n!. \quad (\text{H21})$$

Hence

$$\begin{aligned}2^{-n+1} \sum_{k \text{ even}} x_k^3 \\ = 3\frac{3g^3 n}{2N^3} \left(\frac{n(n+1)}{4} \right) - \frac{g^3}{N^3} \left(\frac{n^2(n+3)}{8} - S(3, n)n! \right) \\ = \frac{g^3 n^3}{N^3} + \frac{3g^3 n^2}{4N^3} + \frac{g^3 S(3, n)n!}{N^3}.\end{aligned}\quad (\text{H22})$$

Similarly,

$$2^{-n+1} \sum_{k \text{ odd}} x_k^3 = \frac{g^3 n^3}{N^3} + \frac{3g^3 n^2}{4N^3} - \frac{g^3 S(3, n)n!}{N^3}. \quad (\text{H23})$$

Hence

$$\left| \langle \epsilon_{0,\sigma} | \epsilon_{0,\sigma} \rangle - \frac{1}{4z_0} \frac{g^2 n}{4N^2} \right| \leq \frac{g^3 n^3}{128N^3 z_0^2}. \quad (\text{H24})$$

Similarly,

$$\left| \langle \epsilon_{1,\sigma} | \epsilon_{1,\sigma} \rangle - \frac{g^2 n}{16N^2 z_1} \right| \leq \frac{g^3 n^3}{128N^3 z_1^2}. \quad (\text{H25})$$

Furthermore, when $n = 3$,

$$\langle \epsilon_{j,\sigma} | \epsilon_{j,\sigma} \rangle = \frac{3g^2}{16N^2 z_j} + (-1)^j \frac{3g^3}{4N^3 z_j^2} - \frac{135g^3}{32N^3 z_j^2} + O(g^4/N^4). \quad (\text{H26})$$

Therefore, for $z_0, z_1 \geq 1/4$ and $gn^2/N \leq 1$, we have

$$\langle \epsilon_{j,\sigma} | \epsilon_{j,\sigma} \rangle \leq \frac{g^2 n}{2N^2}. \quad (\text{H27})$$

Now we can write

$$\begin{aligned} |\psi'_\sigma\rangle &= a|0'_\sigma\rangle + b|1'_\sigma\rangle \\ &= a\sqrt{z_0}|0_\sigma\rangle + b\sqrt{z_1}|1_\sigma\rangle + a|\epsilon_{0,\sigma}\rangle + b|\epsilon_{1,\sigma}\rangle \\ &= \sqrt{\langle \psi'_\sigma | \psi'_\sigma \rangle} (a'|0_\sigma\rangle + b'|1_\sigma\rangle) + a|\epsilon_{0,\sigma}\rangle + b|\epsilon_{1,\sigma}\rangle, \end{aligned} \quad (\text{H28})$$

where $|a'|^2 + |b'|^2 = 1$. Now let $\Pi = |0_\sigma\rangle\langle 0_\sigma| + |1_\sigma\rangle\langle 1_\sigma|$ and $\Pi_1 = |q_{0,\sigma}\rangle\langle q_{0,\sigma}| + |q_{1,\sigma}\rangle\langle q_{1,\sigma}|$, where $|q_{j,\sigma}\rangle = |Q_{j,\sigma}\rangle/\sqrt{\langle Q_{j,\sigma} | Q_{j,\sigma} \rangle}$ and

$$|Q_{j,\sigma}\rangle = \hat{J}^z |j_\sigma\rangle - \langle j_\sigma | \hat{J}^z |j_\sigma\rangle |j_\sigma\rangle. \quad (\text{H29})$$

Let $a'' = a/\sqrt{\langle \psi'_\sigma | \psi'_\sigma \rangle}$ and $b'' = b/\sqrt{\langle \psi'_\sigma | \psi'_\sigma \rangle}$. Then

$$\begin{aligned} p_1 &= 1 - \left\| \Pi \frac{U_\Delta |\psi'_\sigma\rangle}{\sqrt{\langle \psi'_\sigma | \psi'_\sigma \rangle}} \right\|^2 - \left\| \Pi_1 \frac{U_\Delta |\psi'_\sigma\rangle}{\sqrt{\langle \psi'_\sigma | \psi'_\sigma \rangle}} \right\|^2 \\ &= 1 - \left\| \Pi U_\Delta (a'|0_\sigma\rangle + b'|1_\sigma\rangle + a''|\epsilon_{0,j}\rangle + b''|\epsilon_{1,j}\rangle) \right\|^2 \\ &\quad - \left\| \Pi_1 U_\Delta (a'|0_\sigma\rangle + b'|1_\sigma\rangle + a''|\epsilon_{0,j}\rangle + b''|\epsilon_{1,j}\rangle) \right\|^2. \end{aligned} \quad (\text{H30})$$

Simplifying, and using $\langle \psi'_\sigma | \psi'_\sigma \rangle = |a|^2 z_0 + |b|^2 z_1$, we get

$$\begin{aligned} p_1 &\leq p_0 + \|a''|\epsilon_{0,j}\rangle + b''|\epsilon_{1,j}\rangle\|^2 + \|a''|\epsilon_{0,j}\rangle + b''|\epsilon_{1,j}\rangle\|^2 \\ &\leq p_0 + \frac{\max_{j=0,1} \langle \epsilon_{j,\sigma} | \epsilon_{j,\sigma} \rangle}{\langle \psi'_\sigma | \psi'_\sigma \rangle} \\ &\leq p_0 + \frac{g^2 n / (2N^2)}{\min\{z_0, z_1\}}. \end{aligned} \quad (\text{H31})$$

Using $z_0, z_1 \geq 1/4$, we get

$$p_1 \leq p_0 + \frac{2g^2 n}{N^2}. \quad (\text{H32})$$

The normalized state after projecting on the support of Π is

$$|n_0\rangle = \frac{a}{\sqrt{|a|^2 + |b|^2 |u_0|^2}} |0_\sigma\rangle + \frac{be^{i\varphi} u_0}{\sqrt{|a|^2 + |b|^2 |u_0|^2}} |1_\sigma\rangle, \quad (\text{H33})$$

where $u_0 = \frac{\langle 1_\sigma | U_\Delta | 1'_\sigma \rangle}{\langle 0_\sigma | U_\Delta | 0'_\sigma \rangle}$. Hence, we have $a_{1,0} = \langle 0_\sigma | n_0 \rangle$, $b_{1,0} = \sqrt{1 - |a_{1,0}|^2}$ and $\phi_{1,0} = \arctan \frac{\text{Im} u_0}{\text{Re} u_0}$.

Similarly, the normalized state after projecting on the support of Π_1 is proportional to

$$|n_1\rangle = \frac{a}{\sqrt{|a|^2 + |b|^2 |u_1|^2}} |q_{0,\sigma}\rangle + \frac{be^{i\varphi} u_1}{\sqrt{|a|^2 + |b|^2 |u_1|^2}} |q_{1,\sigma}\rangle, \quad (\text{H34})$$

where $u_1 = \frac{\langle q_{1,\sigma} | U_\Delta | 1'_\sigma \rangle}{\langle q_{1,\sigma} | U_\Delta | 0'_\sigma \rangle}$. Hence, we have $a_{1,1} = \langle q_{0,\sigma} | n_1 \rangle$, $b_{1,1} = \sqrt{1 - |a_{1,1}|^2}$ and $\phi_{1,1} = \arctan \frac{\text{Im} u_1}{\text{Re} u_1}$. The state $|n_1\rangle$ is mapped to back to a shifted gnu state by a unitary transformation, mapping the state $|q_{j,\sigma}\rangle$ to $|j_L\rangle$. \square

Appendix I: Approximation bounds

Let u_j be as defined in Theorem 14. Note that

$$\begin{aligned} |u_0| &= \frac{|\langle 1_\sigma | U_\Delta | 1'_\sigma \rangle|}{|\langle 0_\sigma | U_\Delta | 0'_\sigma \rangle|} \\ &\leq \frac{|\langle 1_\sigma | U_\Delta | 1_\sigma \rangle|/\sqrt{2} + g\sqrt{n}/2N}{|\langle 0_\sigma | U_\Delta | 0_\sigma \rangle|/\sqrt{2} - g\sqrt{n}/2N} \\ &= \frac{\frac{|\langle 1_\sigma | U_\Delta | 1_\sigma \rangle|}{|\langle 0_\sigma | U_\Delta | 0_\sigma \rangle|} + \frac{g\sqrt{n}}{\sqrt{2N}|\langle 0_\sigma | U_\Delta | 0_\sigma \rangle|}}{1 - \frac{g\sqrt{n}}{\sqrt{2N}|\langle 0_\sigma | U_\Delta | 0_\sigma \rangle|}} \\ &\leq \frac{1 + \frac{g\sqrt{n}}{\sqrt{2N}|\langle 0_\sigma | U_\Delta | 0_\sigma \rangle|}}{1 - \frac{g\sqrt{n}}{\sqrt{2N}|\langle 0_\sigma | U_\Delta | 0_\sigma \rangle|}}. \end{aligned} \quad (\text{I1})$$

Similarly, we have

$$|u_0| \geq \frac{1 - \frac{g\sqrt{n}}{\sqrt{2N}|\langle 0_\sigma | U_\Delta | 0_\sigma \rangle|}}{1 + \frac{g\sqrt{n}}{\sqrt{2N}|\langle 0_\sigma | U_\Delta | 0_\sigma \rangle|}}. \quad (\text{I2})$$

With the assumption that $|\langle 0_\sigma | U_\Delta | 0_\sigma \rangle| \geq 1/\sqrt{2}$, we get

$$\frac{1 - \frac{g\sqrt{n}}{N}}{1 + \frac{g\sqrt{n}}{N}} \leq |u_0| \leq \frac{1 + \frac{g\sqrt{n}}{N}}{1 - \frac{g\sqrt{n}}{N}}. \quad (\text{I3})$$

Consider the function $f(x) = (1+x)/(1-x)$. Using the Taylor's theorem for the remainder term, we get for $0 < x < 1/4$, the fact that $|f(x) - 1| \leq 4x$. For the function $g(x) = (1-x)/(1+x)$, we get $|g(x) - 1| \leq 2x$. Hence

$$1 - \frac{2g\sqrt{n}}{N} \leq |u_0| \leq 1 - \frac{4g\sqrt{n}}{N}. \quad (\text{I4})$$

Hence $||u_0| - 1| \leq 4g\sqrt{n}/N$. Similarly

$$1 - \frac{2g\sqrt{n}}{N} \leq |u_1| \leq 1 - \frac{4g\sqrt{n}}{N}. \quad (\text{I5})$$

and $||u_1| - 1| \leq 4g\sqrt{n}/N$.

Since $g\sqrt{n} \leq gn \leq N$, we have $(g\sqrt{n}/N)^2 \leq g\sqrt{n}/N$. Therefore

$$1 - \frac{4g\sqrt{n}}{N} \leq |u_j|^2 \leq 1 + \frac{24g\sqrt{n}}{N}. \quad (\text{I6})$$

Hence for any real a with $|a| \leq 1$,

$$\begin{aligned} |a^2 + (1 - a^2)|u_j|^2| &\leq \left| a^2 + (1 - a^2) + (1 - a^2) \frac{24g\sqrt{n}}{N} \right| \\ &\leq |a^2 + (1 - a^2)| + \left| (1 - a^2) \frac{24g\sqrt{n}}{N} \right| \\ &\leq 1 + \frac{24g\sqrt{n}}{N}. \end{aligned} \quad (I7)$$

Moreover,

$$\begin{aligned} |a^2 + (1 - a^2)|u_j|^2| &\geq \left| a^2 + (1 - a^2) - (1 - a^2) \frac{4g\sqrt{n}}{N} \right| \\ &\geq |a^2 + (1 - a^2)| - \left| (1 - a^2) \frac{4g\sqrt{n}}{N} \right| \\ &\geq 1 - \frac{4g\sqrt{n}}{N}. \end{aligned} \quad (I8)$$

Next consider the function $h(x) = 1/\sqrt{1+x}$. Note that $|h(x) - 1| \leq |x|/2$. Hence

$$1 - \frac{12g\sqrt{n}}{N} \leq |a^2 + (1 - a^2)|u_j|^2| \leq 1 + \frac{2g\sqrt{n}}{N}. \quad (I9)$$

This allows us to quantify the perturbation in the amplitudes within the shifted gnu code that results from QEC performed on signal accumulated gnu states with a single deletion. Namely,

$$|a_{1, \text{syn}} - a| \leq |a| \left(1 + \frac{12g\sqrt{n}}{N} - 1 \right) \leq \frac{12g\sqrt{n}}{N}. \quad (I10)$$

Next, we quantify the perturbation $|\phi_{1,j} - \zeta_j|$. For this, consider a function $g(u, v) = \frac{u}{v}$, and the corresponding lemma.

Lemma 24. *Let $u, v \in \mathbb{R}$ such that $|u| = |v| = 1$. Let δ_u, δ_v be real numbers such that $|\delta_u|, |\delta_v| \leq \delta$, where $0 \leq \delta \leq 1/2$. Then*

$$|g(u + \delta_u, v + \delta_v) - g(u, v)| \leq 6\delta. \quad (I11)$$

Proof. Consider $g(u + \delta_u, v + \delta_v)$. We treat this function as a single variable function of u , and then of v . Using this idea, we approximate $g(u + \delta_u, v + \delta_v)$ using $g(u, v + \delta_v)$, and we approximate $g(u, v + \delta_v)$ using $g(u, v)$. This allows us to use the single-variable Taylor's theorem with remainder iteratively. Since $\partial g(u, v)/\partial u = 1/v$, we find that

$$|g(u + \delta_u, v + \delta_v) - g(u, v + \delta_v)| \leq |\delta_u| \frac{1}{|v + \delta_v|}. \quad (I12)$$

Similarly, $\partial g(u, v)/\partial v = -uv^{-2}$, and we find that

$$|g(u, v + \delta_v) - g(u, v)| \leq |\delta_v| \frac{|u|}{(|v| - |\delta_v|)^2}. \quad (I13)$$

Chaining (I12) and (I13) together, we get

$$\begin{aligned} &|g(u + \delta_u, v + \delta_v) - g(u, v)| \\ &= |g(u + \delta_u, v + \delta_v) - g(u, v + \delta_v) + g(u, v + \delta_v) - g(u, v)| \\ &\leq |g(u + \delta_u, v + \delta_v) - g(u, v + \delta_v)| + |g(u, v + \delta_v) - g(u, v)| \\ &\leq |\delta_u| \frac{1}{|v| - |\delta_v|} + |\delta_v| \frac{|u|}{(|v| - |\delta_v|)^2}. \end{aligned} \quad (I14)$$

When we have $|u| = 1$ and $|v| = 1$, and $|\delta_u|, |\delta_v| \leq \delta$, and when $\delta \leq 1/2$, we get $g(u, v) \leq \frac{1}{1-\delta} + \frac{\delta}{(1-\delta)^2} \leq 6\delta$ which gives the result. \square

Next consider the following lemma.

Lemma 25.

$$\left| \frac{\text{Im} \frac{u+\delta_u}{v+\delta_v}}{\text{Re} \frac{u+\delta_u}{v+\delta_v}} - \frac{\text{Im} \frac{u}{v}}{\text{Re} \frac{u}{v}} \right| \leq \frac{12\delta}{|\text{Re} \frac{u}{v}| - 6\delta}. \quad (I15)$$

Proof. We use a telescoping sum together with the triangle inequality to get

$$\begin{aligned} &\left| \frac{\text{Im} \frac{u+\delta_u}{v+\delta_v}}{\text{Re} \frac{u+\delta_u}{v+\delta_v}} - \frac{\text{Im} \frac{u}{v}}{\text{Re} \frac{u}{v}} \right| \\ &= \left| \frac{\text{Im} \frac{u+\delta_u}{v+\delta_v}}{\text{Re} \frac{u+\delta_u}{v+\delta_v}} - \frac{\text{Im} \frac{u}{v}}{\text{Re} \frac{u+\delta_u}{v+\delta_v}} \right| + \left| \frac{\text{Im} \frac{u}{v}}{\text{Re} \frac{u+\delta_u}{v+\delta_v}} - \frac{\text{Im} \frac{u}{v}}{\text{Re} \frac{u}{v}} \right| \end{aligned} \quad (I16)$$

Using Lemma 24 we get

$$\begin{aligned} &\left| \frac{\text{Im} \frac{u+\delta_u}{v+\delta_v}}{\text{Re} \frac{u+\delta_u}{v+\delta_v}} - \frac{\text{Im} \frac{u}{v}}{\text{Re} \frac{u}{v}} \right| \\ &\leq \frac{6\delta}{|\text{Re} \frac{u+\delta_u}{v+\delta_v}|} + \left| \text{Im} \frac{u}{v} \right| \left| \frac{\text{Re} \frac{u}{v} - \text{Re} \frac{u+\delta_u}{v+\delta_v}}{\text{Re} \frac{u}{v} \text{Re} \frac{u+\delta_u}{v+\delta_v}} \right| \\ &\leq \frac{6\delta}{|\text{Re} \frac{u+\delta_u}{v+\delta_v}|} \left(1 + \left| \frac{\text{Im} \frac{u}{v}}{\text{Re} \frac{u}{v}} \right| \right) \\ &\leq \frac{6\delta}{|\text{Re} \frac{u}{v}| - 6\delta} \left(1 + \left| \frac{\text{Im} \frac{u}{v}}{\text{Re} \frac{u}{v}} \right| \right). \end{aligned} \quad (I17)$$

\square

We can write $\phi_{1,0}$ in the form

$$\phi_{1,0} = \arctan \frac{\text{Im} \frac{\langle 1_\sigma | U_\Delta | 1'_\sigma \rangle}{\langle 0_\sigma | U_\Delta | 0'_\sigma \rangle}}{\text{Re} \frac{\langle 1_\sigma | U_\Delta | 1'_\sigma \rangle}{\langle 0_\sigma | U_\Delta | 0'_\sigma \rangle}} = \arctan \frac{\text{Im} \frac{u+\delta_u}{v+\delta_v}}{\text{Re} \frac{u+\delta_u}{v+\delta_v}} \quad (I18)$$

where

$$u = \langle 1_\sigma | U_\Delta | 1_\sigma \rangle / \langle 0_\sigma | U_\Delta | 0_\sigma \rangle \quad (I19)$$

$$\delta_u = \langle 1_\sigma | U_\Delta | \epsilon_{1,\sigma} \rangle / \langle 0_\sigma | U_\Delta | 0_\sigma \rangle \quad (I20)$$

$$v = 1 \quad (I21)$$

$$\delta_v = \langle 0_\sigma | U_\Delta | \epsilon_{0,\sigma} \rangle / \langle 0_\sigma | U_\Delta | 0_\sigma \rangle. \quad (I22)$$

From Lemma 13, $|u| = 1$. Hence, the quantities u, v, δ_u and δ_v satisfy the condition of Lemma 24. Hence we can use Lemma 25 to get

$$|\tan \phi_{1,0} - \tan \zeta_0| \leq \frac{12\delta}{|\operatorname{Re} \frac{u}{v}| - 6\delta}. \quad (\text{I23})$$

We can obtain a lower bound on $|\operatorname{Re} \frac{u}{v}|$. From (88),

$$\begin{aligned} \operatorname{Re} \frac{u}{v} &= \operatorname{Re} \frac{\cos^n(g\Delta/2) + i^n \sin^n(g\Delta/2)}{\cos^n(g\Delta/2) - i^n \sin^n(g\Delta/2)} \\ &= \operatorname{Re} \frac{(\cos^n(g\Delta/2) + i^n \sin^n(g\Delta/2))^2}{\cos^{2n}(g\Delta/2) + \sin^{2n}(g\Delta/2)} \\ &= \frac{\cos^{2n}(g\Delta/2) - \sin^{2n}(g\Delta/2)}{\cos^{2n}(g\Delta/2) + \sin^{2n}(g\Delta/2)}. \end{aligned} \quad (\text{I24})$$

This allows us to obtain $\operatorname{Re} \frac{u}{v} = 1 - \frac{2 \sin^{2n}(g\Delta/2)}{\cos^{2n}(g\Delta/2) + \sin^{2n}(g\Delta/2)}$. And when $|g\Delta/2| \leq \pi/6$, we see that $\frac{2 \sin^{2n}(g\Delta/2)}{\cos^{2n}(g\Delta/2) + \sin^{2n}(g\Delta/2)} \geq 0$, $|\sin(g\Delta/2)| \leq g\Delta/2$ and $\frac{2 \sin^{2n}(g\Delta/2)}{\cos^{2n}(g\Delta/2) + \sin^{2n}(g\Delta/2)} \leq 2 \sin^{2n}(g\Delta/2) \leq 2(g\Delta/2)^{2n} \leq 2(g\Delta/2)^6 \leq 0.05$ and hence

$$0.95 \leq \left| \frac{u}{v} \right| \leq 1. \quad (\text{I25})$$

Now we like to obtain an upper bound on $\frac{1}{0.95-6\delta}$ for small δ . For this, consider the function $1/(1-x)$. Then $|1/(1-x) - 1| = |\frac{x}{1-x}|$, and for $|x| \leq 1/2$, this gives $|1/(1-x) - 1| \leq 2x$. Hence for $6\delta/0.95 \leq 1/2$, we get $\frac{1}{0.95-6\delta} \leq \frac{1}{0.95} + \frac{1}{0.95}(2(6\delta/0.95))$, which gives

$$\frac{1}{0.95-6\delta} \leq 1.06 + 13.3\delta. \quad (\text{I26})$$

To obtain an upper bound on δ , it suffices to obtain upper bounds on $|\delta_u|$ and $|\delta_v|$. For this, we need a lower bound on $|\langle 0_\sigma | U_\Delta | 0_\sigma \rangle|$ and an upper bound on $|\langle j_\sigma | U_\Delta | \epsilon_{j,\sigma} \rangle|$. From the norm of $|\epsilon_{j,\sigma}\rangle$ we have from (H27) and the Cauchy Schwarz inequality, it follows that $|\langle j_\sigma | U_\Delta | \epsilon_{j,\sigma} \rangle| \leq g\sqrt{n}/(\sqrt{2}N)$.

From Lemma 10,

$$|\langle j_L | U_\Delta | j_L \rangle| = |\phi_{n,j}| = \sqrt{\cos^{2n}(g\tau\theta/2) + \sin^{2n}(g\tau\theta/2)}. \quad (\text{I27})$$

For $|g\tau\theta/2| \leq \pi/6$ we have $|\langle j_L | U_\Delta | j_L \rangle| \geq |\cos^n(g\tau/2)|$. Since $\cos x \geq 1 - x^2/2$, and using the Bernoulli inequality, we get

$$|\langle j_L | U_\Delta | j_L \rangle| \geq 1 - ng^2\tau^2\theta^2/4. \quad (\text{I28})$$

Using the inequality $|gn\tau| \leq 1/2$, $|\theta| \leq 1$ and $n \geq 3$, we get

$$|\langle j_L | U_\Delta | j_L \rangle| \geq 1 - 1/4n \geq \frac{11}{12}. \quad (\text{I29})$$

Hence, $\delta = \max_{u,v}\{|\delta_u|, |\delta_v|\} \leq \frac{12g\sqrt{n}}{11\sqrt{2}N} \leq 0.78g\sqrt{n}/N$. Hence we can use Lemma 25 to get

$$\begin{aligned} |\tan \phi_{1,0} - \tan \zeta_0| &\leq (12\delta)(1.06 + 13.3\delta) \\ &\leq \frac{10g\sqrt{n}}{N} + \frac{98g^2n}{N^2}. \end{aligned} \quad (\text{I30})$$

Now consider the function $\arctan x$. Note that $\frac{d \arctan x}{dx} = \frac{1}{1+x^2}$. Hence

$$|\arctan(x + \epsilon) - \arctan x| \leq |\epsilon|. \quad (\text{I31})$$

From this, we conclude that

$$\begin{aligned} |\phi_{1,0} - \zeta_0| &= |\arctan \tan \phi_{1,0} - \arctan \tan \zeta_0| \\ &\leq |\tan \phi_{1,0} - \tan \zeta_0| \\ &\leq \frac{10g\sqrt{n}}{N} + \frac{98g^2n}{N^2}. \end{aligned} \quad (\text{I32})$$

Now consider the following lemma.

Lemma 26. *Let $a, b \in \mathbb{R}$, and let $x \in \mathbb{R}$. Let $|bx| \leq \pi/6$. Then*

$$|\arctan(\tan bx) - bx| \leq 3|bx|^3/2, \quad (\text{I33})$$

$$|\arctan(-\tan bx) - (-bx)| \leq 3|bx|^3/2, \quad (\text{I34})$$

$$|\arctan(\tan^3 bx) - b^3x^3| \leq 1658|bx|^5, \quad (\text{I35})$$

$$|\arctan(-\tan^3 bx) - (-b^3x^3)| \leq 1658|bx|^5. \quad (\text{I36})$$

Proof. From Taylor's theorem with remainder, given a function f with first, second and third derivatives $f', f'',$ and f''' , we have $|f(x) - (f(0) + xf'(0) + x^2f''(0)/2)| \leq \max_{c \in [-|x|, |x|]} |f'''(c)||x|^3/6$. When $bx \leq \pi/6$, we have

$$|\tan bx - bx| \leq \frac{8}{9}|bx|^3, \quad (\text{I37})$$

$$|\tan^3 bx - b^3x^3| \leq 1657|bx|^5. \quad (\text{I38})$$

For all $x \in \mathbb{R}$, we also have

$$|\arctan x - x| \leq \frac{1}{3}|x|^3. \quad (\text{I39})$$

Hence,

$$\begin{aligned} &|\arctan(\tan bx) - bx| \\ &= |\arctan(\tan bx) - \tan bx + \tan bx - bx| \\ &\leq |\arctan(\tan bx) - \tan bx| + |\tan bx - bx| \\ &\leq \frac{|\tan bx|^3}{3} + \frac{8|bx|^3}{9}. \end{aligned} \quad (\text{I40})$$

When $|bx| \leq \pi/6$, we have $\frac{9}{8}|bx| \geq |\tan bx|$. Hence $|\arctan(\tan bx) - bx| \leq \frac{(9/8)^3|bx|^3}{3} + \frac{8|bx|^3}{9} \leq 3|bx|^3/2$. Similarly, $|\arctan(-\tan bx) - (-bx)| \leq 3|bx|^3/2$.

From Taylor's theorem with remainder, given a function f with k th order derivatives $f^{(k)}$,

we have $|f(x) - (f(0) + \sum_{k=1}^4 x^k f^{(k)}(0)/k!)| \leq \max_{c \in [-|x|, |x|]} |f^{(5)}(c)| |x|^5/5!$. Hence

$$\begin{aligned} & |\arctan(\tan^3 bx) - b^3 x^3| \\ &= |\arctan(\tan^3 bx) - \tan^3 bx + \tan^3 bx - b^3 x^3| \\ &\leq |\arctan(\tan^3 bx) - \tan^3 bx| + |\tan^3 bx - b^3 x^3| \\ &\leq \frac{|\tan bx|^9}{3} + 1657|bx|^5 \end{aligned} \quad (\text{I41})$$

When $|bx| \leq \pi/6$, we have $\frac{9}{8}|bx| \geq |\tan bx|$. Hence $|\arctan(\tan^3 bx) - b^3 x^3| \leq \frac{(9/8)^9 (\pi/6)^4 |bx|^5}{3} + 1657|bx|^5 \leq 1658|bx|^5$. Similarly, $|\arctan(-\tan^3 bx) - (-b^3 x^3)| \leq 1658|bx|^5$. \square

Using this lemma, we find that when $n = 3$,

$$|\zeta_0 - (-g\tau\theta/2)^3| \leq 1658(g\tau/2)^5 |\theta|^5 \leq 52g^5 \tau^5 |\theta|^5, \quad (\text{I42})$$

$$|\zeta_1 - (g\tau\theta/2)| \leq 3(g\tau/2)^3 |\theta|^3/2 = \frac{3g^3 \tau^3 |\theta|^3}{16}. \quad (\text{I43})$$

Furthermore,

$$|\phi_{1,0} - (-g\tau\theta/2)^3| \leq +52g^5 \tau^5 |\theta|^5. \quad (\text{I44})$$

Appendix J: Approximation of $\phi_{1,1}$

Now we have

$$\phi_{1,1} = \arctan \frac{\text{Im} \frac{\langle q_{1,\sigma} | U_\Delta | 1'_\sigma \rangle}{\langle q_{0,\sigma} | U_\Delta | 0'_\sigma \rangle}}{\text{Re} \frac{\langle q_{1,\sigma} | U_\Delta | 1'_\sigma \rangle}{\langle q_{0,\sigma} | U_\Delta | 0'_\sigma \rangle}}. \quad (\text{J1})$$

Let us obtain an approximation to $\phi_{1,1}$ to leading order in θ . Hence we write

$$\frac{\langle q_{1,\sigma} | U_\Delta | 1'_\sigma \rangle}{\langle q_{0,\sigma} | U_\Delta | 0'_\sigma \rangle} = \frac{a + a'\theta}{b + b'\theta} + O(\theta^2), \quad (\text{J2})$$

where

$$a = \langle q_{1,\sigma} | 1'_\sigma \rangle, \quad (\text{J3})$$

$$b = \langle q_{0,\sigma} | 0'_\sigma \rangle, \quad (\text{J4})$$

$$a' = -i\tau \langle q_{1,\sigma} | J^z | 1'_\sigma \rangle, \quad (\text{J5})$$

$$b' = -i\tau \langle q_{0,\sigma} | J^z | 0'_\sigma \rangle. \quad (\text{J6})$$

Consider the function $f(x) = \frac{a+a'x}{b+b'x}$. Now $\frac{d}{dx} f(x) = \frac{ba' - ab'}{(b+b'x)^2}$. Hence,

$$f(x) = \frac{a}{b} + \frac{ba' - ab'}{b^2} x + O(x^2). \quad (\text{J7})$$

Hence we can write

$$\frac{\langle q_{1,\sigma} | U_\Delta | 1'_\sigma \rangle}{\langle q_{0,\sigma} | U_\Delta | 0'_\sigma \rangle} = \frac{a}{b} + \frac{ba' - ab'}{b^2} \theta + O(\theta^2) \quad (\text{J8})$$

Since a, b, ia', ib' are real, we have

$$\text{Re} \frac{\langle q_{1,\sigma} | U_\Delta | 1'_\sigma \rangle}{\langle q_{0,\sigma} | U_\Delta | 0'_\sigma \rangle} = \frac{a}{b} + O(\theta^2) \quad (\text{J9})$$

$$\text{Im} \frac{\langle q_{1,\sigma} | U_\Delta | 1'_\sigma \rangle}{\langle q_{0,\sigma} | U_\Delta | 0'_\sigma \rangle} = \theta + O(\theta^2). \quad (\text{J10})$$

Hence

$$\begin{aligned} \tan \phi_{1,1} &= \frac{ba' - ab'}{ib^2} \frac{b}{a} \theta + O(\theta^2) \\ &= \left(\frac{a'}{ia} - \frac{b'}{ib} \right) \theta + O(\theta^2) \\ &= -\tau \left(\frac{\langle q_{1,\sigma} | J^z | 1'_\sigma \rangle}{\langle q_{1,\sigma} | 1'_\sigma \rangle} - \frac{\langle q_{0,\sigma} | J^z | 0'_\sigma \rangle}{\langle q_{0,\sigma} | 0'_\sigma \rangle} \right) \theta + O(\theta^2). \end{aligned} \quad (\text{J11})$$

Hence it remains to evaluate $\langle q_{j,\sigma} | j'_\sigma \rangle$ and $\langle q_{j,\sigma} | J^z | j'_\sigma \rangle$. Now recall the identity $|q_{j,\sigma}\rangle = \frac{2}{g\sqrt{n}} |Q_j\rangle$ where $|Q_j\rangle = J^z |j_\sigma\rangle - \langle j_\sigma | J^z | j_\sigma \rangle |j_\sigma\rangle$. Then we can write

$$\langle Q_{j,\sigma} | j'_\sigma \rangle = \langle j_\sigma | J^z | j'_\sigma \rangle - \langle j_\sigma | J^z | j_\sigma \rangle \langle j_\sigma | j'_\sigma \rangle, \quad (\text{J12})$$

$$\langle Q_{j,\sigma} | J^z | j'_\sigma \rangle = \langle j_\sigma | (J^z)^2 | j'_\sigma \rangle - \langle j_\sigma | J^z | j_\sigma \rangle \langle j_\sigma | J^z | j'_\sigma \rangle. \quad (\text{J13})$$

Hence it remains to evaluate $\langle j_\sigma | j'_\sigma \rangle$, $\langle j_\sigma | J^z | j'_\sigma \rangle$ and $\langle j_\sigma | (J^z)^2 | j'_\sigma \rangle$.

$$\begin{aligned} \langle j_\sigma | \epsilon_{j,\sigma} \rangle &= \langle j_\sigma | (\sqrt{z_j} |j_\sigma\rangle + |\epsilon_{j,\sigma}\rangle) - \sqrt{z_j} \langle j_\sigma | j_\sigma \rangle \\ &= \langle j_\sigma | j'_\sigma \rangle - \sqrt{z_j} \langle j_\sigma | j_\sigma \rangle. \end{aligned} \quad (\text{J14})$$

From (H13), we can rewrite the above as

$$\langle j_\sigma | \epsilon_{j,\sigma} \rangle = 2\sqrt{z_j} \langle \epsilon_{j,\sigma} | \epsilon_{j,\sigma} \rangle. \quad (\text{J15})$$

Hence

$$\langle j_\sigma | j'_\sigma \rangle = \sqrt{z_j} + 2\sqrt{z_j} \langle \epsilon_{j,\sigma} | \epsilon_{j,\sigma} \rangle. \quad (\text{J16})$$

From (H26), for $n = 3$ we get

$$\begin{aligned} \langle j_\sigma | j'_\sigma \rangle &= \sqrt{z_j} + \frac{1}{\sqrt{z_j}} \frac{3g^2}{8N^2} + (-1)^j \frac{3g^3}{2N^3 z_j^{3/2}} \\ &\quad - \frac{135g^3}{16N^3 z_j^{3/2}} + O(g^4/N^4). \end{aligned} \quad (\text{J17})$$

Using our upper bound on $\langle \epsilon_{j,\sigma} | \epsilon_{j,\sigma} \rangle$ and $z_j \leq 1$, we get

$$|\langle j_\sigma | \epsilon_{j,\sigma} \rangle| \leq \frac{g^2 n}{N^2}. \quad (\text{J18})$$

Next

$$\begin{aligned} \langle j_\sigma | J^z | \epsilon_{j,\sigma} \rangle &= (\langle j_\sigma | J^z \rangle (\sqrt{z_j} |j_\sigma\rangle + |\epsilon_{j,\sigma}\rangle - |j_\sigma\rangle)) \\ &= (\langle j_\sigma | J^z \rangle (|j'_\sigma\rangle - |j_\sigma\rangle)) \\ &= \langle j_\sigma | J^z | j'_\sigma \rangle - \langle j_\sigma | J^z | j_\sigma \rangle. \end{aligned} \quad (\text{J19})$$

Now

$$\begin{aligned} & \langle j_\sigma | J^z | j_\sigma \rangle \\ &= 2^{-n+1} \sum_{\text{mod}(k,2)=j} \binom{n}{k} \left(\frac{N}{2} - (gk + s - \sigma) \right) \\ &= \left(\frac{N}{2} - (s - \sigma) \right) - \frac{gn}{2}. \end{aligned} \quad (\text{J20})$$

Let $u = \left(\frac{1}{2} - \frac{gn}{2N} - \frac{s-\sigma}{N} \right)$. Next,

$$\begin{aligned} & \langle j_\sigma | J^z | j'_\sigma \rangle \\ &= 2^{-n+1} \sum_{\text{mod}(k,2)=j} \binom{n}{k} \sqrt{z_j + x_k} \left(\frac{N}{2} - (gk + s - \sigma) \right) \\ &= \frac{N\sqrt{z_j}}{2^{n-1}} \sum_{\text{mod}(k,2)=j} \binom{n}{k} \sqrt{1 + \frac{x_k}{z_j}} (u + x_k) \\ &= \frac{N\sqrt{z_j}}{2^{n-1}} \sum_{\text{mod}(k,2)=j} \binom{n}{k} \left(x_k + \frac{x_k^2}{2z_j} - \frac{x_k^3}{8z_j^2} + \frac{x_k^4}{16z_j^3} + \dots \right) \\ & \quad + \frac{N\sqrt{z_j}}{2^{n-1}} \sum_{\text{mod}(k,2)=j} \binom{n}{k} \left(1 + \frac{x_k}{2z_j} - \frac{x_k^2}{8z_j^2} + \frac{x_k^3}{16z_j^3} + \dots \right). \end{aligned} \quad (\text{J21})$$

Recall from the properties of binomial sums, that $2^{-n+1} \sum_{\text{mod}(k,2)=j} \binom{n}{k} x_k = 0$, $2^{-n+1} \sum_{\text{mod}(k,2)=j} \binom{n}{k} x_k^2 = \frac{g^2 n}{4N^2}$. We also use (H22) and (H23) for $2^{-n+1} \sum_{\text{mod}(k,2)=j} \binom{n}{k} x_k^3$. Therefore

$$\begin{aligned} & \langle j_\sigma | J^z | j'_\sigma \rangle \\ &= Nu\sqrt{z_j} + \frac{N\sqrt{z_j}}{2^{n-1}} \sum_{\text{mod}(k,2)=j} \binom{n}{k} x_k^2 \left(\frac{1}{2z_j} - \frac{u}{8z_j^2} \right) \\ & \quad + \frac{N\sqrt{z_j}}{2^{n-1}} \sum_{\text{mod}(k,2)=j} \binom{n}{k} x_k^3 \left(\frac{u}{16z_j^3} - \frac{x_k^3}{8z_j^2} \right) \\ &= Nu\sqrt{z_j} + N\sqrt{z_j} \frac{g^2 n}{4N^2} \left(\frac{1}{2z_j} - \frac{u}{8z_j^2} \right) + N\sqrt{z_j} \left(\frac{g^3 n^3}{N^3} \right. \\ & \quad \left. + \frac{3g^3 n^2}{4N^3} + (-1)^j \frac{g^3 S(3, n) n!}{N^3} \right) \left(\frac{u}{16z_j^3} - \frac{x_k^3}{8z_j^2} \right) + \dots \\ &= Nu\sqrt{z_j} + \frac{g^2 n}{4N} \left(\frac{1}{2\sqrt{z_j}} - \frac{u}{8z_j^{3/2}} \right) + \frac{g^3 \sqrt{z_j}}{N^2} \left(n^3 + \frac{3n^2}{4} \right. \\ & \quad \left. + (-1)^j S(3, n) n! \right) \left(\frac{u}{16z_j^3} - \frac{x_k^3}{8z_j^2} \right) + \dots \end{aligned} \quad (\text{J22})$$

Now $\left(\frac{1}{2} - \frac{gn}{2N} - \frac{s-\sigma}{N} \right) \leq \frac{1}{2}$. Hence, using the Taylor's Theorem with remainder again for the function

$\sqrt{1 + x_k/z_j}$, and using $|x_k z_j| \leq \frac{gn}{2N z_j}$, we find

$$\begin{aligned} & \left| \langle j_\sigma | J^z | j'_\sigma \rangle - Nu\sqrt{z_j} - \frac{g^2 n}{4N} \left(\frac{1}{2z_j} - \frac{u}{8z_j^2} \right) \right| \\ & \leq N\sqrt{z_j} \frac{gn}{2N z_j} \frac{g^2 n^2}{2^2 N^2 z_j^2} \frac{1}{4(2!)} + N\sqrt{z_j} \frac{3g^3 n^3}{2^3 N^3 z_j^3} \frac{1}{8(3!)} \\ & \leq \frac{g^3 n^3}{2N^2} + \frac{g^3 n^3}{4N^2} = \frac{3g^3 n^3}{4N^2}. \end{aligned} \quad (\text{J23})$$

where the last inequality uses the bound $1/4 \leq z_j \leq 1$. Hence, for $n = 3$,

$$\begin{aligned} \langle q_{j,\sigma} | j'_\sigma \rangle &= \frac{2}{g\sqrt{n}} \left(Nu\sqrt{z_j} + \frac{g^2 n}{4N} \left(\frac{1}{2z_j} - \frac{u}{8z_j^2} \right) \right) \\ & \quad - \frac{2}{g\sqrt{n}} Nu \left(\sqrt{z_j} + \frac{1}{\sqrt{z_j}} \frac{3g^2}{8N^2} \right) + \dots \\ &= \frac{6g}{4N\sqrt{3}} \left(\frac{1}{2z_j} - \frac{u}{8z_j^2} \right) - \frac{6gu}{8N\sqrt{3z_j}} + \dots \end{aligned} \quad (\text{J24})$$

Next,

$$\begin{aligned} & \langle j_\sigma | (J^z)^2 | j'_\sigma \rangle \\ &= 2^{-n+1} \sum_{\text{mod}(k,2)=j} \binom{n}{k} \sqrt{z_j + x_k} \left(\frac{N}{2} - (gk + s - \sigma) \right)^2 \\ &= \frac{N^2 \sqrt{z_j}}{2^{n-1}} \sum_{\text{mod}(k,2)=j} \binom{n}{k} \sqrt{1 + \frac{x_k}{z_j}} (u + x_k)^2 \\ &= \frac{N^2 \sqrt{z_j}}{2^{n-1}} \sum_{\text{mod}(k,2)=j} \binom{n}{k} \left(x_k^2 + \frac{x_k^3}{2z_j} - \frac{x_k^4}{8z_j^2} + \dots \right) \\ & \quad + \frac{N^2 \sqrt{z_j}}{2^{n-1}} 2u \sum_{\text{mod}(k,2)=j} \binom{n}{k} \left(x_k + \frac{x_k^2}{2z_j} - \frac{x_k^3}{8z_j^2} + \dots \right) \\ & \quad + \frac{N^2 \sqrt{z_j}}{2^{n-1}} u^2 \sum_{\text{mod}(k,2)=j} \binom{n}{k} \left(1 + \frac{x_k}{2z_j} - \frac{x_k^2}{8z_j^2} + \frac{x_k^3}{16z_j^3} \dots \right). \end{aligned} \quad (\text{J25})$$

Rearranging terms in the summations, and noting that $2^{-n+1} \sum_{\text{mod}(k,2)=j} \binom{n}{k} x_k = 0$, and setting $u = \left(\frac{1}{2} - \frac{gn}{2N} - \frac{s-\sigma}{N} \right)$, we get

$$\begin{aligned} & \langle j_\sigma | (J^z)^2 | j'_\sigma \rangle \\ &= \frac{N^2 \sqrt{z_j}}{2^{n-1}} \left(1 + \frac{u}{z_j} - \frac{u^2}{8z_j^2} \right) \sum_{\text{mod}(k,2)=j} \binom{n}{k} x_k^2 \\ & \quad + \frac{N^2 \sqrt{z_j}}{2^{n-1}} \left(\frac{1}{2z_j} - \frac{u}{4z_j^2} + \frac{u^2}{16z_j^3} \right) \sum_{\text{mod}(k,2)=j} \binom{n}{k} (x_k^3 + \dots) \\ & \quad + N^2 \sqrt{z_j} u^2. \end{aligned} \quad (\text{J26})$$

Recall from the properties of binomial sums, $2^{-n+1} \sum_{\text{mod}(k,2)=j} \binom{n}{k} x_k^2 = \frac{g^2 n}{4N^2}$. We also use (H22) and (H23) for $2^{-n+1} \sum_{\text{mod}(k,2)=j} \binom{n}{k} x_k^3$. Hence for $n = 3$,

$$\begin{aligned} \langle j_\sigma | (J^z)^2 | j'_\sigma \rangle &= N^2 \sqrt{z_j} u^2 + \frac{g^2 n \sqrt{z_j}}{4} \left(1 + \frac{u}{z_j} - \frac{u^2}{8z_j^2} \right) \\ &+ \frac{g^3}{2N \sqrt{z_j}} \left(n^3 + \frac{3n^2}{4} + 6(-1)^j \right) \left(1 - \frac{u}{2z_j} + \frac{u^2}{8z_j^2} \right) + \dots \end{aligned} \quad (\text{J27})$$

Hence

$$\begin{aligned} &\langle q_{j,\sigma} | J^z | j'_\sigma \rangle \\ &= \frac{2}{g\sqrt{n}} \langle j_\sigma | (J^z)^2 | j'_\sigma \rangle - \frac{2}{g\sqrt{n}} \langle j_\sigma | J^z | j_\sigma \rangle \langle j_\sigma | J^z | j'_\sigma \rangle \\ &= \frac{2}{g\sqrt{n}} \left(N^2 \sqrt{z_j} u^2 + \frac{g^2 n \sqrt{z_j}}{4} \left(1 + \frac{u}{z_j} - \frac{u^2}{8z_j^2} \right) \right) \\ &+ \frac{2}{g\sqrt{n}} \frac{g^3}{2N \sqrt{z_j}} \left(n^3 + \frac{3n^2}{4} + 6(-1)^j \right) \left(1 - \frac{u}{2z_j} + \frac{u^2}{8z_j^2} \right) \\ &- \frac{2}{g\sqrt{n}} N u \left(N u \sqrt{z_j} + \frac{g^2 n}{4N} \left(\frac{1}{2z_j} - \frac{u}{8z_j^2} \right) \right) + \dots \\ &= \frac{g\sqrt{n z_j}}{2} \left(1 + \frac{u}{z_j} - \frac{u^2}{8z_j^2} \right) - \frac{g\sqrt{n} u}{2} \left(\frac{1}{2z_j} - \frac{u}{8z_j^2} \right) + \\ &+ \frac{g^2}{N \sqrt{3z_j}} \left(\frac{135}{4} + 6(-1)^j \right) \left(1 - \frac{u}{2z_j} + \frac{u^2}{8z_j^2} \right) + \dots \end{aligned} \quad (\text{J28})$$

Hence we find that

$$\begin{aligned} &\frac{\langle q_{j,\sigma} | J^z | j'_\sigma \rangle}{\langle q_{j,\sigma} | j'_\sigma \rangle} \\ &= \left(4N \sqrt{n z_j} \left(1 + \frac{u}{z_j} - \frac{u^2}{8z_j^2} \right) - 4N \sqrt{n} u \left(\frac{1}{2z_j} - \frac{u}{8z_j^2} \right) \right) \\ &+ \frac{2g}{\sqrt{3z_j}} \left(135 + 24(-1)^j \right) \left(1 - \frac{u}{2z_j} + \frac{u^2}{8z_j^2} \right) \\ &\times \left(4\sqrt{3} \left(\frac{1}{2z_j} - \frac{u}{8z_j^2} \right) - 2\sqrt{3} u / z_j \right)^{-1} + \dots \end{aligned} \quad (\text{J29})$$

When $s = N/2 - gn/2 + o(g)$, it follows that $z_0 \approx z_1 \approx 1/2$, and $u = o(g/N)$. Then

$$\begin{aligned} &\frac{\langle q_{j,\sigma} | J^z | j'_\sigma \rangle}{\langle q_{j,\sigma} | j'_\sigma \rangle} \\ &= N \left(\frac{1}{\sqrt{2}} - 1 \right) + \frac{g\sqrt{2} (45 + 8(-1)^j)}{4} + \dots, \end{aligned} \quad (\text{J30})$$

and hence

$$\frac{\langle q_{1,\sigma} | J^z | 1'_\sigma \rangle}{\langle q_{1,\sigma} | 1'_\sigma \rangle} - \frac{\langle q_{0,\sigma} | J^z | 0'_\sigma \rangle}{\langle q_{0,\sigma} | 0'_\sigma \rangle} = -4\sqrt{2}g + \dots \quad (\text{J31})$$

Hence

$$\tan \phi_{1,1} = 4\sqrt{2}g\tau\theta + \dots \quad (\text{J32})$$

and

$$\frac{d}{d\theta} \tan \phi_{1,1} = 4\sqrt{2}g\tau + \dots \quad (\text{J33})$$